# Study of: a) the Ge(p,d) and (p,t) reactions, b) the $^{26}Mg(p,t)^{24}Mg$ reaction.

by

R. Fournier

Submitted in partial fulfillment
of the requirements for the degree of
Doctor of Philosophy

Department of Physics,
Faculty of Pure and Applied Science,
The University of Ottawa,
Ottawa, Canada.

1971

Homage profonde

to my wife

à mes parents

## ABSTRACT

### PART I

A systematic study of the (p,d) and (p,t) reactions on all the stable germanium isotopes was made using a 20 MeV proton beam. Level energies in the residual nuclei are deduced and compared to previously measured values. Spin and parity assignments to these levels are suggested whenever possible.

The experimental (p,d) angular distributions are compared to the DWBA theory and absolute spectroscopic factors are extracted. From these, the occupation and center of gravity energy of the $2p_{3/2}$, $1f_{5/2}$, $2p_{1/2}$ and $1g_{9/2}$ shells are calculated and compared to results obtained for neighbouring nuclei and to the predictions of the simple pairing theory. A collective model based on the Nilsson deformed potential to which is added a residual interaction of the pairing type is applied to try and predict the low lying level properties of the odd germanium isotopes.

The (p,t) results are presented without too much emphasis due to the complicated nature of the two nucleon transfer reaction and to the poor knowledge of the wave functions in this mass region.

## PART II

The $^{26}Mg(p,t)^{24}Mg$ reaction was studied with a 20 MeV proton beam. A formalism is presented to calculate the structure amplitudes which are needed for the DWBA calculation. DWBA predictions are compared to the experimental angular distributions, and it is concluded that the large discrepancy between the two for the transition strength to the excited members of the ground state rotational band in $^{24}Mg$ is due to an other reaction mechanism than the direct pick-up of a dineutron, and that the two step process is a good candidate for this other reaction mechanism.

## STATEMENT OF ORIGINALITY

As far as the author is aware, this work constitutes the first systematic investigation of the (p,d) and (p,t) reactions on the stable germanium isotopes, and the first quantitative analysis of the $^{26}Mg(p,t)^{24}Mg$ reaction.

Different authors have tried, with more or less success, to predict from pairing theory the observed occupation and the single quasiparticle energy of the active shells for nuclei in the region $28 \leq Z \leq 34$. As far as he is aware, the author is the first one to have compared the systematics of these two quantities to the predictions of the pairing theory for the whole mass region. Good agreement was found although there exists large discrepancies for certain individual nuclei, which can be attributed to uncertainties in the measured values.

For the first time, the data on the single quasiparticle energies, for this mass region, has been compared in a systematic way to investigate the effect of the short range p-n force in this mass region.

Although the author cannot claim originality in the Coriolis coupling plus pairing interaction model, he is the first to have applied the model to the germanium isotopes and to have further tested the wave functions by calculating the spectroscopic factors for transitions to the predicted levels.

## ACKNOWLEDGEMENTS

I would like to express my gratitude to Dr. T. Hsu who suggested the first project for this thesis and who also helped considerably in the analysis of the data.

I am indebted to Dr. B. Hird for his continued guidance and encouragement during this project, and also for his financial assistance.

I am grateful to Dr. G. Ball for his enlightening discussions and valuable advice, especially in the derivation of the structure factors for the $^{26}Mg(p,t)^{24}Mg$ reaction.

I would also like to thank Dr. W. Davis for making available his program DWUCK, and J. Kroon for his help in carrying out these experiments.

Finally the author would like to acknowledge the financial assistance of the National Research Council of Canada.

TABLE OF CONTENTS.

## LIST OF DIAGRAMS

# LIST OF TABLES

Part I.

## PREFACE

The work for this thesis was done in two parts. In chronological order, the first problem attempted was that of calculating the structure factors for the $^{26}Mg(p,t)^{24}Mg$ reaction. During that investigation, a systematic study of the (p,d) and (p,t) reactions on the stable germanium isotopes was carried out.

Although the second problem is much bigger in scope, it required less effort to carry out than the first one since the whole operation from raw data to the final fitted angular distributions was computerized by the author, and the physics started with this final product.

The first problem dealt with something completely new. A formalism for calculating the structure factors first had to be found and many tries turned out to be dead ends. Then each derivation had to be checked and cross-checked for possible mistakes. Finally, many computer hours were used to try, unsuccessfully, to obtain a good agreement between the observed and predicted transition strengths.

The author has made no attempt at describing theories which are textbook content or well published, and assumes the reader to be more or less familiar with the one and two nucleon DWBA theory, the simple pairing theory, the

Nilsson model of the deformed nucleus and the Coriolis coupling scheme of a nucleon to the deformed core.

## 1.- INTRODUCTION.

The mechanism of single nucleon transfer reactions such as the (p,d) or its inverse, the (d,p), is reasonably well understood in terms of the DWBA theory. These reactions allow, in some cases, to assign spin and parity to the levels populated in the residual nucleus. Furthermore, from the spectroscopic strength distribution to these levels and from the extracted total spectroscopic strength, one can calculate the single particle energy of each subshell in the residual nucleus and the fractional filling of each subshell in the parent nucleus.

Systematic investigations of the (d,p) reactions on the stable even isotopes of Ni, Zn and Se have already been reported. When this work was started, no such systematic study had been made for the germanium isotopes, and the only spectroscopic information available was from the $^{70}Ge(^{3}He,\alpha)^{69}Ge$ reaction and the (d,p) reactions on $^{70}Ge$ and $^{72}Ge$. These are isolated measurements performed at different energies by different authors, so that it is hard to extract systematic behaviour.

To fill the gap between Zn and Se, it was thought worthwhile to perform the (p,d) reaction on all the stable germanium isotopes. By comparing our results to those of neighbouring Ni, Zn and Se one should have a good picture of the shell filling and the behaviour of the single par-

ticle energies for nuclei with neutron number between $N = 30$ and $N = 48$. Such a study also extended our knowledge of the level schemes of the odd germanium isotopes which are not too well known.

The results of the (p,t) reactions are presented without too much emphasis due to the fact that no structure factors can be calculated since no model has been able to successfully describe the germanium isotopes.

## 2.- EXPERIMENTAL.

A 20 MeV proton beam from the Chalk River MP Tandem accelerator was used to bombard isotopically enriched germanium targets supported on a 15 $\mu g/cm^2$ carbon foil and mounted in the center of a precision 34 inch diameter scattering chamber. The beam was well collimated and focused in a 2 to 3 mm diameter spot on the target.

The beam was stopped in a long faraday cup with both electric and magnetic suppression. A precision current integrator (calibrated) yielded the accumulated charge which was used to calculate the cross sections. A 2 mm thick detector, at 20 degrees to the beam direction, and placed behind a 2 mm thick absorber so that the protons elastically scattered from the target were completely stopped, was used to further monitor the beam current by making frequent checks of the ratio of the accumulated charge to monitor counts (under the elastic proton peak and refered to the same target orientation). Beam currents of 50 to 900 nA were used.

The target materials were supplied by Oak Ridge National Laboratories and the quoted isotopic composition from their spectroscopic analysis is listed in Table 1.

The reaction products were detected and analysed with a counter telescope system consisting of three totally depleted silicon counters having thicknesses of 50 $\mu$ ($\Delta$E), 500 $\mu$ (E) and 200 $\mu$ ($\bar{E}$), entirely enclosed in a brass housing

with an entrance slit subtending an angle of 0.000414 strad to the target. The entrance slit to the detector housing was followed by a small permanent magnet for electron suppression; such an arrangement yielded almost background free spectra.

The particle identification uses a method developped by Hird and Ollerhead (69Hil) in which a particular type of particle is identified by making an on-line calculation of the fromt counter thickness for each particle using the known experimental range-energy curve of that particular type of particle. The front counter thickness seen by a particle stopped in the second detector is given by:

$$T = R(E+\Delta E) - R(E),$$

where R(E) is the range of the particle of energy E in the detector material, and $\Delta E$ and E are the energies lost in the front and second counter respectively. The range-energy characteristic of a particular type of particle was stored in the memory of the on-line computer; the particle energies could then be converted into equivalent ranges in the detectors, and the front counter thickness was obtained by substracting two tabulated values. The true front counter thickness will be obtained only for the type of particles whose range-energy characteristic is stored in the computer; for all other particles, different and non constant thicknesses should result. The triton range-energy curve was stored in the computer, since earlier investigations were of the (p,t) reactions for which the cross sec-

tion is much smaller than that of the other competing (p,p), (p,d) and (p,$\alpha$) reactions.

Fig. 1 shows the basic electronic circuit used and can be described as follows: A pulse will appear at the output of the coincidence unit to open the ADCs (Analogue to Digital Converters) only when there is a pulse from the $\Delta E$ and E counters in coincidence and no pulse from the $\bar{E}$ counter; the $\Delta E$ and E pulses are then digitized and transfered to the on-line computer for particle identification. The summed $\Delta E$ and E counter thicknesses is chosen so as to stop the most energetic particles of interest (deuterons in our case), while not being thick enough to stop the elastic protons which will produce a pulse in the $\bar{E}$ counter. In this way, the numerous unwanted elastic protons can be rejected before they reach the relatively slow ADC. The actual electronic circuit used is, of course, much more sophisticated since pulse shaping, delays for accurate timing, gate drivers, inverters, ...etc. are required, but the basic principle of operation is the same as that just described.

By carefully adjusting the amplification of the detection system, the ADC's digitized detector pulse is the appropriate address to the stored range-energy curve. The front counter thickness is thus obtained by adding two channels ($\Delta E+E$), looking up two numbers in the memory whose addresses are $E+\Delta E$ and E, and subtracting these two

numbers.

Fig. 2 shows a typical front counter thickness spectrum obtained; it is seen that not only are the tritons properly identified, but all the Z = 1 particles are well separated. By setting digital windows on the different peaks of the thickness spectrum, one can accumulate the energy spectrum of various particles simultaneously in different regions of the memory. It was thus possible to analyse the (p,d), (p,t) and (p,$\alpha$) spectra at the same time.

Spectra were accumulated at every 5 degree intervals from 15 to 65 degrees and sometimes at 12, 17 or 22 degrees with an energy resolution of 30 to 40 keV. In order to obtain accurate energy scales, measurements with an $^{27}Al$ target from which the well known levels of the residual nucleus $^{26}Al$ provided many calibrated deuteron energies, were made at regular intervals.

The target thicknesses were measured in a separate experiment of the Rutherford scattering at 40 and 60 degrees of 6 MeV alpha particles (the Coulomb barrier for alpha particles on germanium is $\sim$8 MeV). At these angles the elastic scattering peak from germanium is well resolved from that of the carbon backing and other light impurities. Since the elastic cross sections are very large, no particle identification system was required

and only one detector was used in the same detector housing as in the reaction measurements so as to eliminate systematic errors in geometry corrections.

The target thicknesses were calculated using the relation:

$$\frac{d\sigma(\theta)^{el}}{d\Omega} = \frac{N(\theta)^{el}}{w\ t\ N_{inc}} = \sigma(\theta)^{R},$$

where: $\frac{d\sigma(\theta)^{el}}{d\Omega}$ = measured experimental cross section at angle $\theta$,

$N(\theta)^{el}$ = number of elastically scattered particles at the same angle (area under the elastic scattering peak),

$w$ = solid angle of the detector entrance slit,

$t$ = target thickness in atoms/cm$^2$,

$N_{inc}$ = number of particles incident on the target (proportional to the integrated current),

$\sigma(\theta)^{R}$ = Rutherford cross section at angle $\theta$.

Since the targets are not isotopically pure, the calculated thicknesses obtained with the above formulae have to be multiplied by the % content of the particular target isotope to obtain the true thickness. The last column of Table 1 lists the corrected target thickness for the various isotopes.

## 3.- DATA ANALYSIS.

The first step in analysing the data was to calculate the calibration line for each spectrum. Two different methods were used:

a) From the reaction kinematics and the peak position of the carbon and oxygen impurities seen on all the (p,d) spectra, the slope and the intercept of the calibration line were determined for each (p,d) spectrum.

b) The position of the observed peaks from the numerous $^{27}Al(p,d)^{26}Al$ calibration reactions were accurately determined by a peak fitting programme and chi-square fitted to the well known $^{26}Al$ level scheme. The slope of the calibration line was found to be almost constant and an average was taken; the slope intercept varied considerably and was corrected, for each spectrum, by requiring that the oxygen impurity peak in the (p,d) spectrum had the right energy as determined from reaction kinematics.

These two different methods yielded essentially the same calibration line for each spectrum. The calibration line of the corresponding (p,t) spectrum is the same since it only depends on the amplification chain, and the energy loss in the dead layers of the counters is small.

A peak fitting programme which least square fitted a gaussian curve to each peak of each individual spectrum

was used to determine the position and area of each peak. From the known calibration, the mass of the reacting particles and the integrated current as well as the target thickness, the programme then calculated the Q value of each peak and the center of mass cross section and error. This method of analysis is very useful when dealing with partially unresolved peaks and it provides a check that the same level is being studied at all angles by predicting a constant Q value. The error in the final cross section includes statistical and fitting errors. No background corrections were applied since the background in all the spectra was found to be negligiable. From the average Q value of each level, the level scheme of the residual nucleus was obtained.

An alternative method was used to determine the level scheme of the residual nuclei. All the energy spectra of a particular reaction were transformed into Q value spectra using the known calibration of the spectra and the kinematics of the reaction. All the Q value spectra were then summed and the peaks were fitted with a peak fitting programme. The accurately determined peak positions yielded the Q value of all the levels and the level scheme was obtained. After such a summation, many weak peaks which could not be analyzed by the first method grow to a statistically significant size, and their energy can be

determined with more accuracy. These two methods yielded essentially the same level energies within the experimental error of 2 to 5 keV for strong peaks and 10 to 20 keV for weakly excited levels. Figs. 3 to 12 show the summed Q value spectrum for each reaction studied.

Since the targets are not isotopically pure and contain significant amounts of other germanium impurities, the calculated cross sections have to be corrected when two or more levels from different residual nuclei overlap (i.e. have the same Q value). This is especially important in the (p,d) reactions, where the level density of the residual nuclei is high and levels overlap often. The cross sections were corrected, when overlapping of levels occurred, according to the method described in Appendix 1. When 80% of a certain level was accounted for by other impurities it was assumed to be due only to these impurities. Finally, the center of mass cross sections were plotted as a function of the center of mass angle to obtain the angular distributions shown in Figs 13 to 17 for the (p,d) reactions and in Figs. 18 to 22 for the (p,t) reactions.

## 4.- DWBA ANALYSIS.

The DWBA analysis of the (p,d) reactions was made using the DWBA code DWUCK (67Kul) which incorporates finite range and nonlocality corrections into the conventional zero-range DWBA with local potentials. Figs. 13 to 17 show the experimental angular distributions for the (p,d) reactions compared to the theoretical curves calculated for the $\ell_n$ transfers which fit the data best. A basic set of DWBA calculations was performed for all the excited states of the final nuclei using a finite range parameter of 0.65 fm, assuming all the potentials to be local with no spin-orbit interaction and no lower cut-off. Different optical potential parameters taken from the literature were tried for both the entrance and exit channels and the combination which gave the best overall fit to our data is listed in table 2. The proton optical potential parameters were taken from the work of Perey (63Pe1) (for $^{64}$Zn(p,p) at 22 MeV) and the deuteron parameters were taken from the deuteron elastic scattering analysis of Perey and Perey (63Pe2) ( for Cu(d,d) at 15 MeV).

The transferred neutron was assumed to be bound in a Saxon-Woods potential and the customary separation energy prescription was used. The radius and diffuseness of the Saxon-Woods potential were adjusted so as to have the

best simultaneous agreement between the total extracted spectroscopic strengths for each reaction and the expected one, while requiring at the same time that the shapes of the predicted angular distributions fit well the experimental ones. A radius and diffuseness of 1.25 and 0.55 fm seemed to be the most appropriate values, and it was found that for a 10% variation of the diffuseness, the cross sections varied by approximately 10%, while a 5% variation of the radius changed the cross sections by approximately 25%. For these small changes in the bound state parameters, the shape of the predicted curves and the relative cross sections remained reasonably constant. This sensitivity to the bound state parameters is reflected in the accuracy of our extracted absolute spectroscopic factors.

With these parameters, a set of spectroscopic factors was extracted in the usual manner of best fitting the theoretical angular distributions to the experiment, using the relation:

$$\frac{d\sigma}{d\Omega}(\theta)^{exp} = 2.29\, \mathcal{S}\, \sigma_{\ell_n}(\theta)^{DW},$$

where $\mathcal{S}$ is the spectroscopic factor, $\sigma_{\ell_n}(\theta)^{DW}$ the predicted angular distribution and $\ell_n$ the transfered angular momentum. For unresolved doublets, the predicted cross sections for the two relevant $\ell_n$ values were summed according to:

$$\sigma(\theta)^{DW} = A\,\sigma_{\ell_1}(\theta)^{DW} + (1 - A)\,\sigma_{\ell_2}(\theta)^{DW},$$

where A was varied between 0 and 1, and the resultant $\sigma(\theta)^{DW}$ was chi-square fitted to the data in order to determine the best value of A and also sometimes of $\ell_1$ and $\ell_2$.

In Fig. 23 is plotted the calculated absolute cross section at the first maximum for $\ell_n = 1$, 3 and 4 transitions as a function of the Q value. Also indicated on the same figure is the approximate energy of the outgoing deuteron and the range of Q values covered in each reaction which is labelled by the residual nucleus. Consulting Fig. 23 and Table 3, where the experimental summed spectroscopic strengths are compared to the expected ones, it is easy to see that in order to obtain better agreement, one would need a smaller Q-dependence of the calculated cross sections.

Since the deuteron optical potentials were kept constant throughout the basic analysis, and in view of the large range of Q values covered, it was felt important to study the sensitivity of the basic analysis to the addition of energy dependent terms in the optical potential of the outgoing channel.

The real deuteron potential was changed to the form:

$$V_s = 105.1 - 0.25\times(13 - E_d),$$

where $E_d$ is the outgoing deuteron energy. The added energy dependent term is similar to that found by Perey and Perey (63Pe2), and this form was chosen so that for

$E_d \approx 13$ MeV, $Q = -7$ MeV, the real potential is 105.1 MeV, the original value. With this improved potential, it was found that for $Q = -11$ MeV the cross sections decreased by less than 5%, which is negligable and in the wrong direction, so that energy dependent terms in the real deuteron optical potential were not included in our calculations.

From Fig. 20 of Perey and Perey's analysis of deuteron elastic scattering data (63Pe2), it is seen that for our range of deuteron energies (between 9 and 13 MeV) the energy dependence of the imaginary potential is large. A DWBA calculation along these lines for $Q = -11$ Mev ($E_d \approx 9$ MeV) with $W_D = 26$ MeV lowered the calculated cross section by approximately 20% for $\ell_n = 1$, 25% for $\ell_n = 3$ and 35% for $\ell_n = 4$; these variations are also in the wrong direction. A search in the literature of (d,p) experiments performed on Zn at 10 MeV (67Eh1), $^{70}$Ge at 7.5 MeV (68Go1) and $^{52}$Cr at 7.5 MeV (68Ra1) showed that these authors use imaginary well depths of approximately 20 MeV, which are quite different from the suggested values of Perey and Perey (63Pe2). In view of these facts and also because there does not seem to be any simple A dependence of the imaginary potential (70Gr1), the energy dependence of the imaginary potential was also ignored in our final results.

The effect of the non-locality of the optical potentials was also investigated. Since the non-local parameters

for bound states are not well known (70Ehl), only the optical potentials in the scattering channels were assumed to be non-local, with $\beta_p = 0.85$ for the protons and $\beta_d = 0.54$ for the deuterons, which are the values recommended by Kuntz for the programme DWUCK (67Kul). With these parameters, the cross sections were found to vary by only a few percent and the Q dependence was unaltered. Since these effects are small, they were not included in our calculations.

The (p,t) angular distributions were analyzed with a programme which assumed that the two transfered neutrons were bound in a Saxon-Woods potential and the coordinate transformations were made using the point triton approximation (64Rol). The same proton optical potential parameters were used as for the (p,d) reactions. The triton optical potential parameters were obtained from the data of Hafele et. al. (67Hal) for 20 MeV scattering from nickel. Some adjustments were made to the bound state parameters to achieve the best simultaneous fits to the first $L = 0$ and the first $L = 2$ transitions seen in each reaction.

Since wave functions in this mass region are not well known, no structure factor calculations could be made, and no importance was attached on the ratio of the experimental cross sections to the calculated ones.

# 5.- RESULTS.

## 5.1- Generalities.

From shell model considerations, the (p,d) reaction in the germanium region is expected to pick-up neutrons from the partially filled $2p_{3/2}$, $1f_{5/2}$, $2p_{1/2}$ and $1g_{9/2}$ shells. For $0^+$ spin targets, the spin and parity of the observed levels populated by a $\ell_n = 3$ or 4 transition can safely be assigned $5/2^-$ and $9/2^+$ respectively; however, for $\ell_n = 1$ transitions, the final spin can be either $1/2^-$ or $3/2^-$. Different methods were used to try and resolve the ambiguity between $2p_{3/2}$ and $2p_{1/2}$ neutron pick-up:

a) A good test, when (d,p) results are available, is to compare the (p,d) and the (d,p) reaction cross sections to a given $\ell_n = 1$ level. Since in this region $N > 38$, where the $2p_{3/2}$ neutron shell is buried under the almost full $1f_{5/2}$ shell while the $2p_{1/2}$ shell is above the latter, the $2p_{3/2}$ shell should be much fuller than the $2p_{1/2}$; therefore the ratio of the (p,d) over the (d,p) reaction cross section should fall into two different categories: one which is large, corresponding to a stripping or pick-up from a $2p_{3/2}$ shell which has many neutrons but few holes, and one which is smaller, corresponding to a neutron transfer to or from a $2p_{1/2}$ shell in which neutron and neutron holes are available.

b) There seems to be a small angle j-dependence of the Lee-Schiffer type. In their original work, Lee and Schiffer (64Lel) noticed a marked difference at backward angles between angular distributions leading to $j = 1/2^-$ and $3/2^-$ ($\ell_n = 1$) levels, from their work there was also, in some cases, evidence for a similar but much weaker effect at small angles. Sherr et. al. (64Shl), in their analysis of the (p,d) reactions on Fe and Ni, also found weak evidence for a small angle j-dependence whereby the first minimum seemed to be relatively deeper for $1/2^-$ than for $3/2^-$ levels. Evidence for such an effect is more noticeable in the $^{72}Ge(p,d)^{71}Ge$ reaction where the (p,d)/(d,p) ratio yields a spin of $3/2^-$ for the level at 502 keV (See Fig. 14), and a spin of $1/2^-$ for the ground state and the 706 keV level.

c) It seems very likely that the strong $\ell_n = 1$ transition to the 379, 502, 370 and 574 keV level of $^{69}$, $^{71}$, $^{73}$, $^{75}Ge$ respectively (by far the strongest transition in all the spectra as can be seen in Figs. 3 to 7 would correspond to the pick-up of a neutron from the same configuration. This transition is to a $3/2^-$ level (379 keV) in $^{69}Ge$, the spin having been determined in a study of the $\beta^+$ decay of $^{69}As$ (70Mul). Furthermore, from the (p,d)/(d,p) ratio this transition to $^{71}Ge$ (502 keV) and $^{73}Ge$ (370 keV) is also to a $3/2^-$ level.

d) In certain cases, for the low lying levels, a favored spin is suggested by comparing the level scheme of the germanium isotopes to that of neighbouring nuclei who have the same number of neutrons and whose number of protons differ by two.

e) From shell model considerations, one can assume that most of the $2p_{1/2}$ strength will lie at low excitation, while the $2p_{3/2}$ strength which requires more energy to excite since it is buried under the $1f_{5/2}$ should lie at higher energy.

In the case of the odd mass $^{73}$Ge target whose ground state spin is $9/2^+$, pick-up of a $(\ell,j)$ neutron will lead to final states of parity $(-)^{\ell}$ and final spin J which are allowed by Clebsh Gordan coefficient rules for the coupling of 9/2 and j to obtain J. Also, there is now more than one $(\ell,j)$ value which can lead to the same final state.

The (p,d) reaction can populate both $T_<$ and $T_>$ states in the final nucleus ($T_< = T_{target} - 1/2$, $T_> = T_{target} + 1/2$). Using the Q values of the (p,n) reactions on the germanium isotopes and a Coulomb energy displacement of 10 MeV (67Jal), the calculated energy of the first $T_>$ level in the germanium isotopes is at approximately 7, 9, 7, 10 and 12 MeV in $^{69}$, $^{71}$, $^{72}$, $^{73}$, $^{75}$Ge, respectively, well above the highest excitation energy seen in each isotope; therefore only $T_<$

states are populated. The spectroscopic strength will be divided between the $T_<$ and $T_>$ states and according to a sum rule of Macfarlane and French (60Mal), the total strength to the $T_<$ levels is:

$$\sum S_j(T_<) = n_j - p_j/(2T+1) ,$$

where $n_j$ and $p_j$ are the number of neutrons and protons in the j subshell of the target nucleus, T is the isotopic spin of the target nucleus and the sum runs over all the states of spin j. Since the proton distribution in the germanium isotopes (Z = 32) is not known, one has to make the assumption that the four additional protons outside the Z = 28 closed shell are in the $2p_{3/2}$ shell as predicted by the shell model. This is a drastic assumption as one expects that the four additional protons will be distributed mainly between the $2p_{3/2}$ and the $1f_{5/2}$ shells since these two shells are closely spaced. From that assumption, since $p_j \neq 0$ only for the $2p_{3/2}$ shell, the maximum spectroscopic strength to the $1f_{5/2}$, $2p_{1/2}$ and $1g_{9/2}$ shells should be 6, 2 and 10 respectively. For the $2p_{3/2}$ shell, the expected total strength is 3.43 for $^{70}$Ge (T = 3), 3.56 for $^{72}$Ge (T = 4), 3.60 for $^{73}$Ge (T = 4.5), 3.64 for $^{74}$Ge (T = 5) and 3.70 for $^{76}$Ge (T = 6). The total spectroscopic strength to all the shells should be 9.43 for $^{70}$Ge, 11.56 for $^{72}$Ge, 12.60 for $^{73}$Ge, 13.64 for $^{74}$Ge and 15.70 for $^{76}$Ge. If a different

states are populated. The spectroscopic strength will be divided between the $T_<$ and $T_>$ states and according to a sum rule of Macfarlane and French (60Mal), the total strength to the $T_<$ levels is:

$$\sum S_j(T_<) = n_j - p_j/(2T+1) ,$$

where $n_j$ and $p_j$ are the number of neutrons and protons in the j subshell of the target nucleus, T is the isotopic spin of the target nucleus and the sum runs over all the states of spin j. Since the proton distribution in the germanium isotopes (Z = 32) is not known, one has to make the assumption that the four additional protons outside the Z = 28 closed shell are in the $2p_{3/2}$ shell as predicted by the shell model. This is a drastic assumption as one expects that the four additional protons will be distributed mainly between the $2p_{3/2}$ and the $1f_{5/2}$ shells since these two shells are closely spaced. From that assumption, since $p_j \neq 0$ only for the $2p_{3/2}$ shell, the maximum spectroscopic strength to the $1f_{5/2}$, $2p_{1/2}$ and $1g_{9/2}$ shells should be 6, 2 and 10 respectively. For the $2p_{3/2}$ shell, the expected total strength is 3.43 for $^{70}$Ge (T = 3), 3.56 for $^{72}$Ge (T = 4), 3.60 for $^{73}$Ge (T = 4.5), 3.64 for $^{74}$Ge (T = 5) and 3.70 for $^{76}$Ge (T = 6). The total spectroscopic strength to all the shells should be 9.43 for $^{70}$Ge, 11.56 for $^{72}$Ge, 12.60 for $^{73}$Ge, 13.64 for $^{74}$Ge and 15.70 for $^{76}$Ge. If a different

proton distribution is assumed, the expected spectroscopic strength to the individual subshells will be changed, but the total strength to all the shells will be the same. The values listed above were used to normalize the spectroscopic strengths of each reaction.

From the summed spectroscopic strengths to each subshell, the occupation of the shell (i.e. how full the shell is) was deduced according to:

$$\text{Occupation } (\%) = 100 \times \Sigma S_j^{exp} / S_j^{max} \quad ,$$

where $S_j^{max}$ is the maximum possible strength to shell j, and $\Sigma S_j^{exp}$ is the observed total strength.

From the spectroscopic strength distribution of a particular j shell, one can calculate the single particle energy or center of gravity energy ( $\varepsilon_j$) of that particular shell defined as:

$$\varepsilon_j = \Sigma S_j E_j / \Sigma S_j \quad ,$$

where $S_j$ is the spectroscopic strength to the level of energy $E_j$, and the sum runs over all levels of spin j.

5.2- <u>The $^{70}$Ge(p,d)$^{69}$Ge reaction</u>.

Very little information is available on the $^{69}$Ge level scheme. Fou et. al. (67Fol) established five low-lying levels with the $^{70}$Ge($^3$He,$\alpha$)$^{69}$Ge reaction, and were able to determine $\ell_n$ values and spectroscopic factors to these

levels. Muszynski and Mark (70Mul), in analysing the gamma ray spectra following the beta decay of $^{69}As$, assigned spin and parity to some low lying levels. A $9/2^+$ state at 398 keV was reported by Christiansen et. al. (70Chl) who measured the magnetic moment of that state populated in a $^{69}Ga(p,n)^{69}Ge$ reaction.

Fig. 3 shows the summed Q value spectrum of the reaction, while in Fig. 13 are drawn the deduced angular distributions with their fitted theoretical curves, and Table 4 lists the relevant spectroscopic information obtained. From Fig. 13, it can be seen that the theoretical fits to the most prominent peaks are very good. Since we could not resolve the $9/2^+$ level reported by Christiansen et. al. (70Chl) at 398 keV from the strong $\ell_n = 1$ peak at 379 keV, a mixture of $\ell_n = 1 + 4$ was attempted for that level, yielding a spectroscopic factor of 1.26 for the $\ell_n = 4$ transition, which is in agreement with other results in this mass region. For the transitions to the weaker levels the fits are not as good and the $\ell_n$ assignments are sometimes ambiguous. The 815 kev state which seems to be a multiplet can only be fitted by mixtures of $\ell_n = 1 + 3$ or $\ell_n = 1 + 4$. The 1307 keV state, as well as the 2103 and 2136 keV doublet contain significant amount of $\ell_n = 1$, as is indicated by the forward peaking. Even though the $\ell_n = 3$ fits to the 1417 and 1477 keV levels are not very good, one can rule out $\ell_n = 4$ transfers to

these levels as can be seen by the dotted $\ell_n = 4$ curve drawn for the angular distribution to the 1477 keV level.

In Table 10 our results for the low lying levels of $^{69}$Ge are compared to those of Fou et. al. (67Fol) and Muszynski and Mark (70Mul). There is very good agreement on the level energies, and our $\ell_n$ values to these levels fit very well with the spin and parity assignments of Muszynski and Mark (70Mul). The spectroscopic factors from the ($^3$He,$\alpha$) reaction of Fou et. al. (67Fol) and our (p,d) reaction show similar trends even though they differ in detail. We are able to exclude their tentative $\ell_n = 3$ assignment for pick-up to the 88 keV level.

One can tentatively rule out the possible $\ell_n = 4$ assignment to the 815 keV state since, in the (p,d) reaction on the other even germanium isotopes, the $\ell_n = 4$ strength is concentrated into only one low lying $9/2^+$ level which in $^{69}$Ge has been reported at 398 keV (70Chl). From the apparent small angle j-dependence mentioned above, it seems that the 995 keV level would have a prefered $1/2^-$ spin and parity. This assignment is also in accord with the low lying level scheme of the neighbouring nucleus $^{67}$Zn (67Ehl) which is compared in Fig. 24 to the $^{69}$Ge level scheme. The 815 keV level was assigned a prefered $3/2^-$ spin since it could correspond to the 888 keV level of $^{67}$Zn which has that spin. The 2103 and 2136 keV doublet

was assigned a spin of $3/2^-$ since it is unlikely that the $2p_{1/2}$ strength would fractionate to such high energies.

The summed spectroscopic strengths for the p, f and g shells obtained from the preceding spin assignments are shown in Table 9, along with the center of gravity energies of $^{69}Ge$. From the summed spectroscopic factors the occupation of the different subshells was calculated and is compared in Table 11 to the results of the $^{70}Ge(d,p)^{71}Ge$ reaction of Goldman (68Gol) and to the neighbouring nucleus $^{68}Zn$ studied in the $^{68}Zn(d,p)^{69}Zn$ reaction (67Ehl), where the experimental $\sum_J (2j+1)S_j$ for the (d,p) reactions has been normalized to 12, which is the expected number of holes predicted by the shell model. The last row of Table 11 represents the results obtained in reanalysing Goldman's results (68Gol) by comparing our $^{72}Ge(p,d)^{71}Ge$ reaction to his $^{70}Ge(d,p)^{71}Ge$ reaction as will be discussed in the next section dealing with the $^{72}Ge(p,d)^{71}Ge$ reaction.

From Table 11, one can draw the following conclusions:

a) Since the results of the two (d,p) experiments of row 3 or 4 on $^{68}Zn$ and row 5 on $^{70}Ge$ of Table 11-a give almost identical results for the occupation of each shell, the neutron configuration is affected very little by the addition of two protons to $^{68}Zn$.

b) Since the first and last row of Table 11-a which represent our (p,d) and Goldman's (d,p) respectively disa-

gree significantly only in the occupation of the $2p_{3/2}$ shell, it seems that some $2p_{3/2}$ strength was missed. In view of the poor statistics for this reaction, the missed strength could be in the weak levels for which we could not obtain angular distributions.

c) Since the occupation of the $2p_{1/2}$, $1f_{5/2}$ and $1g_{9/2}$ shells agree so well (probably within the uncertainty of the optical potentials) then their strengths must have been almost completely exhausted in all three experiments. Thus the $2p_{1/2}$ strength appears not to fractionate significantly above 1 MeV and most of the $1f_{5/2}$ strength lies below 2 MeV. The extracted $1g_{9/2}$ strength, obtained by fitting the 379 keV transition with $\ell_n = 1+4$, is consistent with that obtained from the $^{70}Ge(d,p)^{71}Ge$ reaction and seems to be concentrated into only one transition as it will be seen that this is also the case for the other germanium isotopes.

5.3- <u>The $^{72}Ge(p,d)^{71}Ge$ reaction</u>.

Earlier investigations of $^{71}Ge$ were through the beta decay of $^{71}As$ and the $^{70}Ge(d,p)^{71}Ge$ reaction (66Nd1), and the high resolution study of the $^{70}Ge(d,p)^{71}Ge$ reaction by Goldman (68Go1) using a multigap spectrograph showed a high level density at low excitations. In his measurements the excitation energies were determined with an accu-

racy of 10 keV for most of the levels and spins and parities for the stronger transitions were assigned. Measurements with the $^{71}$Ga(p,n) and (p,n$\gamma$) reactions by Malan et. al. (70Mal) at energies between 1.5 and 3.0 MeV, using high resolution neutron and gamma ray spectroscopy confirmed most of Goldman's levels and established several new ones below 2 MeV excitation with an accuracy of 0.5 to 1.0 keV. Recent measurements of the gamma rays following the decay of $^{71}$As (71Mul) confirmed some of the previous levels and also some of the assigned spins and parities.

Fig. 4 shows the summed Q value spectrum of the reaction, while in Fig. 14 are drawn the angular distributions which were obtained with their fitted DWBA curves and Table 5 lists the relevant spectroscopic information which was extracted. As can be seen from Fig. 14, the theoretical fits to the experimental angular distributions are satisfactory and allow unambiguous $\ell_n$ assignments. The poor fit to the second maximum of the 706 kev level is attributed to an incomplete separation, at a few angles, of the 706 ($\ell_n = 1$) and 757 ($\ell_n = 3$) keV peaks which are only partially resolved as can be seen from the summed Q value spectrum of Fig. 4. The spectroscopic factor to the 706 keV level was increased by 40% since it is only for the first two angles that the separation is questiona-

ble. Similarily, an incomplete separation of the 1166 and 1210 keV levels yielded $\ell_n = 1$ plus some admixture of $\ell_n=3$ for the 1166 keV level and $\ell_n=3$ with some forward peaking for the 1210 keV level. So as not to lose any $\ell_n=3$ strength, the two peaks were summed and fitted with a mixture of $\ell_n=1+3$ transfers, assuming the 1166 and 1210 keV states to be populated by pure $\ell_n=1$ and 3 transitions respectively.

Our deduced level energies are compared in Table 12 to those obtained with the $^{71}$Ga (p,n), (p,n $\gamma$) reactions of Malan et. al. (70Mal) and the $^{70}$Ge(d,p)$^{71}$Ge reaction of Goldman (68Gol). With our resolution of 35 to 40 keV we cannot see as much structure as in the other high resolution experiments. In our individual energy spectra, as well as in the summed Q value spectrum, there is no evidence for the 60 keV level reported by Goldman (68Gol). Peaks which were too weak to assign energies were seen between 502 and 706 keV, 807 and 1025 keV, 1595 and 1742 keV, 1966 and 2354 keV and above the 2354 keV peak.

In Table 13 our deduced spectroscopic information is compared to that of the $^{70}$Ge(d,p)$^{71}$Ge reaction of Goldman (68Gol) for levels below 2.5 MeV excitation. For levels which have the same energy, the $\ell_n$ assignments frequently differ but this is understandable since many of Goldman's assignments are doubtful. The 1966 keV state which shows

up as a clear $\ell_n = 0$ in Goldman's data and an unambiguous $\ell_n = 1$ in our data must be a doublet. The 2040 keV state of Goldman which shows as a strong $\ell_n = 1$ transition in his (d,p) experiment is too weakly populated in our work to assign energy or obtain an angular distribution; it is strange that such a state at high excitation should show so strongly in a (d,p) reaction and be very weak in a (p,d) reaction, expecially for pick-up from an almost full $2p_{3/2}$ shell, as is expected at that excitation.

Also shown in Table 13 is the (p,d)/(d,p) ratio of the cross sections for the $\ell_n = 1$ transitions. The spread in values is small and since the ground state has a known $1/2^-$ spin, it seems that an upper limit of 3.2 on the ratio for transitions leading to $1/2^-$ states can be used. With that criterion, the 706 and 1096 keV levels could possibly be $1/2^-$ states, while all the other $\ell_n = 1$ transitions (except the ground state transition) would preferentially be to $3/2^-$ states. If a spin of $1/2^-$ is assigned to the 706 and 1096 keV levels, in accord with Goldman's assignment based on the Lee-Schiffer effect and the (p,d)/(d,p) ratio, then the summed spectroscopic strength of 1.56 to the $2p_{1/2}$ shell does not agree with that of the other germanium isotopes as can be seen in Table 9; furthermore, Hauser-Feshbach calculations for the $^{71}Ga(p,n)^{71}Ge$ reaction of Malan et. al. (70Mal) yield a prefered $3/2^-$ spin for these

two levels, in accord with a more recent assignment based on the analysis of the gamma rays following the beta decay of $^{71}As$ (71Mul). These two levels were therefore assigned a spin of $3/2^-$. The 502 keV level cannot be assigned a $1/2^-$ spin since it would more than completely exhaust the available $2p_{1/2}$ strength; moreover, a spin of $3/2^-$ is favored from the systematics of that transition which appears as the strongest in all our (p,d) reactions and was identified as a $2p_{3/2}$ neutron pick-up in the $^{70}Ge(p,d)^{69}Ge$ reaction. This assignment agrees with the Hauser-Feshbach calculation of Malan et. al. (70Mal) and with the recent work of Murray et. al. (71Mul); it is strange that it disagrees with Goldman's assignment based on the Lee-Schiffer effect from which there is good evidence for a $1/2^-$ state.

In the last column of Table 13 is presented a reanalysis of Goldman's data using his tabulated maximum cross sections with our assigned $\ell_n$ transfers and spins. These results are listed in the last row of Table 11-a. His data, when analysed in this way, was previously shown to be in good agreement with the results from our $^{70}Ge(p,d)^{69}Ge$ reaction.

The summed spectroscopic strengths to the different subshells on the basis of the spin assignments of Table 5 are shown in Table 9, along with the single particle energies of $^{71}Ge$. From the summed spectroscopic factors, the occupation of the different subshells was deduced and are com-

pared in Table 14 to that of the neighbouring nucleus $^{70}$Zn (67Eh1) which has the same number of neutrons; in the same table the center of gravity energies are compared to Goldman's results (68Go1) and to those of $^{69}$Zn (67Eh1). The reanalysis of Goldman's data, as described previously, is in better agreement with our results for the center of gravity energies of $^{71}$Ge, even though there is still a large discrepancy for the $1f_{5/2}$ shell. It is seen that the addition of two protons to $^{70}$Zn to produce $^{72}$Ge, leaves the occupation of the $2p_{3/2}$ and $1f_{5/2}$ shells essentially unaltered, while that of the $2p_{1/2}$ shell is increased at the expense of the $1g_{9/2}$ shell.

5.4- The $^{73}$Ge(p,d)$^{72}$Ge reaction.

$^{72}$Ge, the residual nucleus of the $^{73}$Ge(p,d)$^{72}$Ge reaction has been extensively studied because of the anomalous low energy of its $0^+$ first excited state. Earlier investigations of the level scheme of that nucleus are summarized in Ref. 66Nd1. More recent high resolution studies of the gamma rays following the beta decay of $^{72}$As and $^{72}$Ga (68Ca1, 68Ot1, 71Re1, 71Re2) as well as proton (70Cu1) and deuteron (67Kr1) inelastic scattering experiments on $^{72}$Ge have extended the level scheme to approximately 4 MeV excitation and shown its complexity. The spin and parity of most of the levels seen in the preceding experiments have been

limited to two values.

There has been much speculations to understand the nature of the low lying levels of $^{72}Ge$, especially the anomalous $0^+$ first excited state. Even though some of the low excited states can be qualitatively interpreted as arising from a simple vibrator (71Re2), the $0^+$ first excited state seems to be of a single particle nature (69Mol, 56Br1). Kregar and Mihailovic (67kr2) have applied the Davydov (61Da1) non-adiabatic model and found the ground and first excited $0^+$ state to be prolate and oblate ellipsoids respectively.

Fig. 5 shows the summed Q value spectrum of the reaction, while in Fig. 15 the calculated angular distributions are drawn with their fitted DWBA curves and Table 6 lists the spectroscopic information extracted. In Fig. 25 our energy levels are compared to those of Camp (68Ca1) and Rester et. al. (71Re1, 71Re2). The agreement between their proposed level schemes and our observed energies is satisfactory even though our resolution does not allow us to see as much structure as in their high resolution gamma ray spectroscopy. The position of the first $0^+$ excited state at 691 keV is indicated in Fig. 5 by the arrow labelled $0^{+\prime}$, and from the present measurements, the transition to that level is estimated to be less than 0.5% of the ground state transition strength. The

2505 keV level is an unresolved doublet corresponding probably to the 2464 and 2515 keV levels of Camp (68Cal), and from our energy spectra there is evidence for a very weak peak at approximately 2.4 MeV which would correspond to the 2402 keV level of Camp. We do not see the 3094 keV level of Camp and Rester et. al. but instead see a closely spaced doublet at 3077 and 3119 keV. Since the 3035, 3077 and 3119 keV levels form a partially unresolved and weakly excited triplet, our energy assignment to these levels is not very accurate and it is possible that our 3077 keV level corresponds to their 3094 keV state. The 3119 keV ($\ell_n = 1$) peak must correspond to a level in $^{72}$Ge since it is different from the 457 keV ($\ell_n = 3$) level from the $^{76}$Ge(p,d)$^{75}$Ge reaction which has the same Q value, and cannot be attributed to levels from the other germanium impurities since their ground state Q values are more negative than that of the 3119 keV level. We see levels at 3235, 3398 and 3965 keV which are missing in the decay schemes of Camp and Rester et. al. These three levels overlap with levels from the other germanium isotopes present in the target as impurities and after correction, there still remains a strong enough cross section to attribute them as transitions to levels in $^{72}$Ge. In order to rule out the possibility of these new levels as arising

from incomplete impurity subtraction due to large errors in the quoted target composition, the $^{73}Ge(p,t)^{71}Ge$ reaction in which the ground state peaks from all the germanium isotopes are seen and well separated, along with the (p,t) reaction data on the other germanium isotopes, were used to calculate the impurity contents of the target. That calculation yielded the following isotopic composition: 2.9 to 3.6% of $^{70}Ge$, 9.6 to 11.1% of $^{72}Ge$, 77.7 to 73.4% of $^{73}Ge$, 9.1 to 10.8% of $^{74}Ge$ and 0.8 to 1.0% of $^{76}Ge$. These numbers are in good agreement with the manufacturer's quoted composition of Table 1, and the observed additional levels must be levels of $^{72}Ge$. These levels at 3077, 3119, 3235, 3398 and 3965 keV which are missing from the decay schemes of Camp and Rester et. al. cannot be reasonably accounted for by their unplaced gamma rays. It could be that these levels are high spin states which would be weakly populated in the beta decay of $^{72}As$ or $^{72}Ga$ and also by the gamma decay from higher levels in $^{72}Ge$ with low spins. We cannot confirm the 3419, 3439 and 3455 keV triplet of Camp and Rester et. al. since it overlaps the first excited state from the $^{74}Ge(p,d)^{73}Ge$ reaction which accounts for approximately 80% of the cross section to that peak. Our 3659 keV peak seems to confirm Camp's doubtful level at 3667 keV. Many levels were observed above 4.5 MeV excitation but they

were partially unresolved and too weak to attempt energy assignments.

The apparent strong background in the summed Q value spectrum (Fig. 5) which starts to increase rapidly at the 2754 keV peak (peak No. 7) is attributed to the overlapping of many weak peaks due to the high level density above the 2754 keV level. No three body breakup process could explain the position at which this apparent background starts. The low lying even parity levels (up to 2.05 MeV) are weakly populated since they correspond to $\ell_n = 2$ or 4 transfers which quickly exhaust the available spectroscopic strength of these shells (total strength of 3 for $\ell_n = 4$); in contrast, from the work of Camp and Rester et. al., most levels at higher excitation energy are of negative parity and are expected to be strongly populated since they correspond to $\ell_n = 1$ or 3 transfers for which the available spectroscopic strength is 4 and 6 respectively.

From Fig. 15, it is seen that the fits to the angular distributions are acceptable and allow, in most cases, unambiguous $\ell_n$ assignments. The angular distributions to the partially unresolved 3754 and 3804 kev doublet which both showed admixtures of $\ell_n = 1+3$ or $\ell_n = 1+4$ transfers were added together so as not to loose any $\ell_n = 3$ or 4 strength. It is not possible to distinguish unambiguously

between $\ell_n = 1+3$ and $\ell_n = 1+4$ transfers for the 3398, 3659, 4339 and the 3754 + 3804 keV doublet. $\ell_n = 1+4$ transfer was assigned only to the 3754 + 5804 keV doublet since the other peaks do not seem to be doublets.

Since the target ($^{73}$Ge) ground state spin is $9/2^+$, selection rules allow population of the following states in the final nucleus: $4^-$ and $5^-$ for $2p_{1/2}$ pick-up, $3^-$ to $6^-$ for $2p_{3/2}$ pick-up, $2^+$ to $7^+$ for $2d_{5/2}$ pick-up, $2^-$ to $7^-$ for $1f_{5/2}$ pick-up and $0^+$, $2^+$, $4^+$, $6^+$, $8^+$ for $1g_{9/2}$ pick-up. It is seen that no $1^\pm$ states can be populated. Applying these selection rules, one can see that our $\ell_n$ transfers are in good agreement with the proposed spins and parities of Camp and Rester et. al. ( See Fig. 25). The $1^+$, $2^+$, $3^+$ possible spin assignments of Rester et. al. to the 2754 keV level disagree with our observed $\ell_n = 1$ transfer to that level. Our 2936 keV ($\ell_n = 3$) would most probably correspond to the 2943 keV ($3^-$) level of Camp and Rester et. al. Our $\ell_n = 1+4$ assignment to the 3754 and 3804 keV doublet is not in agreement with the proposed spins of Camp and Rester et. al. since they report no positive parity levels in that region.

The summed spectroscopic strengths (unnormalized) to the different subshells is 2.08, 5.06, 2.78 and 0.06 for the $1g_{9/2}$, $1f_{5/2}$, $2p_{3/2} + 2p_{1/2}$ and $2d_{5/2}$ shells respectively with a total sum of 9.98. To take into

account the missed and non-negligible strength to the numerous unresolved excited states above 4.5 MeV, the area from 4.5 to 5.5 MeV was summed in each spectrum and the angular distribution which was obtained is shown in Fig. 26. The angular distribution was best fitted with a mixture of $\ell_n = 1 + 3 + 4$ with respective spectroscopic factors of 0.6, 1.2 and 1.2. This brings the spectroscopic strength distribution to 3.28, 6.26, 3.38 and 0.06 for the $1g_{9/2}$, $1f_{5/2}$, $2p_{1/2} + 2p_{3/2}$ and $2d_{5/2}$ shells respectively with a total sum of 12.98. Most of the available spectroscopic strength is then exhausted but there now seems to be too much $\ell_n = 3$ and 4, and too little $\ell_n = 1$ strength. This seems to indicate that some $\ell_n$ values have been wrongly assigned, which is quite probable in view of our poor resolution as compared to the high level density.

The strong $\ell_n = 1$ transition which was seen at low energy in the two preceding reactions, and was identified as a $2p_{3/2}$ neutron pick-up, is expected to fractionate into four relatively strong $\ell_n = 1$ transitions, corresponding to the population of the various states of the configuration $\left[2p_{3/2}^{-1} \times {}^{73}Ge^{gs.}_{9/2^+}\right]$ $3^-$, $4^-$, $5^-$, $6^-$. Similarily, the strong $\ell_n = 3$ transition observed to the ground state of $^{69}Ge$ and to the 186 keV level of $^{71}Ge$ is also expected to fractionate to the various members of the configuration $\left[1f_{5/2}^{-1} \times {}^{72}Ge^{gs.}_{9/2}\right]$ $2^-$, $3^-$, $4^-$, $5^-$, $6^-$, $7^-$.

The spectroscopic strength to the different spin states should be distributed in a $(2I+1)$ fashion, where I is the spin of the final state. In Table 15 are shown the strongest $\ell_n = 1$ and 3 transitions taken from Table 6. The 3035 keV level is populated by a pure $\ell_n = 3$ transfer, in agreement with the $2^-$ spin assignment of Camp and Rester et. al. to that level. The small spectroscopic factor for that transition makes that level a good candidate for the lowest member of the $\left[1f_{5/2}^{-1} \times {}^{73}Ge^{gs.}_{9/2^+}\right]$ $2^-$, $3^-$, $4^-$, $5^-$, $6^-$, $7^-$ configuration. The 3890 keV level is also populated by a pure $\ell_n = 3$ transfer and its large spectroscopic factor makes it a good candidate for the $7^-$ highest member of the same configuration. This high spin assignment is also in agreement with the fact that this level is missing in the decay schemes of Camp and Rester et. al. Also shown in the same table are the renormalized spectroscopic factors $S_\ell / \Sigma S_\ell$, assuming that the 3398, 3659, 4047 and 4339 keV levels are the members of the $\left[2p_{3/2}^{-1} \times {}^{73}Ge^{gs.}_{9/2^+}\right]$ $3^-$, $4^-$, $5^-$, $6^-$ for the $\ell_n = 1$ transitions and the two additional levels at 3035 and 3890 keV are the additional $2^-$ and $7^-$ members of the $1f_{5/2}$ neutron hole coupled to the $^{73}Ge$ ground state. A sequence of spin assignments is proposed and the normalized values of $(2J+1)/40$ for the spins of $3^-$, $4^-$, $5^-$, $6^-$ and $(2J+1)/60$ for the spins of $2^-$, $3^-$, $4^-$, $5^-$, $6^-$, $7^-$ can be com-

pared to the experimental values. There is a good agreement for the $\ell_n = 1$ normalized strengths. The poor agreement on the $\ell_n = 3$ strength distribution is attributed to the fact that these levels are fitted with a mixture of $\ell_n = 1 + 3$, where the $\ell_n = 1$ strength is well determined by the first maximum while the $\ell_n = 3$ component is not; a small fitting error will not affect the $\ell_n = 1$ strength considerably while the $\ell_n = 3$ will be. It must be noted that the proposed spins are only very tentative and it is amazing that such a simple model fits so well with the experimental data. Similar results would be expected with the configuration $\left[2p_{1/2}^{-1} \times {}^{73}Ge^{gs.}_{9/2^+}\right] 4^-, 5^-$, but the cross sections would be much smaller in this case, and the two members would be hard to identify amongst the many weaker transitions seen.

## 5.5- The $^{74}Ge(p,d)^{73}Ge$ reaction.

Earlier investigations of the low lying levels of $^{73}Ge$ were mainly confined to the analysis of the gamma rays following the beta decay of $^{73}As$ and $^{73}Ga$ (66Nd1); (d,p) experiments extended the level scheme up to 3.95 MeV (66Nd1). More recently Heymann et. al. (69Hè1) identified 37 levels using the $^{72}Ge(d,p)^{73}Ge$ reaction and 19 levels using the $^{73}Ge(p,p')^{73}Ge$ reaction; $\ell_n$ values as well as spin and parities were assigned to the stronger (d,p) transitions.

Fig. 6 shows the summed Q value spectrum of the reaction, while in Fig. 16 the angular distributions are drawn with their fitted theoretical curves and Table 7 lists the relevant spectroscopic information deduced. Again, the fits to the angular distributions are satisfactory and allow many unambiguous $\ell_n$ assignments. The first angular distribution corresponds to the unresolved ground state ($9/2^+$, $\ell_n = 4$) and 13.5 keV ($5/2^+$, $\ell_n = 2$) while the third corresponds to the unresolved 363 and 392 keV doublet of Ref. 66Nd1.

In Table 16 our results are compared to those of Heymann et. al. (69He1) and to the energies of Ref. 66Nd1 with the spins of Ref. 70Ky1 for the low lying states. Below 0.7 MeV there is good agreement between the four results for the excitation energy of the levels. In our spectra, there is no evidence for the 67.03 keV level ($7/2^+$) of Ref. 66Nd1 which is most probably of a collective nature and is expected to be weakly populated in a (p,d) reaction. The 396 keV level of Heymann et. al. for which no $\ell_n$ assignment is given, is seen from their published spectrum (peak No. 4) to be stronger than the 562, 666 and 864 keV levels; it is strange that such a strong peak was left out of their analysis. Our $\ell_n = 2$ assignment to the 494 keV level, which fits the data poorly, is in agreement with the $\Delta\ell = 2$ assignment of Heymann et. al.

from their (p,p') reaction leading to that level (their 498 keV level), and in disagreement with the $\ell_n = 1$ assignment from their (d,p) reaction to the corresponding 512 keV level which is seen to be poorly fitted by their published curves. The $\ell_n = 3$ assignment to the 666 keV level seen in their (d,p) reaction is questionable since it should be much stronger in a (p,d) reaction, and from our spectra, we only have weak evidence for a peak at that position; that assignment is also in disagreement with the $\Delta\ell = 2$ assignment from their (p,p') reaction data. Our 1261 keV level which has a clear $\ell_n = 1$ stripping pattern cannot correspond to the 1274 keV level of Heymann et. al. which is clearly an $\ell_n = 0$ transition in their (d,p) reaction. Similarily our 1610 ($\ell_n = 3$) and 1653 ($\ell_n = 1$) keV levels must be distinct from their 1617 ($\ell_n = 2$) and 1646 ($\ell_n = 2$) keV levels since they are populated so strongly in the (d,p) reaction. Several weak and partially unresolved peaks were seen in our deuteron spectra between the 1744 and 2030 keV levels; we do not see the strong $\ell_n = 1$ transition of Heymann et. al. to their 1936 and 1983 keV levels which should be populated even stronger in a (p,d) reaction if they are $2p_{3/2}$ states. Above 2 MeV our energy levels are expected to be different from the (d,p) since the (p,d) reaction preferen-

tially populates levels for which $\ell_n = 1$ and 3, while the (d,p) tends to populate levels via $\ell_n = 0$ and 2. Table 16 also lists the (p,d)/(d,p) ratio for the $\ell_n = 1$ transitions, which allows to assign a spin of $1/2^-$ to the 63 and 897 keV levels and a spin of $3/2^-$ to the 370 and 1039 keV levels. The other $\ell_n = 1$ transitions were assigned a $3/2^-$ spin because these levels are either not seen or too weak in the (d,p) reaction. These spin assignments do not agree with Heymann et. al.'s assignment of a spin $1/2^-$ to the lower excited levels and $3/2^-$ to the higher ones. Our $3/2^-$ assignment to the 370 keV level is in agreement with the observed systematics of that strong $\ell_n = 1$ transition observed in the other spectra and previously identified as a $2p_{3/2}$ neutron pick-up.

The high value of 0.51 for the total $\ell_n = 2$ spectroscopic strength seen in this reaction is not reliable, since it mostly comes from the ground state transition which was fitted by a mixture of $\ell_n = 2 + 4$, but which is just resolved from the strong $\ell_n = 1$ transition to the 63 keV level, so that some of the small angle contributions to the ground state peak may come from the 63 keV peak; the other $\ell_n = 2$ strength mainly comes from the 494 keV level which is seen to be poorly fitted by an $\ell_n = 2$.

The summed spectroscopic strengths for the different subshells of $^{74}$Ge is listed in Table 9, along with the

center of gravity energies of $^{73}$Ge. From the summed spectroscopic factors, the occupation of the different subshells was deduced and is compared in Table 17 to that of the neighbouring nucleus $^{76}$Se (65Lil); in the same table, the center of gravity energies of $^{73}$Ge are compared to those of $^{71}$Zn (67Ehl). The poor agreement on the shell occupation of $^{74}$Ge and $^{76}$Se is probably due to the high occupation (upper limit) found for the $1g_{9/2}$ shell in $^{76}$Se; by lowering the occupation of that shell, the occupation of the other shells will increase, which would be in better agreement with our results. There is a relatively good agreement on the center of gravity energies except for the $2p_{1/2}$ shell which is much lower in $^{71}$Zn than in $^{73}$Ge.

5.6- <u>The $^{76}$Ge(p,d)$^{75}$Ge reaction</u>.

The only available information on the $^{75}$Ge level scheme is from the $^{74}$Ge(d,p)$^{75}$Ge reaction and through the analysis of the gamma rays following the beta decay of $^{75}$Ga (66Ndl). There is no spin parity assignment to these levels except for the ground state spin whose $1/2^-$ value has been measured recently (70011) and a possible $7/2^+$ spin for the 48 sec. isomeric state at 139 keV (66Ndl).

Fig. 7 shows the summed Q value spectrum of the reaction while in Fig. 17 the angular distributions are drawn

with their fitted theoretical curves, and Table 8 lists the spectroscopic information extracted. In Table 18, our energy levels are compared to those of Ref. 66Nd1. In our spectra, there is no evidence for the 62 keV level of Ref. 66Nd1, which should be resolved from the ground state; there is evidence for a weak peak at 140 ± 20 keV which is partially unresolved from the strong 197 keV peak. There is no evidence for the 360 keV level of Ref. 66Nd1 and our peak at 457 keV which is a weak $\ell_n = 3$ transition is expected to be much weaker in a (d,p) experiment from which most of the levels of Ref. 66Nd1 were determined. Above 1 MeV excitation, there is little agreement between the two level schemes; this is probably due to the fact that $\ell_n = 0$ and 2 transitions are favored in the (d,p) reaction in this mass region, while the (p,d) will preferentially pick-up neutrons from the p and f shells. The 2043 and 2105 keV levels are seen as two distinct peaks to which we can assign accurate excitation energies; the angular distribution of the 2043 keV level had an $\ell_n = 1$ shape, while that of the 2105 keV had a $\ell_n = 3$ stripping pattern with some forward peaking. Since the non negligible contribution from 6 impurities had to be substracted in this region, the area under the two peaks was summed at each angle, then corrected for the impurities and the

resultant angular distribution was fitted with a mixture of $\ell_n = 1$ and 3. The known $1/2^-$ ground state spin is in agreement with the small angle j-dependence mentioned before. In Fig. 27, the low lying levels of $^{75}$Ge are compared to those of $^{77}$Se obtained from the $^{76}$Se(d,p)$^{77}$Se reaction of Lin (65Lil); it is seen that our 250 keV level can either have a $1/2^-$ or $3/2^-$ spin. Our $3/2^-$ assignment to the 574 keV level based on the systematics of that strong transition is in agreement with the spectroscopic sum rules since if it was a $1/2^-$ state, the combined strength to that level and the ground state would more than exhaust the available spectroscopic strength of 2 for a $2p_{1/2}$ shell. A $3/2^-$ spin was assigned to the 899 keV level on the assumption that it corresponds to the 830 keV level of $^{77}$Se. For higher excitation energies, a $3/2^-$ spin assignment to all the $\ell_n = 1$ transitions was made on the basis of the shell model.

The summed spectroscopic strengths for the different subshells of $^{76}$Ge is listed in Table 9, along with the center of gravity energies of $^{75}$Ge. From the summed spectroscopic factors, the occupation of the different subshells was deduced and is compared in Table 19 to that of the neighbouring nucleus $^{78}$Se; In the same table, the center of gravity energies of $^{75}$Ge are compared to those of $^{77}$Se. On comparing the $2p_{1/2}$ and $2p_{3/2}$ shell occupation

of $^{76}$Ge and $^{78}$Se, it appears that we have too much $2p_{3/2}$ strength and too little $2p_{1/2}$ strength. This seems to indicate that the 889 keV level could possibly be a $1/2^-$ level rather than $3/2^-$ as assigned; the center of gravity energies also suggest this. As for the $1f_{5/2}$ shell, the Se data is not very reliable since Lin (65Lil) reports only one $\ell_n = 3$ transition in his (d,p) reaction and from our data it is known that the $1f_{5/2}$ spreads significantly to higher excitations.

5.7- The $^{70}$Ge(p,t)$^{68}$Ge reaction.

When this work was started, no excited states in $^{68}$Ge were known and only estimates of its mass excess were available. Recently, the energy of three levels in $^{68}$Ge was measured in an analysis of the gamma rays following heavy ion bombardment of the nickel isotopes (70Nol). Paradellis et. al. (71Pal), in a more recent analysis of the gamma rays following the beta decay of $^{68}$As populated in the $^{70}$Ge(p,3n)$^{68}$As reaction, have proposed a decay scheme of $^{68}$Ge which contains 10 excited states.

Six excited states were identified in the summed Q value spectrum of Fig. 8 and they are listed in Table 20 along with the results of Nolte et. al. (70Nol) and Paradellis et. al. (71Pal). Of these, three were strong enough to appear at all angles, and the angular distributions of these three levels are shown in Fig. 18, along

with the DWBA predictions assuming a pure $(1f_{5/2})^2$ (solid line) and a $(1g_{9/2})^2$ (dotted line) neutron configuration for L = 0, 2 and 4, and a $(1f_{5/2}, 1g_{9/2})$ neutron configuration for L = 3.

It is seen that the $(1f_{5/2})^2$ and $(1g_{9/2})^2$ configurations fit the data equally well and one cannot distinguish between these two transitions. Since the DWBA predictions are very sensitive to the choice of optical parameters, one cannot assign a definite L transfer to the 2648 keV level which can be a L = 3 or 4, or a doublet with both components present. From an other point of view, pick-up of $(1g_{9/2})^2$ and $(1f_{5/2}, 1g_{9/2})$ neutron pairs can be assumed to be very small since between N = 36 and 38, the $1g_{9/2}$ shell has not started to fill, while the $1f_{5/2}$ shell is filling rapidly as can be seen in Figs. 29 and 31 which show the shell filling in this mass region and will be discussed later. An L = 4 assignment to the 2648 keV level thus seems more probable than L = 3.

No excited $0^+$ state was seen and an upper limit of 2% of the ground state intensity can be established for a $0^+$ excited state below 3 MeV.

The absolute Q value of the $^{70}Ge(p,t)^{68}Ge$ reaction was obtained by a careful comparison of the ground state triton peak with the $^{27}Al(p,d)^{26}Al$ calibration peaks. Since the mass excess of $^{70}Ge$ is accurately known, this

measurement yields a mass excess of -66.969 ± 0.013 MeV for $^{68}$Ge. This new value is in much better agreement with mass systematics than the previous estimate.

5.8- The $^{72}$Ge(p,t)$^{70}$Ge reaction.

Kregar and Elbek (67Kr1) investigated the low lying levels of $^{70}$Ge with the (d,d′) reaction and suggested that $^{70}$Ge and $^{72}$Ge might be slightly deformed in their ground state. The studies of Brown et. al. (67Br1), Van Patter et. al. (68Pa1), de Ruiter et. al. (68Ru1) and Hinrichsen et. al. (69Hi2) extended the level scheme up to approximately 5.5 MeV, proposing spins and parities to most of the levels.

We observe 14 excited states of $^{70}$Ge in the summed Q value spectrum of Fig. 9, and they are listed in Table 21, along with the results of Hinrichsen et. al. (69Hi2). Of these, 12 were strong enough to obtain angular distributions, and L assignments were attempted to most of them. Fig. 19 shows the angular distributions with the fitted DWBA predictions. For the ground and first excited state, pick-up of pure $(1g_{9/2})^2$ (solid line) and $(1f_{5/2})^2$ (broken line) neutron pairs were assumed. It is seen that the $(1g_{9/2})^2$ neutron configuration fits the data better, as is expected, since the $1g_{9/2}$ shell is now filling rapidly while the $1f_{5/2}$ shell is almost full as can be verified

from Figs. 29 and 31. For the other excited states, pick-up of $(1g_{9/2})^2$ and $(1f_{5/2}, 1g_{9/2})$ neutron configurations were assumed for even L and odd L, respectively. For states above 2.5 MeV, it is impossible to make unambiguous L assignments. This could be attributed to the fact that the states we observe above that energy are most probably unresolved multiplets due to our poor resolution as compared to the high level density in that region. Our L assignments to the transitions below 2.5 MeV are in agreement with the previously known spins of these levels as can be verified from Table 21.

## 5.9- The $^{73}Ge(p,t)^{71}Ge$ reaction.

Seven excited states were identified in the summed Q value spectrum of Fig. 10; they are listed in Table 22 and compared in Table 13 to the previously measured energy levels of $^{71}Ge$. Five transitions were strong enough to obtain angular distributions and they are shown in Fig. 20 along with the DWBA predictions assuming the pick-up of a $(1g_{9/2})^2$ neutron pair for even L and $(1f_{5/2}, 1g_{9/2})$ neutron pair for odd L.

Unambiguous L = 0 transitions were observed to the 198 and 1038 keV levels of $^{71}Ge$; the first is in agreement with the $9/2^+$ spin assignment from the $^{72}Ge(p,d)^{71}Ge$ reaction to the corresponding 186 keV level, while the

second is in disagreement with our observed $\ell_n = 2$ transition to the corresponding level populated in the (p,d) reaction, and also in disagreement with the proposed $3/2, 5/2^-$ possible spin assignments of Malan et. al. (70Mal) to their 1.03 MeV level. Even though there is a poor $\ell_n = 2$ fit in the (p,d) reaction to that level (1025 keV level of Fig.14), a $\ell_n = 4$, as would be required to have agreement, would clearly be unacceptable.

It is impossible to distinguish between L = 2 and L = 3 for the transition to the 515 keV level; an L = 2 assignment would agree with the observed $\ell_n = 2$ transition to this level seen in the $^{70}Ge(d,p)^{71}Ge$ reaction of Goldman (68Gol). In our energy spectra, the 1183 keV peak seems to be a doublet and probably corresponds to the unresolved 1166 and 1210 kev levels seen in our (p,d) reaction. An unambiguous L assignment to this transition is not possible and both L = 2 and L = 3 seem to be present. It is therefore impossible to confirm our $\ell_n = 1$ and 3 assignment to these two levels which were obtained in our (p,d) reaction measurements or to confirm Goldman's (68Gol) $\ell_n = 2$ assignment to these two levels from his (d,p) reaction data. The 1955 keV peak also appears to be a doublet and may correspond to the unresolved 1940 and 1960 keV levels of Goldman (68Gol); again, it is impossible to make an unambiguous L assignment to this transition.

5.10- The $^{74}Ge(p,t)^{72}Ge$ reaction.

In this reaction, 12 levels in $^{72}Ge$ were identified from the summed Q value spectrum of Fig. 11; they are listed in Table 23, and compared in Fig. 25 with our previous results of the $^{73}Ge(p,d)^{72}Ge$ reaction and with the proposed level schemes of Camp (68Cal) and Rester et. al. (71Rel, 71Re2). There is good agreement on the level energies deduced from the (p,t) and the (p,d) reactions; furthermore, these new results seem to confirm our previous levels at 3077 and 3119 keV which were missing, as discussed previously, in the decay scheme of Camp (68Cal) and Rester et. al. (71Rel, 71Re2). Angular distributions could be obtained for only 7 levels and they are shown in Fig. 21 along with the calculated DWBA curves for the assumed pick-up of $(1g_{9/2})^2$ and $(1g_{9/2}, 1f_{5/2})$ neutron pairs for even L and odd L, respectively. The L assignments to the ground state, the 690, 835, 1465 and 2513 keV levels are consistent with the previously proposed spins of these levels ( Fig. 25); it is however impossible to make a definite L assignment to the transitions to the 3323 and 3411 keV levels.

5.11 The $^{76}Ge(p,t)^{74}Ge$ reaction.

The level scheme of $^{74}Ge$ has been recently investigated by Camp et. al. (71Cal) in a high resolution study of the gamma rays following the beta decay of $^{74}Ga$. The

same paper also contains a summary of previous studies of $^{74}Ge$.

We observe 15 excited states in the summed Q value spectrum of Fig. 12 and our deduced energies are compared in Table 24 to those of Camp et. al. (71Cal). With few exceptions, the energies are in good agreement and we confirm most of their levels below 3.6 MeV; the region between 1479 and 2181 keV is masked by other germanium impurities so it is impossible to confirm their levels in that region. On the other hand, there is no evidence for any of the new levels suggested by Moreh et. al. (70Mol) at 1717, 2229 and 2600 keV.

Seven peaks were strong enough to be resolved at all angles and their angular distributions are shown in Fig. 22 along with the predicted DWBA curves calculated assuming the pick-up of a $(1g_{9/2})^2$ neutron pair for even L and a $(1g_{9/2}, 1f_{5/2})$ neutron pair for odd L. The ground and first excited states are well fitted by L = 0 and 2 respectively, while the other angular distributions, which are much weaker, are poorly fitted. It is impossible to distinguish between L = 2 and 3 or L = 3 and 4 for these weakly excited levels so that no additional spin information can be deduced from the present measurements.

## 6.- DISCUSSION.

The results of the (p,d) investigations on the even germanium isotopes are summarized in Fig. 32 which shows the spectroscopic strength distribution to each residual nucleus. On the horizontal axis is shown the excitation energy in the residual nuclei, and on the vertical axis is plotted the spectroscopic factor for the three transfered $\ell_n$ values of interest.

For the $\ell_n = 1$ transitions, the bold lines represent $1/2^-$ final spin states, while the thinner lines are the $3/2^-$ spin states. It is seen that the $\ell_n = 1$ transfer is characterized by two strong transitions at low excitations: One to a $1/2^-$ level and a much stronger one to a $3/2^-$ level at approximately 0.5 MeV. The $\ell_n = 3$ transfer is characterized by a single strong transition to a state below 0.5 MeV except in $^{75}$Ge, where the strength seems to fractionate into three levels. The systematics of the $\ell_n = 4$ transfer are simple in that only one transition is observed which carries almost all of the available spectroscopic strength. It thus seems that these 4 transitions must be to good single particle states since they account for most of the available single particle strengths.

In Figs. 28 to 31 our extracted information on the occupation and center of gravity energies of the four

subshells of interest has been collected and compared to other available data in this mass region: the Ni data was taken from the work of Turkiewicz et. al. (70Tul), the Zn data from the work of von Ehrenstein et. al. (67Eh1), the Se data from the work of Lin (65Li1), and the As data comes from our analysis of the $^{75}As(p,d)^{74}As$ reaction (71Fo1). The two curves drawn represent pairing calculations which will be discussed later. As can be seen from these figures, there is an overall good agreement between all these data on the shell filling and center of gravity energy of the different subshells. The only major discrepancy is in the center of gravity energy of the $1f_{5/2}$ shell (Fig. 29), where it is seen that the selenium single particle energy is much lower than in germanium. This is attributed to the fact that Lin (65Li1) reports only one low energy $\ell_n = 3$ transition in his $^{76,78}Se(d,p)^{77,79}Se$ reactions, while from our (p,d) reactions, which are more sensitive in detecting $1f_{5/2}$ strength since the shell is almost full, we know that the $1f_{5/2}$ strength spreads considerably to higher excitations. By this type of comparison, it was hoped to detect the effect of the short range p-n force: In comparing Ni and Zn, Zn and Ge, or Ge and Se the addition of two protons (mainly $2p_{3/2}$ and $1f_{5/2}$) in going from one isotope to the other should cause the center of gravity

energies of the $2p_{3/2}$ and $1f_{5/2}$ shells to be much higher in Se, Ge or Zn than in Ge, Zn or Ni, respectively, due to the added p-n interaction in these two shells. In view of the good agreement on the occupation and center of gravity energy of these two shells, except for the discrepancy discussed previously, one must conclude that either this type of data is not sensitive enough to detect the effect of the short range p-n force or that the short range force is weak in this mass region.

The occupation numbers and center of gravity energies of the $2p_{3/2}$ and $1f_{5/2}$ shells are almost identical as can be seen by comparing Fig. 28 and 29, indicating that these two shells are very closely spaced; the agreement is even better for the $2p_{1/2}$ and $1g_{9/2}$ shells which must therefore be also very closely spaced.

Another interesting result from the (p,d) reactions is the observed $\ell_n = 2$ transitions with total spectroscopic strengths of 0.09, 0.06 and 0.05 to $^{71,72,75}$Ge, respectively. These values indicate that the probability of finding a $(2d_{5/2})^2$ neutron pair in the ground state wave functions of $^{72,73,76}$Ge is approximately 2% to 5%, indicating that the shell closure at N= 50 is very good. These results are in good agreement with the results of the $^{90}$Zr(p,d)$^{89}$Zr reaction studied by Ball et. al. (68Bal).

The systematics of the transitions to the low

lying levels populated in the (p,t) reactions on the even germanium isotopes are presented in Fig. 33, where the cross sections indicated for L=0 and 2 transfers are the experimental cross sections measured at the second maxima and first maximum, respectively. The transitions to the ground states and to the first excited $2^+$ states do not differ markedly from one isotope to another. The experimental relative ratio of 90/100/80/80 for the ground state to ground state transition to $^{68}Ge/^{70}Ge/^{72}Ge/^{74}Ge$ is in good agreement with the calculated DWBA ratio of 64/100/86/73 which is obtained by assuming the pick-up of a $(1f_{5/2})^2$ neutron pair for the $^{70}Ge(p,t)^{68}Ge$ reaction and a $(1g_{9/2})^2$ neutron pair for the other (p,t) reactions. For the $2^+$ first excited states, the relative experimental ratio of 59/100/90/100 is to be compared with the calculated ratio of 55/100/140/190. The transition strength to the first excited $0^+$ state varies considerably, and is anomalously strong to $^{72}Ge$, indicating that the nature of that state is very different from that of the corresponding first $0^+$ excited state in neighbouring $^{70}Ge$ and $^{74}Ge$. Except for that anomalously strong transition, the weak transition strengths to the other first excited $0^+$ levels, the second excited $2^+$ and first $4^+$ levels are in good agreement with a vibrational model description for the germanium isotopes. In that model members of the two

phonon triplet are forbidden to a 2 nucleon transfer reaction since they are described as 4 quasi particle states. They can, however, be reached by a two step process as described by Glendenning (69Gl1). However, measurements by Darcey (64Dal) on the $^{72}Ge(t,p)^{74}Ge$ reaction showed that the transition to the first excited $0^+$ level in $^{74}Ge$ has a transition strength of approximately 30% of that of the ground state strength, which disagrees with this vibrational model.

Monahan and Arns (69Mol) have suggested that the anomalous first excited $0^+$ level in $^{72}Ge$ could be similar to the corresponding situation in $^{90}Zr$, where the anomalous $0^+$ first excited state of $^{90}Zr$ was explained by Bayman et. al. (59Bal) as arising from a proton configuration orthogonal to that of the ground state. Since $^{90}Zr$ has 40 protons and $^{72}Ge$ has 40 neutrons, one could possibly explain the anomalous first excited $0^+$ state in $^{72}Ge$ as arising from a neutron configuration orthogonal to that of the ground state.

A summary of the (p,d) and (p,t) reactions leading to $^{72}Ge$ is presented in Fig. 34, where the wave functions written for the ground states refer to the main neutron configurations as deduced from our (p,d) data, and the double arrows represent strong transitions. With these wave functions it is possible, in the (p,t) reaction, to

populate the anomalous $0^+$ level by pick-up of a $(2p_{1/2})^2$ neutron pair, while that state cannot be populated in the (p,d) reaction, in agreement with our observed measurements. The other low lying levels in $^{72}Ge$ seem to be adequately described by the vibrational model since the 2 phonon and higher phonon states are weakly populated in both the (p,d) and (p,t) reactions, in accord with such a description.

# 7.- MODEL CALCULATIONS.

## 7.1- Simple pairing theory model.

Nuclei in the mass region of the germanium isotopes have so far not been adequately described by any reasonable model. Shell model calculations in this region are prohibitive due to the large number of particles (or holes) outside the nearest closed core and the large number of available states. The even-even germanium isotopes are poorly described by the vibrational model, and the calculations of Kisslinger and Sorensen (63Kil), using the pairing Hamiltonian with a long range quadrupole-quadrupole residual interaction, failed to reproduce the systematics of the low lying levels of the odd mass isotopes in this region. On the other hand, simple pairing theory is usually successful at predicting the occupation number and the center of gravity energy ( quasi particle energy) of a particular shell; these depend more on the "bulk properties" of the nuclei, in contrast to the level energies which are sensitive to fine details in the nuclear wave function.

The simple pairing theory as applied to the nuclear problem by Kisslinger and Sorensen (60Kil) is very attractive due to its simplicity. In their notation, one merely has to determine the values of $\lambda$ and $\Delta$ by solving the

"gap equation":

$$\frac{G}{2} \sum_j \frac{\Omega_j}{\sqrt{(\varepsilon_j - \lambda)^2 + \Delta^2}} = 1 \qquad (1)$$

$$n = \sum_j \Omega_j \left[1 - \frac{\varepsilon_j - \lambda}{\sqrt{(\varepsilon_j - \lambda)^2 + \Delta^2}}\right] \qquad (2)$$

where: G is the strength parameter for the pairing force,

$\Omega_j = j + 1/2$ ,

$\varepsilon_j$ is the single particle energy of shell j,

n = number of particles (neutrons in our case) outside the nearest closed shell,

$\Delta$ is the gap energy,

$\lambda$ is a Lagrangian multiplier which insures that the ground state has the right number of particles and is equivalent to a chemical potential.

The single quasi particle energies ($E_j$) and the shell occupation ( $V_j^2$ ) are given by:

$$E_j = \sqrt{(\varepsilon_j - \lambda)^2 + \Delta^2} \quad - \text{const.} \qquad (3)$$

$$V_j^2 = \frac{1}{2}\left[1 - \frac{\varepsilon_j - \lambda}{\sqrt{(\varepsilon_j - \lambda)^2 + \Delta^2}}\right] \qquad (4)$$

and these can be compared to the experimental center of gravity energy and shell occupation. The constant in equation (3) was set equal to $-\Delta$, which corresponds to setting $E_j = 0$ for the single quasiparticle state which is half filled ($V_j^2 = 0.5$, $\varepsilon_j = \lambda$ ).

The gap equation is easily solved with an iterative method. The pairing force strength parameter G was taken to be 24/A, the value recommended by Kisslinger and Sorensen (63Kil) for this mass region. Only the $2p_{3/2}$, $1f_{5/2}$, $2p_{1/2}$ and $1g_{9/2}$ shells were considered, and within each shell the single particle energies were given a smooth A dependence of the same form as that used by Kisslinger and Sorensen (63Kil). A first calculation using the recommended single particle energies of Kisslinger and Sorensen (63Kil), namely $\mathcal{E}^{\circ}(2p_{3/2}) = \mathcal{E}^{\circ}(1f_{5/2}) = 0$ MeV, $\mathcal{E}^{\circ}(2p_{1/2}) = 3$ MeV and $\mathcal{E}^{\circ}(1g_{9/2}) = 4$ MeV for A = 58, overestimated considerably the observed splitting of the $2p_{1/2}$ and $1g_{9/2}$ shells. Using different single particle energies, it was found that values of $\mathcal{E}^{\circ}(2p_{3/2}) \approx \mathcal{E}^{\circ}(1f_{5/2}) \approx$ 0 Mev and $\mathcal{E}^{\circ}(2p_{1/2}) \approx \mathcal{E}^{\circ}(1g_{9/2}) \approx 3$ MeV (for A = 58) yielded satisfactory fits to the center of gravity energy and occupation of all four subshells. In Figs. 28 to 31, the solid curves correspond to the set $\mathcal{E}^{\circ}(2p_{3/2}) = \mathcal{E}^{\circ}(1f_{5/2}) = 0$ MeV, $\mathcal{E}^{\circ}(2p_{1/2}) = 2.6$ MeV and $\mathcal{E}^{\circ}(1g_{9/2}) = 2.8$ MeV for A = 58, while the dotted line is for the set $\mathcal{E}^{\circ}(2p_{3/2}) = 0$ Mev, $\mathcal{E}_{\circ}(1f_{5/2}) = 0.3$ MeV, $\mathcal{E}_{\circ}(2p_{1/2}) = 2.8$ MeV and $\mathcal{E}^{\circ}(1g_{9/2}) = 3$ MeV for A = 58.

The gap energy $\Delta$ which is determined by solving the gap equation can also be evaluated from the even-odd mass difference, using the relation:

$$\Delta \approx \frac{1}{4}\left[\left|\text{S.E.}(n) - \text{S.E.}(n-1)\right| + \left|\text{S.E.}(n) - \text{S.E.}(n+1)\right|\right],$$

where n is the number of neutrons in the nucleus for which $\Delta$ is calculated, and S.E.(n) is the separation energy of 1 neutron from the nucleus which has n neutrons. Using the tabulated values of mass excess of the nuclei, $\Delta$ was calculated to be approximately 1.5 MeV in this mass region, and a value of approximately 1.3 MeV was obtained by solving the gap equations. This is taken to mean that the strength of the pairing force parameter is adequate for this mass region since the value of the gap energy $\Delta$ is sensitive to the chosen value of G.

From these calculations, one concludes that the simple pairing theory reproduces quite well the systematics of the center of gravity energy and occupation of the active shells in this mass region.

## 7.2- Coriolis coupling model with a pairing interaction.

As pointed our by Scholz and Malik (68Scl), it is interesting to note that the odd nuclei in the mass region of $71 \leq A \leq 85$ have high level densities at low excitations, some have quite large quadrupole moments compared to the single particle estimates and sometimes even differ in sign with that estimate. These and other electrical properties of these nuclei are consistent, qualitatively, with a rotator treated in the frame work of the Coriolis coupling model as discussed by Scholz and Malik (68Scl). They also indicate the importance of introducing a residual interaction between the nucleons moving in the deformed potential and choose for it the simple pairing interaction.

Their model can be described qualitatively as follows: The unpaired particle moves in a deformed Nilsson potential and the band-head energies are found in the usual way of solving the Nilsson hamiltonian. These band-head energies will be displaced by the residual interaction, and their new position (or value) will be obtained by making a pairing calculation using the unperturbed band-head energies as the single particle energies. Finally, the unpaired quasiparticle moving in the new Nilsson orbits is coupled by the Coriolis force to the rotational motion of the core.

The calculation of Scholz and Malik (68Sc1) takes into account the blocking effect in the pairing calculation, whereby a state occupied by two quasiparticles is not accessible to other quasiparticles. This necessitates the use of different values of $\lambda$ and $\Delta$ for each orbit considered. Since this blocking effect is known to be not too serious (61Ni1), and in order to use the already existing program written for the previous pairing calculations, this effect was neglected and the calculation was made along the lines of Imanishi et. al. (69Im1) who used a similar model for the description of the As isotopes without including the blocking effect. This simplifies the calculations considerably and still allows to see how good, qualitatively, the model can predict experimental results.

The eigenvalues and eigenfunctions of the Nilsson hamiltonian were calculated with an already existing programme, and no major shell mixing or higher order (hexadecapole) corrections were included. The Nilsson hamiltonian has only four parameters: $\mathring{\omega}_0$, $\kappa$, $\mu$ and $\eta$ (55Ni1); it is customary to choose $\hbar\mathring{\omega}_0 = 41A^{-1/3}$ MeV, which corresponds to the conventional harmonic oscillator level spacing. The parameters $\kappa$ and $\mu$ were taken to be:

The calculation of Scholz and Malik (68Scl) takes into account the blocking effect in the pairing calculation, whereby a state occupied by two quasiparticles is not accessible to other quasiparticles. This necessitates the use of different values of $\lambda$ and $\Delta$ for each orbit considered. Since this blocking effect is known to be not too serious (61Nil), and in order to use the already existing program written for the previous pairing calculations, this effect was neglected and the calculation was made along the lines of Imanishi et. al. (69Iml) who used a similar model for the description of the As isotopes without including the blocking effect. This simplifies the calculations considerably and still allows to see how good, qualitatively, the model can predict experimental results.

The eigenvalues and eigenfunctions of the Nilsson hamiltonian were calculated with an already existing programme, and no major shell mixing or higher order (hexadecapole) corrections were included. The Nilsson hamiltonian has only four parameters: $\mathring{\omega}_o$, $\kappa$, $\mu$ and $\eta$ (55Nil); it is customary to choose $\hbar\mathring{\omega}_o = 41A^{-1/3}$ MeV, which corresponds to the conventional harmonic oscillator level spacing. The parameters $\kappa$ and $\mu$ were taken to be:

| N | $\kappa$ | $\mu$ |
|---|---|---|
| 2 | 0.05 | 0.0 |
| 3 | 0.0339 | 0.284 |
| 4 | 0.05 | 0.5 |
| 5 | 0.05 | 0.45 |

where N is the total number of oscillator quanta ($2n + l$). These values were taken from the combined work of Nilsson (55Nil), Imanishi et. al. (69Iml) and Scholz and Malik (68Scl).

The Nilsson hamiltonian was diagonalized for values of the deformation parameter $\delta$ varying between -0.2 and +0.2. For each value of $\delta$, the band-head energies of each orbit were used as single particle energies in the pairing calculation in which all the neutrons above the closed $1d_{3/2}$ shell (N = 20) were allowed to scatter to all the available orbits ( a total of 52 available orbits). The values of $\lambda$ and $\Delta$ were determined by solving the gap equations, and using these the quasiparticle energy $E_\Omega$ and the occupation $V^2_\Omega$ was calculated for each orbit ($\Omega$).

Using the calculated coefficients $V^2_\Omega$, the quasiparticle energies $E_\Omega$ and the Nilsson wave functions described by the $c_{j\Omega}$ coefficients, the Coriolis hamiltonian was diagonalized to yield the perturbed energies and the mixing amplitudes. The decoupling parameter was taken to be that given by the expression (55Nil):

$$a = -\sum_{j} (-)^{j+1/2} (j+1/2) \left| c_{j\ 1/2} \right|^2$$

The rotational constant $\hbar^2/2\mathcal{J}$ which enters in the calculation was chosen as a free parameter since not much is known of it in this mass region; it was also taken to be the same for all the Nilsson orbits. Therefore, there are only two free parameters in this type of calculation: The deformation $\delta$ and the rotational constant $\hbar^2/2\mathcal{J}$. $\delta$, as mentioned previously, was varied between -0.2 and +0.2. Different values of $\hbar^2/2\mathcal{J}$ were tried and it was found that values in the vicinity of 0.08 to 0.12 MeV yielded satisfactory results.

In Figs. 35 to 38 are shown the results of this calculation. The first column to the left is the experimental energy levels of the particular germanium isotope, while the second column is the best (qualitative) fit to the experiment. The sets of curves on the right hand side of these figures illustrate the variation of the energy levels as a function of the deformation $\delta$ for different values of $\hbar^2/2\mathcal{J}$.

Besides trying to reproduce the experimental energy levels of the odd germanium isotopes, it was decided to further test these wave functions by calculating the spectroscopic factors for transitions to these levels, using

the formulae (67Del):

$$S_j = 2\left[\sum_{\Omega} V_{\Omega} W_{j\Omega} c_{j\Omega}\right]^2 ,$$

where: $V_{\Omega}$ = Occupation of orbit $\Omega$ ,

$W_{j\Omega}$ = mixing amplitude of orbit $\Omega$ into the level of spin j,

$c_{j\Omega}$ = Nilsson expansion coefficient for orbit $\Omega$ .

The value obtained for each choice of calculated energy levels is indicated on top of each horizontal bar representing the energy level and can be compared to the corresponding experimental value.

As can be verified from Figs. 35 to 38, the agreement between the predictions and the experimental values is surprisingly good, except for $^{73}$Ge where the model completely fails. The model also fails to reproduce the strong $\ell_n = 1$ ($2p_{3/2}$ neutron pick-up) transition observed to a low lying level of each germanium isotope in the (p,d) reaction.

That model also predicts low lying even parity states but these are below the ground state and for this reason, they were not drawn in the figures. In particular, the first $9/2^+$ state is considerably low, probably due to the fact that different values of the rotational parameter $\hbar^2/2\mathcal{J}$

should be used. However, the spectroscopic factor to this $9/2^+$ state agrees quite well with the experimental value except for $^{75}Ge$.

Table 1. Isotopic content and thickness of the germanium targets.

| Target | Isotopic content (%) | | | | | Target thickness ($\mu g/cm^2$) |
|---|---|---|---|---|---|---|
| | $^{70}Ge$ | $^{72}Ge$ | $^{73}Ge$ | $^{74}Ge$ | $^{76}Ge$ | |
| $^{70}Ge$ | 92.6 | 2.66 | 0.73 | 2.91 | 1.06 | 30.5 |
| $^{72}Ge$ | 2.7 | 89.2 | 2.2 | 4.3 | 1.6 | 36.8 |
| $^{73}Ge$ | 2.2 | 7.6 | 78.0 | 11.1 | 0.9 | 84.4 |
| $^{74}Ge$ | 1.71 | 2.21 | 0.91 | 94.5 | 0.7 | 19.4 |
| $^{76}Ge$ | 7.69 | 6.65 | 1.69 | 10.1 | 73.9 | 19.5 |

Table 2. Optical model potentials used in the DWBA analysis of the (p,d) and (p,t) reactions on the germanium isotopes. The notation is that of Perey (63Pe1).

| | $V_s$ (MeV) | $r_{os}$ (fm) | $a_s$ (fm) | $W_D$ (MeV) | $r_{oI}$ (fm) | $a_I$ (fm) |
|---|---|---|---|---|---|---|
| protons[a] | 46.1 | 1.25 | 0.65 | 13.7 | 1.25 | 0.47 |
| deuterons[b] | 105.1 | 1.07 | 0.962 | 20.25 | 1.366 | 0.668 |
| tritons[c] | 155.0 | 1.24 | 0.678 | 21.9 | 1.45 | 0.841 |
| neutron | | 1.25 | 0.55 | | | |
| dineutron | | 1.29 | 0.60 | | | |

a) From ref. 63Pe1

b) From ref. 63Pe2

c) From ref. 67Ha1

Table 3. Summed spectroscopic strengths for the $\ell_n$=1, 2, 3 and 4 transitions.

| Target | $\ell_n$=1 | $\ell_n$=2 | $\ell_n$=3 | $\ell_n$=4 | Total | Expected total |
|---|---|---|---|---|---|---|
| $^{70}$Ge | 3.94 | 0.0 | 5.75 | 1.26 | 10.95 | 9.43 |
| $^{72}$Ge | 4.74 | 0.09 | 5.49 | 1.93 | 12.25 | 11.56 |
| $^{73}$Ge | 3.39 | 0.061 | 6.29 | 3.31 | 13.05 | 12.60 |
| $^{74}$Ge | 4.03 | (0.503) | 4.62 | 3.35 | 12.50 | 13.64 |
| $^{76}$Ge[a)] | 3.75 | 0.053 | 5.35 | 4.2 | 13.36 | 15.70 |
| $^{76}$Ge[b)] | 3.75 | 0.053 | 4.85 | 4.2 | 12.85 | 15.70 |

a) Assuming that the transition to the 1690 ke level of $^{75}$Ge is a $\ell_n$=3.

b) Assuming that the transition to the 1690 keV level of $^{75}$Ge is not a $\ell_n$=3.

Table 4. Summary of the results of the $^{70}Ge(p,d)^{69}Ge$ reaction.

| Peak | Excitation (keV) | $\ell_n$ | Proposed $J^\pi$ | $\frac{d\sigma}{d\Omega}^{max}$ (mb/sr) | $\theta_{lab}$ | S |
|---|---|---|---|---|---|---|
| 1 | 0 | 3 | $5/2^-$ | 0.77 | 30-35 | 3.30 |
| 2 | 88 ± 5 | 1 | $1/2^-$ | 1.73 | 15 | 0.70 |
| 3 | 234 ± 5 | 1 | $3/2^-$ | 0.33 | 12 | 0.13 |
| 4 | 379 ± 5 | 1<br>4 | $3/2^-$<br>$9/2^+$ | 4.50 | 15 | 2.29<br>1.26 |
| 5* | 815 ± 5 | 1<br>3 | $3/2^-,(1/2^-)$<br>$5/2^-$ | 0.17 | 15 | 0.07<br>0.40 |
| 6 | 995 ± 5 | 1 | $1/2^-,(3/2^-)$ | 0.65 | 15 | 0.37 |
| 7 | 1162 ± 10 | | | | | |
| 8 | 1212 ± 10 | | | | | |
| 9 | 1307 ± 5 | 1 | $1/2^-,3/2^-$ | 0.20 | 15 | 0.14 |
| 10 | 1417 ± 5 | 3 | $5/2^-$ | 0.08 | 17-25 | 0.49 |
| 11 | 1477 ± 5 | 3 | $5/2^-$ | 0.15 | 30 | 1.56 |
| 12 | 1614 ± 10 | | | | | |
| 13* | 1760 ± 15 | | | | | |
| 14 | 1907 ± 15 | | | | | |
| 15 | 1955 ± 15 | | | | | |
| 16 | 2103 ± 10 | 1 | $3/2^-,(1/2^-)$ | 0.18 | 15 | 0.24 |
| 17 | 2136 ± 10 | | | | | |
| 18 | 2184 ± 10 | | | | | |

Table 4. (con'd)

| Peak | Excitation (keV) | $\ell_n$ | Proposed $J^\pi$ | $\frac{d\sigma}{d\Omega}^{max}$ (mb/sr) | $\theta_{lab}$ | S |
|---|---|---|---|---|---|---|
| 19 | 2356 ± 10 | | | | | |
| 20 | 2389 ± 10 | | | | | |
| 21 | 2469 ± 15 | | | | | |
| 22 | 2645 ± 15 | | | | | |
| 23 | 2747 ± 15 | | | | | |

* Broad peaks, probably multiplets.

Table 5. Summary of the results of the $^{72}Ge(p,d)^{71}Ge$ reaction.

| Peak | Excitation (keV) | $\ell_n$ | Proposed $J^{\pi}$ | $\frac{d\sigma}{d\Omega}^{max}$ (mb/sr) | $\theta_{lab}$ | S |
|---|---|---|---|---|---|---|
| 1 | 0 | 1 | $1/2^-$ | 3.05 | 15 | 0.98 |
| 2* | 186 ± 5 | 3 | $5/2^-$ | 1.20 | 30-35 | 3.64 |
| | | 4 | $9/2^+$ | | | 1.93 |
| 3 | 502 ± 5 | 1 | $3/2^-$ | 5.0 | 17 | 2.32 |
| 4 | 706 ± 5 | 1 | $3/2^-,(1/2^-)$ | 0.45 | 15 | 0.24 |
| 5 | 757 ± 10 | 3 | $5/2^-$ | 0.06 | 35 | 0.24 |
| 6 | 807 ± 10 | 2 | $5/2^+$ | 0.05 | 25 | 0.03 |
| 7 | 1025 ± 5 | 2 | $5/2^+$ | 0.05 | 25 | 0.03 |
| 8 | 1096 ± 5 | 1 | $3/2^-,(1/2^-)$ | 0.72 | 15 | 0.37 |
| 9 | 1166 ± 10 | 1 | $3/2^-,(1/2^-)$ | 0.15 | 17 | 0.05 |
| 10 | 1210 ± 10 | 3 | $5/2^-$ | | | 0.40 |
| 11 | 1288 ± 5 | 1 | $3/2^-,(1/2^-)$ | 0.36 | 17 | 0.18 |
| 12 | 1354 ± 10 | 2 | $5/2^+$ | 0.05 | 25 | 0.03 |
| 13 | 1410 ± 10 | 3 | $5/2^-$ | 0.05 | 30 | 0.26 |
| 14 | 1507 ± 5 | 3 | $5/2^-$ | 0.09 | 35 | 0.53 |
| 15 | 1595 ± 10 | 1 | $3/2^-,(1/2^-)$ | 0.16 | 15 | 0.09 |
| 16 | 1742 ± 5 | 1 | $3/2^-,(1/2^-)$ | 0.11 | 17 | 0.09 |
| 17 | 1786 ± 10 | 3 | $5/2^-$ | 0.09 | 25 | 0.42 |
| 18 | 1966 ± 5 | 1 | $3/2^-,(1/2^-)$ | 0.25 | 15 | 0.18 |
| 19 | 2354 ± 5 | 1 | $3/2^-,(1/2^-)$ | 0.19 | 15 | 0.18 |

* Broad peak.

Table 6. Summary of the results of the $^{73}Ge(p,d)^{72}Ge$ reaction.

| Peak | Excitation (keV) | $\ell_n$ | Proposed $J^\pi$ | $\frac{d\sigma}{d\Omega}^{max}$ (mb/sr) | $\theta_{lab}$ | S |
|---|---|---|---|---|---|---|
| 1 | 0 | 4 | $0^+$ | 0.34 | 35 | 0.52 |
| 2 | 830 ± 5 | 2 | $2^+$ | 0.21 | 20 | 0.04 |
| 3 | 1455 ± 5 | 2 | $2^+$ | 0.07 | 17 | 0.014 |
| 4 | 1723 ± 5 | 4 | $4^+$ | 0.09 | 35 | 0.23 |
| 5 | 2049 ± 10 | 2 | | 0.032 | 20 | 0.008 |
| 6* | 2505 ± 5 | 1 | | 0.84 | 15 | 0.19 |
| | | 4 | | | | 0.19 |
| 7 | 2754 ± 15 | 1 | | 0.21 | 15 | 0.049 |
| 8 | 2936 ± 10 | 3 | | 0.04 | 30 | 0.11 |
| 9 | 3035 ± 15 | 3 | | 0.06 | 30 | 0.22 |
| 10 | 3077 ± 15 | | | | | |
| 11 | 3119 ± 15 | 1 | | 0.25 | 15 | 0.062 |
| 12 | 3228 ± 10 | 1 | | 0.22 | 15 | 0.055 |
| 13 | 3316 ± 10 | 1 | | 0.34 | 15 | 0.088 |
| 14 | 3398 ± 5 | 1 | | 1.15 | 15 | 0.28 |
| | | 3 | | | | 0.50 |
| 15 | 3554 ± 10 | 1 | | 0.29 | 15 | 0.073 |
| | | 3 | | | | 0.18 |
| 16 | 3659 ± 5 | 1 | | 1.18 | 15 | 0.32 |
| | | 3 | | | | 1.28 |

Table 6. (con'd)

| Peak | Excitation (keV) | $\ell_n$ | Proposed $J^\pi$ | $\frac{d\sigma}{d\Omega}^{max}$ (mb/sr) | $\theta_{lab}$ | S |
|---|---|---|---|---|---|---|
| 17 | 3754 ± 5 | 1 | | 1.57 | 15 | 0.36 |
| 18 | 3804 ± 5 | + 4 | | | | 1.14 |
| 19 | 3890 ± 10 | 3 | | 0.34 | 25 | 1.23 |
| 20 | 3965 ± 10 | 1 | | 0.50 | 17 | 0.15 |
| | | + 3 | | | | 0.50 |
| 21 | 4047 ± 10 | 1 | | 0.78 | 15 | 0.24 |
| | | + 3 | | | | 0.53 |
| 22 | 4194 ± 5 | 1 | | 0.78 | 15 | 0.27 |
| 23 | 4339 ± 5 | 1 | | 0.97 | 15 | 0.37 |
| | | + 3 | | | | 0.51 |
| 24 | 4458 ± 5 | 1 | | 0.66 | 15 | 0.27 |

* Broad peak, probably a multiplet.

Table 7. Summary of the results of the $^{74}Ge(p,d)^{73}Ge$ reaction.

| Peak | Excitation (keV) | $\ell_n$ | Proposed $J^\pi$ | $\frac{d\sigma^{max}}{d\Omega}$ (mb/sr) | $\theta_{lab}$ | S |
|---|---|---|---|---|---|---|
| 1 | 0 | 4 | $9/2^+$ | 0.92 | 22-35 | 3.35 |
| | | 2 | $5/2^+$ | | | 0.21 |
| 2 | 63 ± 5 | 1 | $1/2^-$ | 1.85 | 15 | 0.56 |
| 3* | 370 ± 5 | 1 | $3/2^-$ | 6.95 | 15 | 2.03 |
| | | 3 | $5/2^-$ | | | 2.58 |
| 4 | 494 ± 5 | 2 | $5/2^+$ | 0.45 | 20 | 0.18 |
| 5 | 557 ± 15 | 2 | $5/2^+$ | 0.12 | 20 | 0.06 |
| 6 | 730 ± 15 | | | | | |
| 7 | 810 ± 10 | | | | | |
| 8 | 897 ± 5 | 1 | $1/2^-,(3/2^-)$ | 0.50 | 15 | 0.19 |
| 9 | 1039 ± 5 | 1 | $3/2^-,(1/2^-)$ | 1.13 | 15 | 0.45 |
| 10 | 1139 ± 10 | 3 | $5/2^-$ | 0.14 | 30 | 0.64 |
| 11 | 1186 ± 10 | 3 | $5/2^-$ | 0.14 | 30 | 0.62 |
| 12 | 1261 ± 10 | 1 | $3/2^-,1/2^-$ | 0.25 | 20 | 0.12 |
| 13 | 1312 ± 10 | 1 | $3/2^-,(1/2^-)$ | 0.34 | 15 | 0.17 |
| 14 | 1610 ± 10 | 3 | $5/2^-$ | 0.15 | 35 | 0.78 |
| 15 | 1653 ± 10 | 1 | $3/2^-,(1/2^-)$ | 0.07 | 15-20 | 0.07 |
| 16 | 1744 ± 15 | 2 | $5/2^+$ | 0.09 | 20 | 0.06 |
| 17 | 2030 ± 10 | 1 | $3/2^-,(1/2^-)$ | 0.30 | 15 | 0.18 |
| 18 | 2122 ± 10 | 1 | $3/2^-,(1/2^-)$ | 0.17 | 15 | 0.11 |
| 19 | 2270 ± 15 | 1 | $3/2^-,(1/2^-)$ | 0.07 | 15 | 0.05 |
| 20 | 2329 ± 15 | 1 | $3/2^-,(1/2^-)$ | 0.16 | 15 | 0.10 |

* Broad peak, possibly a multiplet.

Table 8. Summary of the results of the $^{76}Ge(p,d)^{75}Ge$ reaction.

| Peak | Excitation (keV) | $\ell_n$ | Proposed $J^\pi$ | $\frac{d\sigma^{max}}{d\Omega}$ (mb/sr) | $\theta_{lab}$ | S |
|---|---|---|---|---|---|---|
| 1 | 0 | 1 | $1/2^-$ | 2.60 | 15 | 0.61 |
| 2 | 197 ± 5 | 4 | $9/2^+$ | 1.2 | 35 | 4.2 |
| 3 | 250 ± 5 | 1 | $1/2^-, 3/2^-$ | 0.65 | 15 | 0.16 |
| 4 | 314 ± 5 | 3 | $5/2^-$ | 0.55 | 30 | 1.38 |
| 5 | 457 ± 5 | 3 | $5/2^-$ | 0.12 | 35 | 0.32 |
| 6* | 574 ± 5 | 1 | $3/2^-$ | 6.0 | 15 | 1.59 |
| | | 3 | $5/2^-$ | | | 1.59 |
| 7 | 671 ± 15 | 2 | $5/2^+$ | 0.15 | 25 | 0.05 |
| 8 | 889 ± 10 | 1 | $3/2^-, (1/2^-)$ | 0.48 | 15 | 0.14 |
| 9 | 988 ± 10 | | | | | |
| 10 | 1250 ± 5 | | | | | |
| 11* | 1403 ± 5 | 1 | $3/2^-, (1/2^-)$ | 0.62 | 15 | 0.20 |
| | | 3 | $5/2^-$ | | | 0.47 |
| 12* | 1501 ± 5 | 1 | $3/2^-, (1/2^-)$ | 1.3 | 15 | 0.48 |
| 13 | 1593 ± 10 | 3 | $5/2^-$ | 0.18 | 30 | 0.64 |
| 14* | 1690 ± 5 | (3) | $(5/2^-)$ | 0.12 | 30 | (0.51) |
| 15* | 1803 ± 5 | 1 | $3/2^-, (1/2^-)$ | 0.60 | 15 | 0.22 |
| 16 | 2043 ± 10 | 1 | $3/2^-, (1/2^-)$ | 0.16 | 15 | 0.06 |
| 17 | 2105 ± 10 | 3 | $5/2^-$ | | | 0.45 |
| 18 | 2198 ± 15 | | | | | |
| 19 | 2316 ± 10 | 1 | $3/2^-, (1/2^-)$ | 0.45 | 15 | 0.18 |
| 20 | 2670 ± 10 | 1 | $3/2^-, (1/2^-)$ | 0.19 | 15 | 0.11 |

* Broad peaks, probably multiplets.

## Table 9.

a) Summed spectroscopic strengths (normalized).

| Nucleus | $2p_{1/2}$ | $2p_{3/2}$ | $2p_{1/2}$ $2p_{3/2}$ | $1f_{5/2}$ | $1g_{9/2}$ |
|---|---|---|---|---|---|
| $^{70}$Ge | 0.92 - 1.04 | 2.35 - 2.47 | 3.39 | 4.95 | 1.09 |
| $^{72}$Ge | 0.98 | 3.49 | 4.47 | 5.18 | 1.82 |
| $^{73}$Ge | | | 3.27 | 6.07 | 3.20 |
| $^{74}$Ge | 0.82 - 0.95 | 3.44 - 3.58 | 4.39 | 5.04 | 3.66 |
| $^{76}$Ge | 0.72 - 0.97 | 3.50 - 3.92 | 4.41 - 4.70 | 6.06 - 6.29 | 4.94 - 5.26 |

b) Center of gravity energies ( $\varepsilon_j$ in MeV).

| Nucleus | $\varepsilon(2p_{1/2})$ | $\varepsilon(2p_{3/2})$ | $\varepsilon(1f_{5/2})$ | $\varepsilon(1g_{9/2})$ |
|---|---|---|---|---|
| $^{69}$Ge | 0.40 - 0.51 | 0.54 - 0.57 | 0.55 | 0.40 |
| $^{71}$Ge | 0.00 | 0.84 | 0.59 | 0.19 |
| $^{73}$Ge | 0.27 - 0.41 | 0.79 - 0.81 | 0.80 | 0.00 |
| $^{75}$Ge | 0.00 - 0.05 | 1.05 - 1.10 | 0.80 - 0.93 | 0.20 |

Table 10. Low lying energy levels of $^{69}Ge$.

| $^{70}Ge(p,d)^{69}Ge$ (present work) | | | | $^{70}Ge(^{3}He,\alpha)^{69}Ge$ (67Fol) | | | $^{69}As(\beta^{+},\gamma)$ (70Mul) | |
|---|---|---|---|---|---|---|---|---|
| Peak | Energy (keV) | $\ell_n$ | S | Energy (keV) | $\ell_n$ | S | Energy (keV) | $J^{\pi}$ |
| 1 | 0 | 3 | 3.30 | 0 | 3 | 3.4 | 0 | $5/2^-$ |
| 2 | 88 | 1 | 0.70 | 90 | (3) | 0.6 | 87 | $1/2^-$ |
| 3 | 234 | 1 | 0.13 | 230 | (1) | 0.2 | 233 | $3/2^-$ |
| 4 | 379 | 1 + 4 | 2.29<br>1.26 | 380 | 1 | 3.9 | 374<br>(398) | $3/2^-$ |
| 5 | 815 | | | | | | | |
| 6 | 995 | 1 | 0.37 | 1000 | 1 | 0.7 | | |

Table 11. Shell occupation for N = 38 and center of gravity energies for N = 37 nuclei.

a) Shell occupation for some N = 38 nuclei (%)

| Nucleus | $2p_{1/2}$ | $2p_{3/2}$ | $2p_{3/2}+2p_{1/2}$ | $1f_{5/2}$ | $1g_{9/2}$ |
|---|---|---|---|---|---|
| $^{70}Ge$ 1) | 45-51 | 67-70 | 55 | 84 | 11 |
| $^{70}Ge$ 2) | 42 | 97 | 78 | 66 | 13 |
| $^{68}Zn$ 3) | 34-39 | 80-82 | 66 | 75 | 15 |
| $^{68}Zn$ 4) | 41-45 | 82-84 | 75 | 81 | 10 |
| $^{70}Ge$ 5) | 34-56 | 83-88 | 77 | 75 | 9 |

b) Shell center of gravity energies for N = 37 (MeV)

| Nucleus | $2p_{1/2}$ | $2p_{3/2}$ | $1f_{5/2}$ | $1g_{9/2}$ |
|---|---|---|---|---|
| $^{69}Ge$ 1) | 0.40-0.51 | 0.54-0.57 | 0.58 | 0.40 |
| $^{67}Zn$ 3) | 0.35-0.38 | 0.43-0.47 | 0.0 | 0.60 |
| $^{67}Zn$ 4) | 0.36-0.40 | 0.43-0.48 | 0.0 | 0.60 |
| $^{65}Ni$ 6) | 0.32 | 0.62 | 0.40 | 1.17 |

1) Our results with the spin assignments of Table 4

2) Goldman's results from the $^{70}Ge(d,p)^{71}Ge$ (68Gol)

3) From Ref. 67Ehl, using Set a

4) From Ref. 67Ehl, using Set b

5) Reanalyzed Goldman's results (68Gol) as discussed in text

6) From Ref. 70Tul

Table 12. Level energies of $^{71}Ge$.

| Peak | $^{72}Ge(p,d)^{71}Ge$ Present work (keV) | $^{71}Ga(p,n\gamma)^{71}Ge$ (70Mal) (keV) | $^{70}Ge(d,p)^{71}Ge$ (68Gol) (keV) |
|---|---|---|---|
| 1 | 0 | 0 | 0 |
| | | | 60 |
| | | 175 | 190 |
| 2 | 186 | 198 | 190 |
| 3 | 502 | 500 | 480 |
| | | 524 | 510 |
| | | 589 | 570 |
| | | | 620 |
| | | | 630 |
| 4 | 706 | 708 | 700 |
| 5 | 757 | 747 | 730 |
| 6 | 807 | 808 | 790 |
| | | 831 | 810 |
| | | | 890 |
| | | | 950 |
| | | | 970 |
| 7 | 1025 | 1026 | 1030 |
| 8 | 1096 | 1096 | 1090 |
| | | 1139 | 1120 |
| 9 | 1166 | | 1160 |
| | | 1204 | |
| 10 | 1210 | 1212 | 1200 |

Table 12. (con'd)

| Peak | $^{72}Ge(p,d)^{71}Ge$ (keV) | $^{71}Ga(p,n\gamma)^{71}Ge$ (keV) | $^{70}Ge(d,p)^{71}Ge$ (keV) |
|---|---|---|---|
| 11 | 1288 | 1288 | 1280 |
| | | 1299 | |
| 12 | 1354 | 1349 | 1340 |
| | | 1379 | 1380 |
| 13 | 1410 | 1415 | 1410 |
| | | 1454 | 1450 |
| | | 1477 | 1470 |
| 14 | 1507 | 1507 | 1500 |
| | | 1543 | |
| | | 1566 | 1550 |
| 15 | 1595 | 1599 | 1590 |
| | | 1629 | |
| | | 1699 | 1690 |
| 16 | 1742 | 1744 | |
| 17 | 1786 | 1792 | 1780 |
| | | | 1870 |
| | | 1938 | 1940 |
| 18 | 1966 | 1965 | 1960<br>2040<br>2120<br>2170<br>2220<br>2270<br>2330 |
| 19 | 2354 | | 2350<br>2410<br>2480 |

Table 13. Comparison of the $^{72}Ge(p,d)^{71}Ge$ and the $^{70}Ge(d,p)^{71}Ge$ reaction.

| $^{72}Ge(p,d)^{71}Ge$ Present work | | | | $^{70}Ge(d,p)^{71}Ge$ (68Col) | | | | Ratio pd/dp | Goldman's data reanalyzed | | | $^{73}Ge(p,t)^{71}Ge$ | |
|---|---|---|---|---|---|---|---|---|---|---|---|---|---|
| Energy (keV) | $\ell_n$ | $\frac{d\sigma}{d\Omega}^{max}$ (mb/sr) | $J^\pi$ | Energy (keV) | $\ell_n$ | $\frac{d\sigma}{d\Omega}^{max}$ (mb/sr) | $J^\pi$ | | $\ell_n$ | $J^\pi$ | (2J+1)S | Energy (keV) | L |
| 0 | 1 | 3.05 | $1/2^-$ | 0 | 1 | 0.94 | $1/2^-$ | 3.2 | 1 | $1/2^-$ | 0.55 | | |
| | | | | 60 | | | | | | | | | |
| 186 | {3 + 4 | 1.20 | $5/2^-$ $9/2^+$ | 160 | 3 | 0.07 | $5/2^-$ | | 3 | $5/2^-$ | 0.4 | | |
| | | | | 190 | 4 | 0.61 | $9/2^+$ | | 4 | $9/2^+$ | 7.3 | 198 | 0 |
| 502 | 1 | 5.0 | $3/2^-$ | 480 | 1 | 0.60 | $1/2^-$ | 8.3 | 1 | $3/2^-$ | 0.27 | | |
| | | | | 510 | 2 | 0.75 | | | | | | 515 | (2,3) |
| | | | | 570 | | 0.01 | | | | | | 587 | |
| | | | | 620 | | 0.04 | | | | | | | |
| | | | | 630 | | | | | | | | | |
| 706 | 1 | 0.45 | $3/2^-$,$(1/2^-)$ | 700 | (1) | 0.13 | $1/2^-$ | 3.5 | 1 | $3/2^-$ | 0.05 | | |
| 757 | 3 | 0.06 | $5/2^-$ | { 730 | (2) | 0.03 | | | } 3 | $5/2^-$ | 0.14 | | |
| | | | | 790 | | 0.01 | | | | | | | |
| 807 | 2 | 0.05 | $5/2^+$ | 810 | | 0.02 | | | | | | | |
| | | | | 890 | (1) | 0.04 | $1/2^-$ | | | | | | |
| | | | | 950 | | | | | | | | | |
| | | | | 970 | | 0.04 | | | | | | | |
| 1025 | 2 | 0.05 | $5/2^+$ | 1030 | | 0.06 | | | | | | 1028 | |
| 1096 | 1 | 0.72 | $3/2^-$,$(1/2^-)$ | 1090 | 1 | 0.28 | $1/2^-$ | 2.6 | 1 | $3/2^-$ | 0.1 | | |
| | | | | 1120 | | 0.28 | | | | | | | |
| 1166 | 1 | } 0.15 | $3/2^-$,$(1/2^-)$ | 1160 | 2? | 0.04 | | 4.0 | 1 | $3/2^-$ | 0.02 | 1183 | (3,2) |
| 1210 | 3 | | $5/2^-$ | 1200 | 2? | 0.05 | | | 3 | $5/2^-$ | 0.18 | | |
| 1288 | 1 | 0.36 | $3/2^-$,$(1/2^-)$ | 1280 | | 0.06 | | 6.1 | 1 | $3/2^-$ | 0.02 | | |
| 1354 | 2 | 0.05 | $5/2^+$ | 1340 | 0? | 0.63 | | | | | | | |
| | | | | 1380 | (2) | 0.26 | | | | | | | |
| 1410 | 3 | 0.05 | $5/2^-$ | 1410 | | | | | 3 | $5/2^-$ | 0.03 | | |
| | | | | 1450 | | 0.03 | | | | | | | |
| | | | | 1470 | (3) | 0.14 | $(5/2^-)$ | | | | | 1472 | |
| 1507 | 3 | 0.09 | $5/2^-$ | 1500 | (2) | 0.08 | | | 3 | $5/2^-$ | 0.30 | | |
| | | | | 1550 | 2? | 0.28 | | | | | | | |
| 1595 | 1 | 0.16 | $3/2^-$,$(1/2^-)$ | 1590 | | 0.40 | | 4.0 | 1 | $3/2^-$ | 0.01 | | |
| | | | | 1690 | (3) | 0.16 | $(5/2^-)$ | | | | | | |
| 1742 | 1 | 0.11 | $3/2^-$,$(1/2^-)$ | | | | | | | | | | |
| 1786 | 3 | 0.09 | $5/2^-$ | 1780 | (1) | 0.04 | $(3/2^-)$ | | 3 | $5/2^-$ | 0.16 | | |
| | | | | 1870 | | 0.01 | | | | | | | |
| | | | | 1940 | | 0.02 | | | | | | | |
| 1966 | 1 | 0.25 | $3/2^-$,$(1/2^-)$ | 1960 | 0 | 0.30 | $1/2^+$ | | | | | 1955 | |
| | | | | 2040 | 1 | 0.32 | $3/2^-$ | | | | | | |
| | | | | 2120 | (3) | 0.03 | $(5/2^-)$ | | | | | | |
| | | | | 2170 | | 0.02 | | | | | | | |
| | | | | 2220 | 0 | 2.00 | $1/2^+$ | | | | | | |
| | | | | 2270 | 2 | 0.44 | | | | | | | |
| | | | | 2330 | | 0.05 | | | | | | | |
| 2354 | 1 | 0.19 | $3/2^-(1/2^-)$ | 2350 | | 0.17 | | | 1 | $3/2^-$ | 0.05 | | |
| | | | | 2410 | 0 | 0.16 | $1/2^+$ | | | | | | |
| | | | | 2480 | 0 | 0.36 | $1/2^+$ | | | | | | |

Table 14. Shell occupation for N = 40 and center of gravity energies for N = 39 nuclei.

a) Shell occupation for some N = 40 nuclei (%)

| Nucleus | $2p_{1/2}$ | $2p_{3/2}$ | $2p_{3/2}+2p_{1/2}$ | $1f_{5/2}$ | $1g_{9/2}$ |
|---|---|---|---|---|---|
| $^{72}Ge$ 1) | 49 | 88 | 75 | 87 | 18 |
| $^{70}Zn$ 2) | 30-35 | 86-89 | 70 | 80 | 31 |
| $^{70}Zn$ 3) | 35-40 | 80-90 | 68 | 84 | 27 |

b) Shell center of gravity energies for N = 39 (MeV)

| Nucleus | $2p_{1/2}$ | $2p_{3/2}$ | $1f_{5/2}$ | $1g_{9/2}$ |
|---|---|---|---|---|
| $^{71}Ge$ 1) | 0.00 | 0.84 | 0.59 | 0.19 |
| $^{71}Ge$ 4) | 0.30 | 2.0 | 1.3 | 0.19 |
| $^{71}Ge$ 5) | 0.00 | 0.88 | 0.96 | 0.19 |
| $^{69}Zn$ 2) | 0.00-0.13 | 0.84-0.98 | 0.53 | 0.44 |
| $^{69}Zn$ 3) | 0.00-0.13 | 0.84-0.97 | 0.53 | 0.44 |

1) Present results

2) From Ref. 67Ehl, using Set a

3) From Ref. 67Ehl, using Set b

4) Goldman's results from the $^{70}Ge(d,p)^{71}Ge$ (68Gol)

5) Reanalyzed Goldman's data (68Gol) as discussed in the text.

Table 15. Strong $\ell_n = 1$ and 3 transitions from the $^{73}Ge(p,d)^{72}Ge$ reaction.

| Energy (keV) | $S_{\ell=1}$ | $S_{\ell=3}$ | $\frac{S_{\ell=1}}{\Sigma S_{\ell=1}}$ | $\frac{S_{\ell=3}}{\Sigma S_{\ell=3}}$ | $J^\pi$ | $\frac{\ell=1}{\frac{2J+1}{40}}$ | $\frac{\ell=3}{\frac{2J+1}{60}}$ |
|---|---|---|---|---|---|---|---|
| 3035 | | 0.22 | | 0.05 | $2^-$ | | 0.08 |
| 3398 | 0.28 | 0.50 | 0.22 | 0.11 | $4^-$ | 0.23 | 0.15 |
| 3659 | 0.32 | 1.28 | 0.26 | 0.29 | $5^-$ | 0.28 | 0.18 |
| 3754<br>3804 | 0.36 | | | | | | |
| 3890 | | 1.23 | | 0.29 | $7^-$ | | 0.25 |
| 3965 | 0.15 | 0.50 | | | | | |
| 4047 | 0.24 | 0.53 | 0.19 | 0.12 | $3^-$ | 0.18 | 0.12 |
| 4194 | 0.27 | | | | | | |
| 4339 | 0.37 | 0.51 | 0.31 | 0.12 | $6^-$ | 0.33 | 0.22 |
| 4458 | 0.27 | | | | | | |

Table 16. Comparison of the $^{74}Ge(p,d)^{73}Ge$, $^{72}Ge(d,p)^{73}Ge$ and $^{73}Ge(p,p')^{73}Ge$ reactions.

| $^{74}Ge(p,d)^{73}Ge$ Present work | | | | pd/dp ratio | $^{72}Ge(d,p)^{73}Ge$ (69Hel) | | | | $^{73}Ge(p,p')^{73}Ge$ (69Hel) | | Nuclear data (66Ndl) | |
|---|---|---|---|---|---|---|---|---|---|---|---|---|
| Energy (keV) | $\ell_n$ | $\frac{d\sigma}{d\Omega}^{max}$ (mb/sr) | $J^\pi$ | | Energy (keV) | $\ell_n$ | $\frac{d\sigma}{d\Omega}^{max}$ (mb/sr) | $J^\pi$ | Energy (keV) | ΔL | Energy (keV) | $J^\pi$ |
| 0 | 4 | 0.92 | $9/2^+$ | | 0 | 4 | 0.66 | $9/2^+$ | 0 | 0 | 0 | $9/2^+$ |
| | 2 | | $5/2^+$ | | 13 | 2 | 0.22 | $5/2^+$ | | | 14 | $5/2^+$ |
| 63 | 1 | 1.85 | $1/2^-$ | 2 | 67 | 1 | 0.91 | $1/2^-$ | 67 | 2 | 66.8 | $1/2^-$ |
| | | | | | | | | | | | 67 | $7/2^+$ |
| 370 | 1 | 6.95 | $3/2^-$ | 9 | 368 | 1 | 0.75 | $1/2^-$ | | | 363 | |
| | 3 | | $5/2^-$ | | 396 | | | | | | 392 | |
| 494 | 2 | 0.45 | $5/2^+$ | | 512 | 1 | 0.64 | $1/2^-$ | 498 | 2 | (520) | |
| 557 | 2 | 0.12 | $5/2^+$ | | 562 | 2 | 0.37 | $5/2^+$ | 551 | 2 | 554 | |
| | | | | | 666 | 3 | 0.16 | $5/2^-$ | 656 | 2 | 647 | |
| 730 | | | | | 727 | | | | | | | |
| | | | | | | | | | 778 | | (770) | |
| 810 | | | | | | | | | 825 | | 820 | |
| 897 | 1 | 0.50 | $1/2^-$,$(3/2^-)$ | 1 | 864 | 1 | 0.20 | $1/2^-$ | 867 | | 879 | |
| | | | | | 904 | 1 | 0.40 | $1/2^-$ | | | | |
| | | | | | 926 | | | | 918 | 2 | 950 | |
| | | | | | | | | | 997 | 2 | | |
| 1039 | 1 | 1.13 | $3/2^-$,$(1/2^-)$ | 6 | 1051 | 1 | 0.24 | $1/2^-$ | 1039 | 2 | 1040 | |
| 1139 | 3 | 0.14 | $5/2^-$ | | 1141 | | | | 1132 | 2 | 1134 | |
| 1186 | 3 | 0.14 | $5/2^-$ | | 1176 | | | | | | | |
| 1261 | 1 | 0.25 | $3/2^-$,$1/2^-$ | | 1274 | 0 | 0.21 | $1/2^+$ | | | | |
| 1312 | 1 | 0.34 | $3/2^-$,$(1/2^-)$ | | 1322 | | | | 1318 | 2 | | |
| | | | | | 1344 | | | | 1338 | 2 | | |
| | | | | | | | | | | | 1570 | |
| 1610 | 3 | 0.15 | $5/2^-$ | | 1617 | 2 | 0.53 | $5/2^+$ | 1614 | 2 | | |
| 1653 | 1 | 0.07 | $3/2^-$,$(1/2^-)$ | | 1646 | 2 | 1.26 | $5/2^+$ | 1659 | | 1690 | |
| 1744 | 2 | 0.09 | $5/2^+$ | | 1756 | 2 | 2.22 | $5/2^+$ | 1767 | 2 | | |
| | | | | | 1804 | 2 | 0.55 | $5/2^+$ | | | 1810 | |
| | | | | | 1936 | 1 | 0.67 | $3/2^-$ | | | 1960 | |
| | | | | | 1983 | 1 | 0.42 | $3/2^-$ | | | | |
| 2030 | 1 | 0.30 | $3/2^-$,$(1/2^-)$ | 1 | 2010 | | | | | | | |
| | | | | | 2053 | 1 | 0.28 | $3/2^-$ | | | | |
| | | | | | 2093 | 2 | 0.98 | $5/2^+$ | 2088 | | | |
| 2122 | 1 | 0.17 | $3/2^-$,$(1/2^-)$ | | | | | | | | 2140 | |
| | | | | | 2164 | | | | | | | |
| 2270 | 1 | 0.07 | $3/2^-$,$(1/2^-)$ | | 2251 | 2 | 0.42 | $5/2^+$ | | | | |
| 2329 | 1 | 0.16 | $3/2^-$,$(1/2^-)$ | | 2312 | 2 | 0.16 | $5/2^+$ | | | | |
| | | | | | 2353 | 2 | 0.24 | $5/2^+$ | 2364 | 3 | | |
| | | | | | 2411 | 1 | 0.31 | $3/2^-$ | | | | |
| | | | | | 2495 | 2 | 1.25 | $5/2^+$ | 2454 | 3 | 2480 | |

Table 17. Shell occupation for N = 42 and center of gravity energies for N = 41 nuclei.

a) Shell occupation of some N = 42 nuclei (%)

| Nucleus | $2p_{1/2}$ | $2p_{3/2}$ | $2p_{3/2}+2p_{1/2}$ | $1f_{5/2}$ | $1g_{9/2}$ |
|---|---|---|---|---|---|
| $^{74}Ge$ 1) | 41-48 | 84-99 | 78 | 84 | 37 |
| $^{76}Se$ 2) | 39 | 76 | 63 | 72 | >59 |

b) Shell center of gravity energies for N = 41 (MeV)

| Nucleus | $2p_{1/2}$ | $2p_{3/2}$ | $1f_{5/2}$ | $1g_{9/2}$ |
|---|---|---|---|---|
| $^{73}Ge$ 1) | 0.27-0.41 | 0.79-0.81 | 0.80 | 0.0 |
| $^{71}Zn$ 3) | 0.00-0.04 | 0.79-0.88 | 0.47 | 0.16 |
| $^{71}Zn$ 4) | 0.00-0.04 | 0.80-0.89 | 0.47 | 0.16 |

1) Present data

2) From Ref. 65Li1

3) From Ref. 67Eh1, using Set a

4) From Ref. 67Eh1, using Set b

Table 18. Energy levels of $^{75}Ge$.

| Present work (keV) | Nuclear Data (66Nd1) (keV) |
|---|---|
| 0 | 0 |
| | 62 |
| (140) | 139 |
| 197 | 180 |
| | 215 |
| 250 | 261 |
| 314 | 326 |
| | 360 |
| 457 | |
| 574 | 593 |
| 671 | 685 |
| 889 | 885 |
| 988 | 940 |
| 1250 | 1110 |
| | 1320 |
| 1403 | |
| | 1470 |
| 1501 | |
| 1593 | 1570 |
| 1690 | |
| | 1740 |
| 1803 | |

Table 18. (con'd)

| Present work (keV) | Nuclear Data (keV) |
|---|---|
| | 1870 |
| 2043 | |
| | 2080 |
| 2105 | |
| 2198 | 2190 |
| | 2230 |
| 2316 | |
| | (2460) |
| 2670 | 2680 |
| | (2830) |
| | 3020 |

Table 19. Shell occupation for N = 44 and center of gravity energies for N = 43 nuclei.

a) Shell occupation of some N = 44 nuclei (%)

| Nucleus | $2p_{3/2}$ | $2p_{1/2}$ | $2p_{3/2}+2p_{1/2}$ | $1f_{5/2}$ | $1g_{9/2}$ |
|---|---|---|---|---|---|
| $^{76}Ge$ 1) | 36-48 | 96-100 | 77-82 | 100 | 49-53 |
| $^{78}Se$ 2) | 63 | 83 | 76 | 85 | 63 |

b) Shell center of gravity energies for some N = 43 nuclei (MeV)

| Nucleus | $2p_{1/2}$ | $2p_{3/2}$ | $1f_{5/2}$ | $1g_{9/2}$ |
|---|---|---|---|---|
| $^{75}Ge$ 1) | 0.00-0.05 | 1.05-1.10 | 0.80-0.93 | 0.20 |
| $^{77}Se$ 2) | 0.19 | 1.10 | 0.32 | 0.19 |

1) Present data

2) From Ref. 65Lil

Table 20. Energy levels, L values from the $^{70}Ge(p,t)^{68}Ge$ reaction.

| $^{70}Ge(p,t)^{68}Ge$ Present work | | | $^{68}As(\beta^+, \gamma)$ (71Pa1) | | Ni($^{16}O$,xnyp) (70No1) | |
|---|---|---|---|---|---|---|
| Peak | Energy (keV) | L | Energy (keV) | $J^\pi$ | Energy (keV) | $J^\pi$ |
| 1 | 0 | 0 | 0 | $0^+$ | 0 | $0^+$ |
| 2 | 1017 ± 5 | 2 | 1017 | $2^+$ | 1016 | $2^+$ |
| 3 | 1767 ± 10 | | 1779 | $2^+$ | 1777 | $2^+$ |
| | | | 2270 | $(4^\pm)$ | 2264 | $4^+$ |
| | | | 2429 | | | |
| | | | 2454 | (1,2) | | |
| 4 | 2648 ± 5 | (3,4) | 2651 | $(3^-,4^+)$ | | |
| 5* | 2826 ± 10 | | | | | |
| 6 | 2949 ± 10 | | | | | |
| 7 | 3011 ± 10 | | | | | |
| | | | 3043 | | | |
| 8 | 3175 ± 10 | | | | | |
| | | | 3788 | | | |
| | | | 4075 | | | |
| | | | 4237 | | | |

* Broad peak, possibly a multiplet.

Table 21. Energy levels, L values from the $^{72}Ge(p,t)^{70}Ge$ reaction.

| $^{72}Ge(p,t)^{70}Ge$ Present work | | | $^{70}Ge(p,p')$, $(p,p'\gamma)$ (69Hi2) | |
|---|---|---|---|---|
| Peak | Energy (keV) | L | Energy (keV) | $J^{\pi}$ |
| 1 | 0 | 0 | 0 | $0^+$ |
| 2 | 1036 | 2 | 1041 | $2^+$ |
| 3 | 1213 | 0 | 1216 | $0^+$ |
| 4 | 1708 | 2 | 1708 | $2^+$ |
| | | | 2153 | $4^+$ |
| 5 | 2148 | 2 | 2157 | $2^+$ |
| 6 | 2301 | (0) | 2307 | $0^+$ |
| | | | 2452 | (3) |
| | | | 2536 | $(1^{\pm},2^+)$ |
| 7 | 2558 | (3,4) | 2562 | $3^-$ |
| | | | 2807 | $(4^+)$ |
| | | | 2887 | 0 |
| 8 | 2937 | | 2945 | (2,1) |
| | | | 3047 | $3^+$ |
| 9 | 3058 | 4,(3) | 3059 | $4^+$ |
| | | | 3107 | (0) |
| | | | 3182 | |
| 10 | 3187 | | 3195 | |
| | | | 3242 | 1 |

Table 21. (con'd)

| Peak | Energy | L | Energy | $J^{\pi}$ |
|---|---|---|---|---|
| | | | 3296 | |
| | | | 3316 | 1 |
| 11 | 3327 | | 3336 | |
| | | | 3345 | |
| | | | 3351 | |
| | | | 3419 | |
| | | | 3428 | |
| 12 | 3430 | | 3432 | |
| | | | 3456 | |
| | | | 3483 | (1,2) |
| | | | 3489 | 3,4 |
| 13 | 3566 | (3,4) | 3563 | |
| | | | 3570 | |
| | | | 3581 | |
| | | | 3593 | 3,4 |
| 14 | 3628 | (2,3) | 3633 | |
| | | | 3667 | |
| 15 | 3676 | | 3678 | 3,4 |
| | | | 3691 | |
| | | | 3710 | |

Table 22. Energy levels, L values from the $^{73}Ge(p,t)^{71}Ge$ reaction.

| Peak | Energy (keV) | L |
|---|---|---|
| 1 | 198 | 0 |
| 2 | 515 | (2,3) |
| 3* | 587 | |
| 4 | 1038 | 0 |
| 5 | 1183 | (2,3) |
| 6 | 1472 | |
| 7* | 1955 | (4) |

*Broad peak, possibly a multiplet.

Table 23. Energy levels, L values from the $^{74}Ge(p,t)^{72}Ge$ reaction.

| Peak | Energy (keV) | L |
|---|---|---|
| 1 | 0 | 0 |
| 2 | 690 | 0 |
| 3 | 835 | 2 |
| 4 | 1465 | 2 |
| 5 | 2405 | |
| 6 | 2513 | 3 |
| 7 | 2942 | |
| 8 | 3074 | |
| 9 | 3129 | |
| 10 | 3323 | 3,(2) |
| 11 | 3411 | (2,3) |

Table 24. Energy levels, L values from the $^{76}Ge(p,t)^{74}Ge$ reaction.

| $^{76}Ge(p,t)^{74}Ge$ Present work | | | $^{74}Ga(\beta^+,\gamma)^{74}Ge$ (71Cal1) | |
|---|---|---|---|---|
| Peak | Energy (keV) | L | Energy (keV) | $J^\pi$ |
| 1 | 0 | 0 | 0 | $0^+$ |
| 2 | 597 | 2 | 596 | $2^+$ |
| 3 | 1206 | 2,3 | 1204 | $2^+$ |
| | | | 1464 | $4^+$ |
| 4 | 1479 | | 1483 | $0^+$ |
| | | | 1697 | $(3^+)$ |
| | | | 2165 | $4^+$ |
| 5 | 2181 | | 3198 | $2^+$ |
| 6 | 2535 | 3 | 2537 | $3^-$ |
| 7 | 2672 | | 2694 | $(2,3^-)$ |
| 8 | 2838 | | 2822 | $(2,4^+)$ |
| 9 | 2941 | | 2949 | $3^-$ |
| 10 | 3024 | 2,3 | 3034 | $(2^+)$ |
| 11 | 3137 | 3,4 | 3140 | $3^-$ |
| | | | 3176 | $(2,3^-)$ |
| 12 | 3210 | | 3342 | $(2^+)$ |
| 13 | 3373 | | | |
| 14 | 3495 | | 3478 | $3^-$ |
| 15 | 3575 | | 3567 | $(2,4^+)$ |
| | | | 3639 | $(1^-,2^+)$ |

Table 24. (con'd)

| Peak | Energy | L | Energy | $J^{\pi}$ |
|---|---|---|---|---|
| | | | 3697 | |
| | | | 3722 | $(3^-)$ |
| | | | 3807 | |
| | | | 3829 | |
| | | | 3895 | $(2^{\pm})$ |
| 16 | 3936 | | 3949 | |
| | | | 3976 | |
| | | | 4201 | |

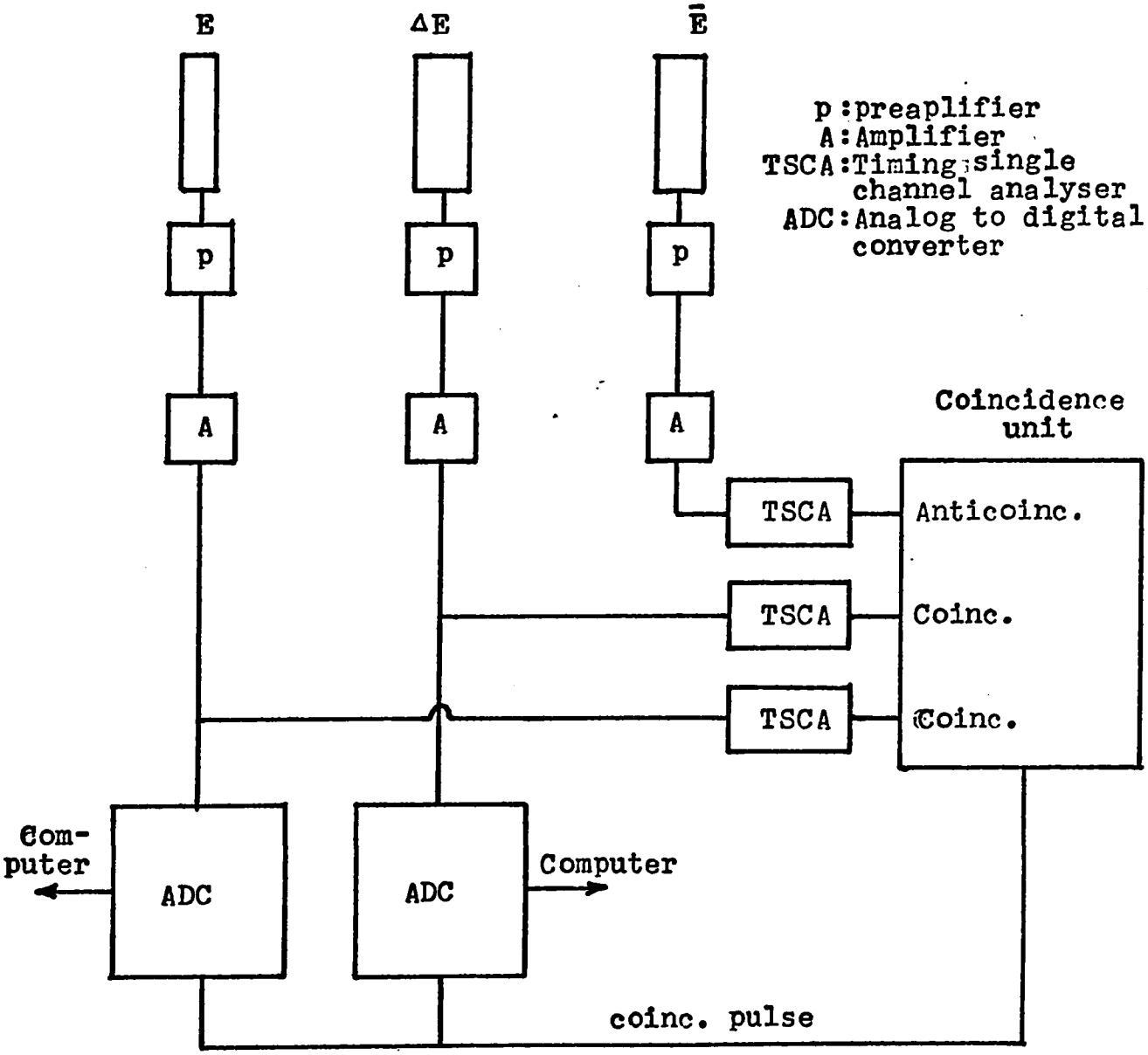


Fig. 1 Electronics.

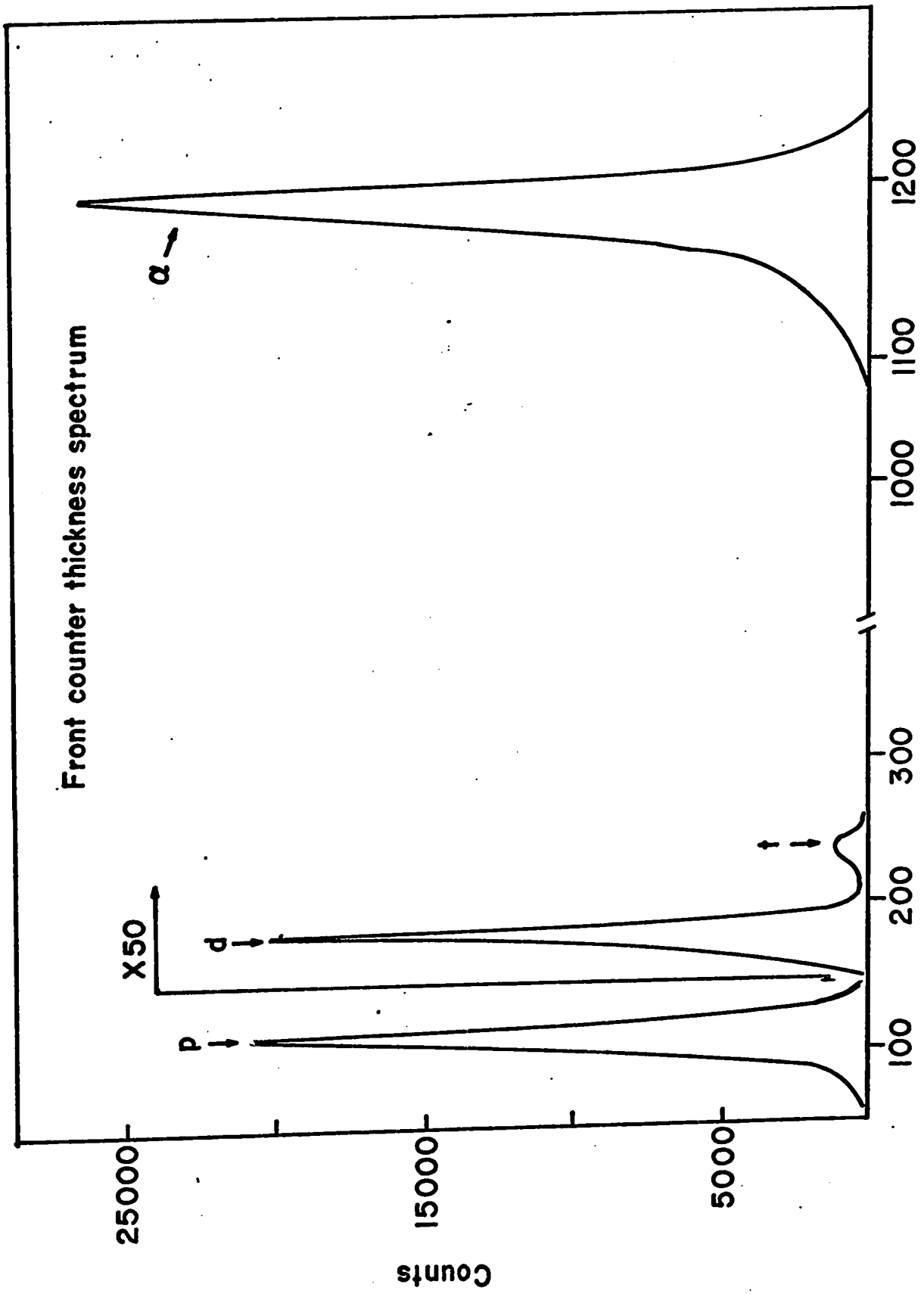


Fig. 2 Mass spectrum

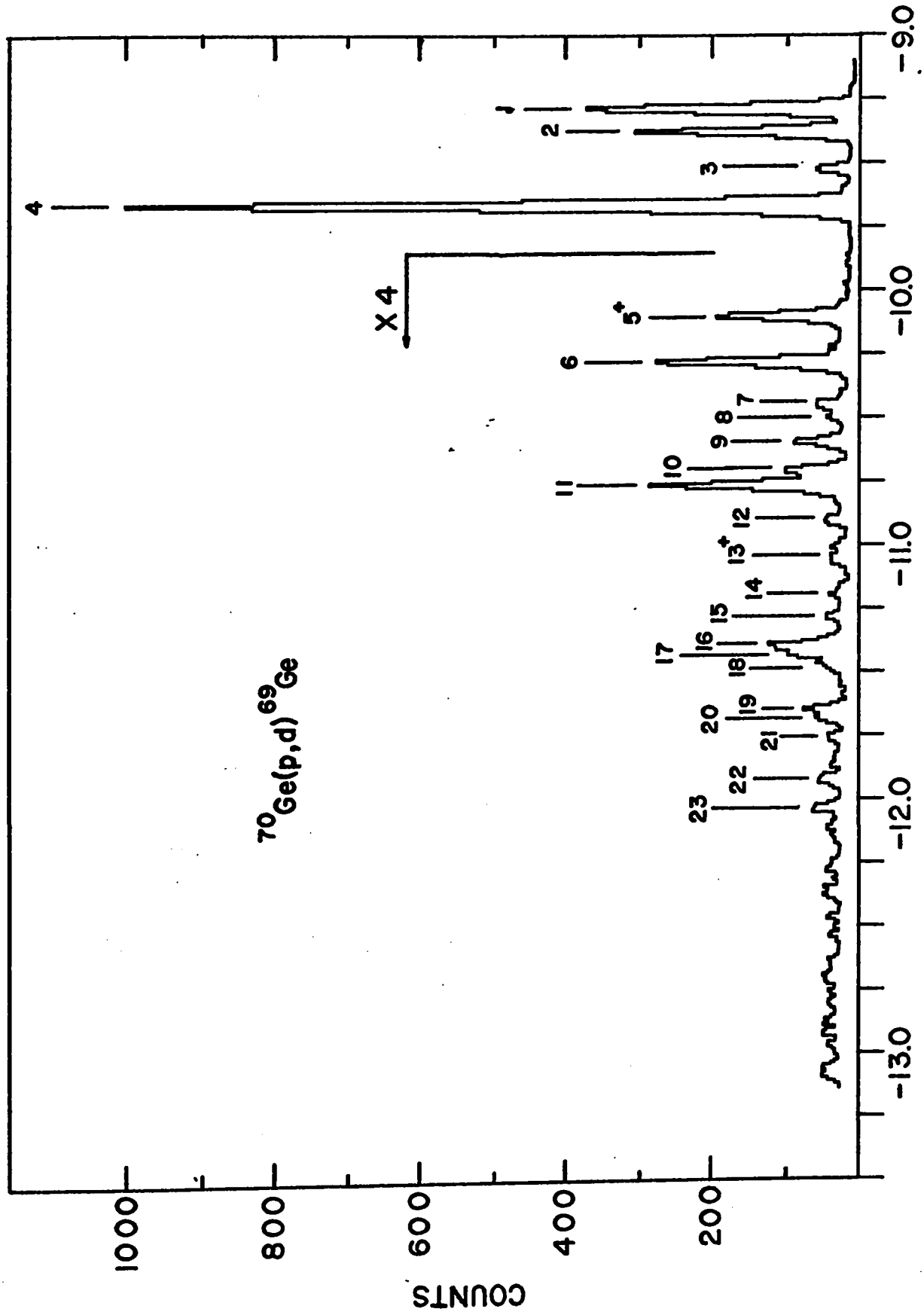


Fig. 3 Summed Q value spectrum of the $^{70}Ge(p,d)^{69}Ge$ reaction.

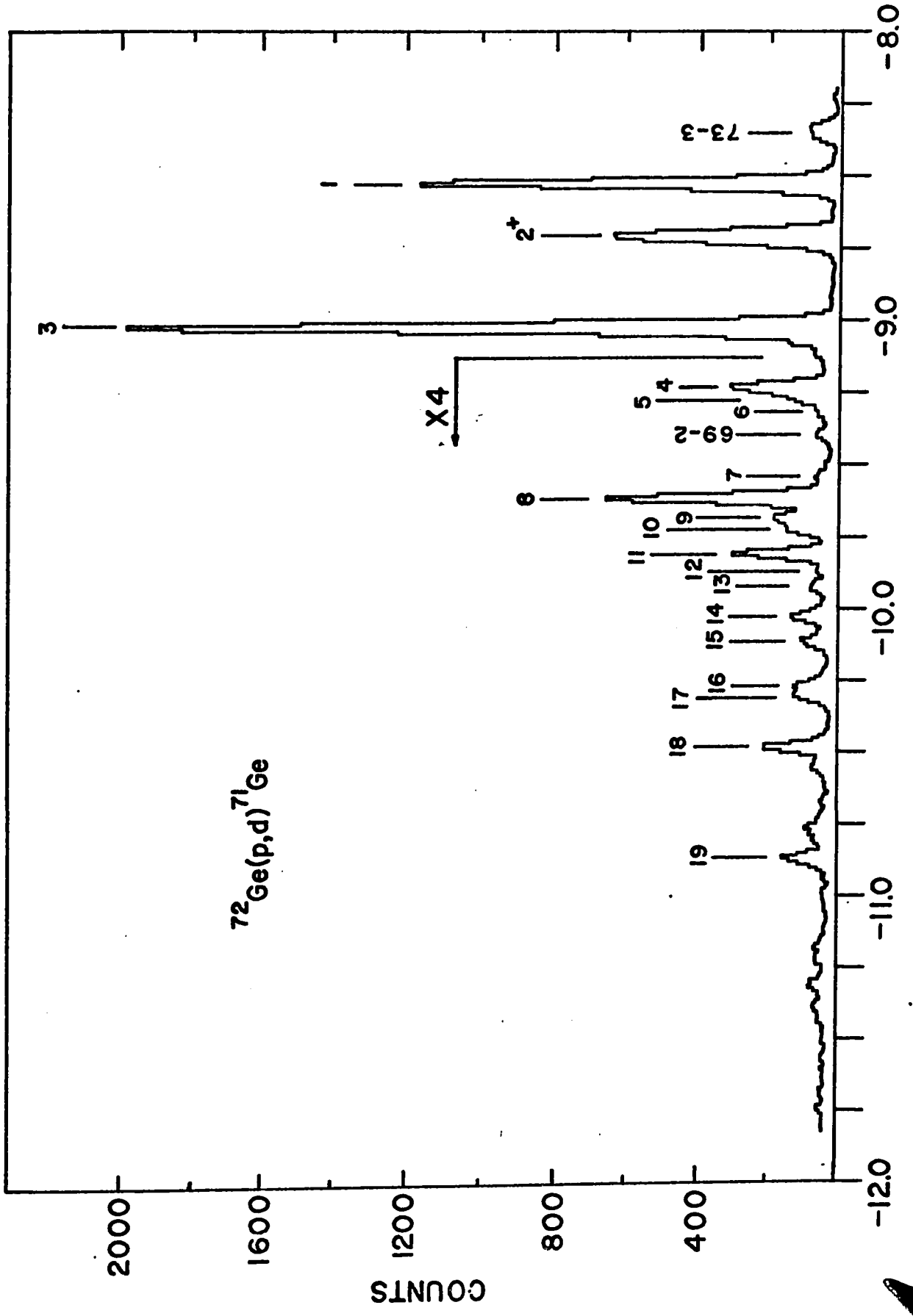


Fig. 4 Summed Q value spectrum of the $^{72}$Ge(p,d)$^{71}$Ge reaction.

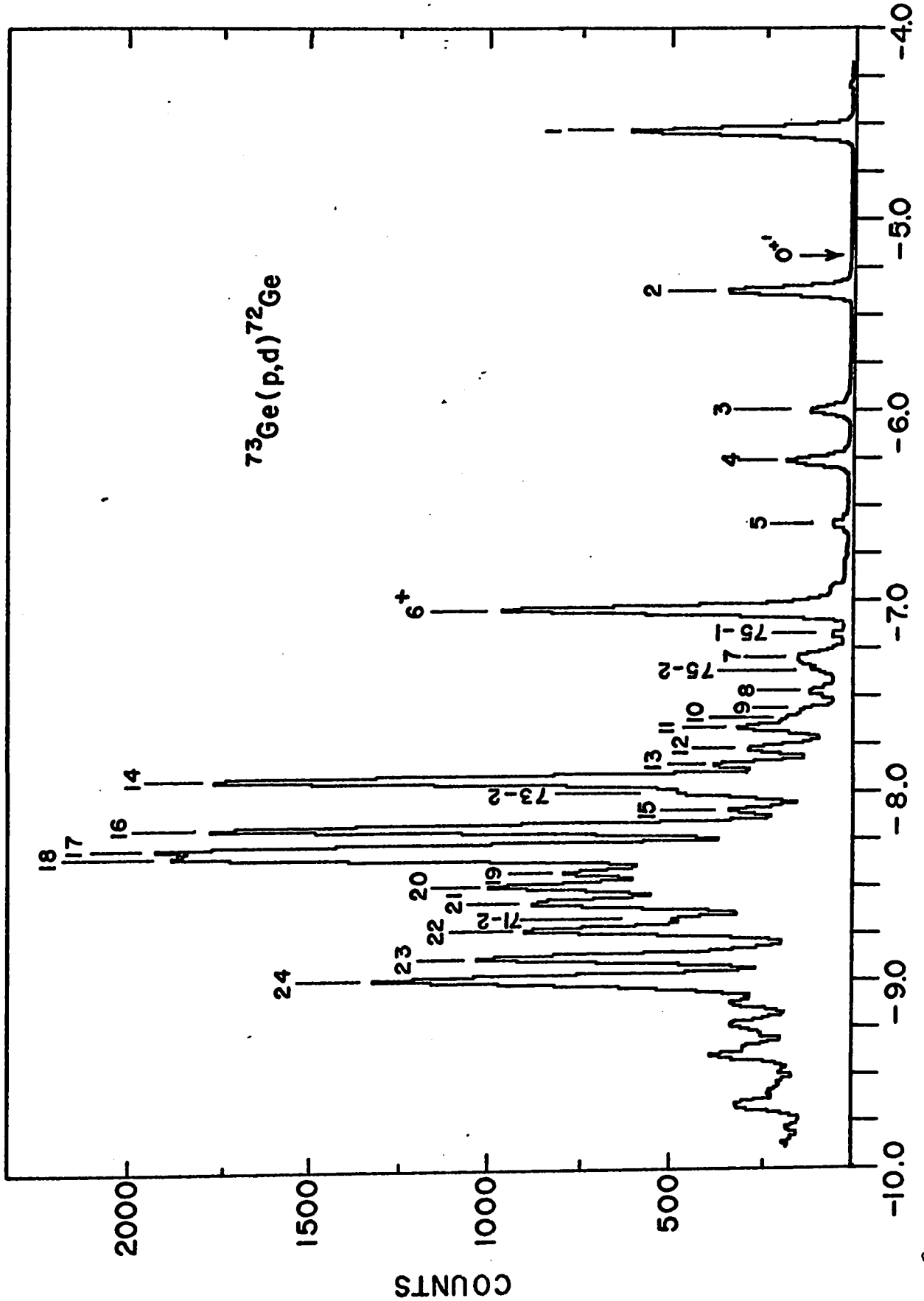


Fig. 5 Summed Q value spectrum of the $^{73}Ge9p,d)^{72}Ge$ reaction.

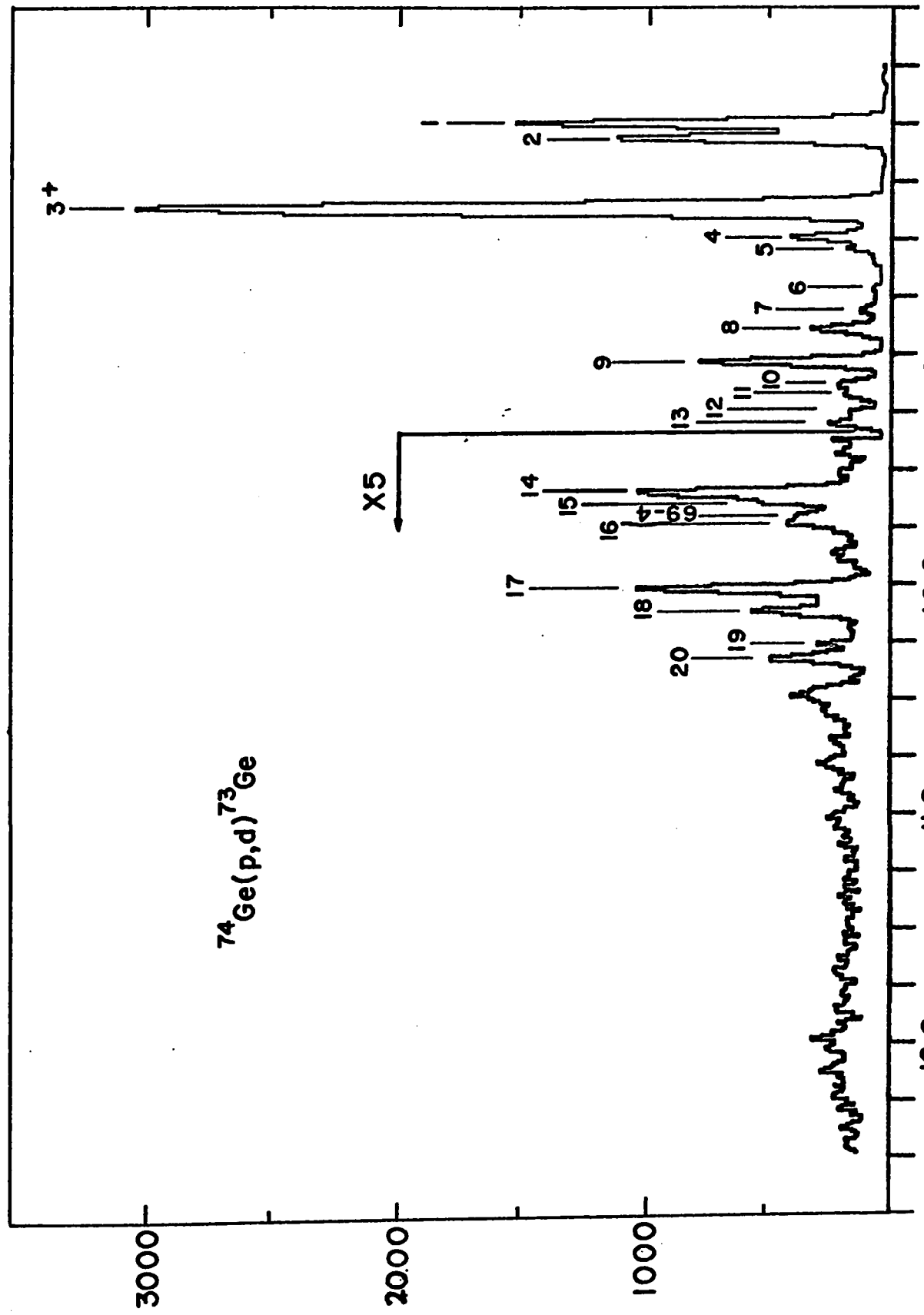


Fig. 6 Summed Q value spectrum of the $^{74}$Ge(p,d)$^{73}$Ge reaction.

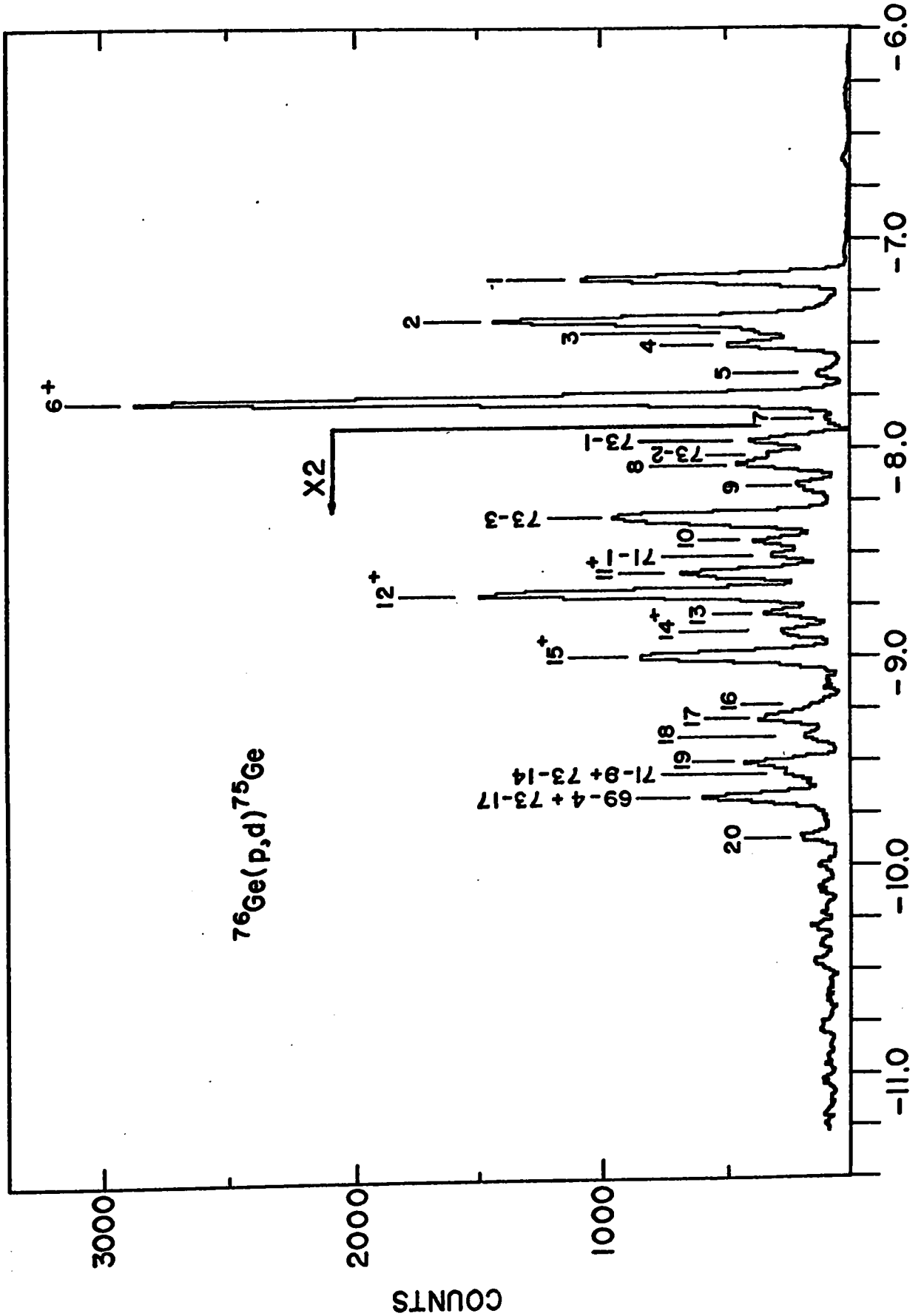


Fig. 7 Summed Q value spectrum of the $^{76}$Ge(p,d)$^{75}$Ge reaction.

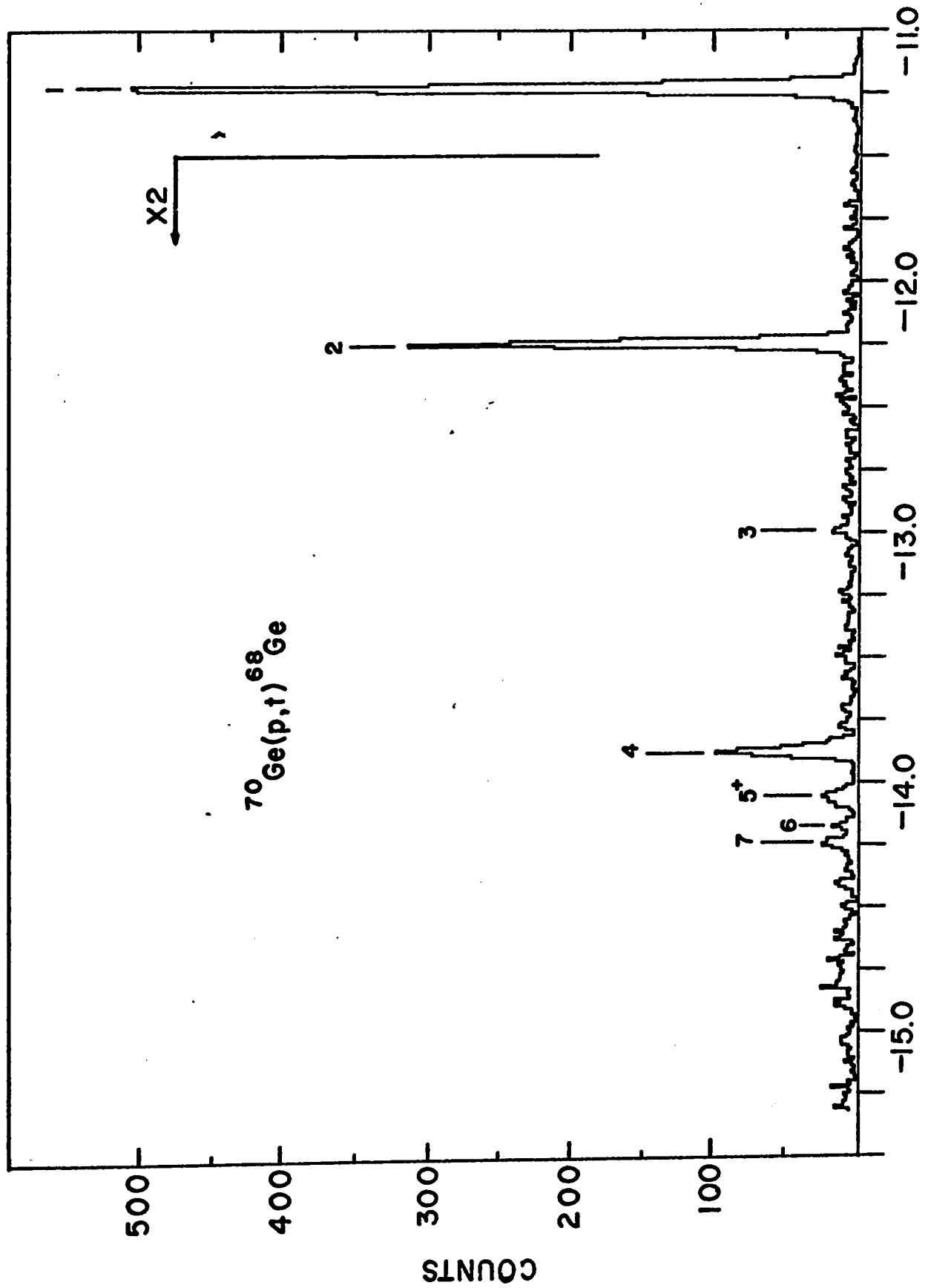


Fig. 8 Summed Q value spectrum of the $^{70}$Ge(p,t)$^{68}$Ge reaction.

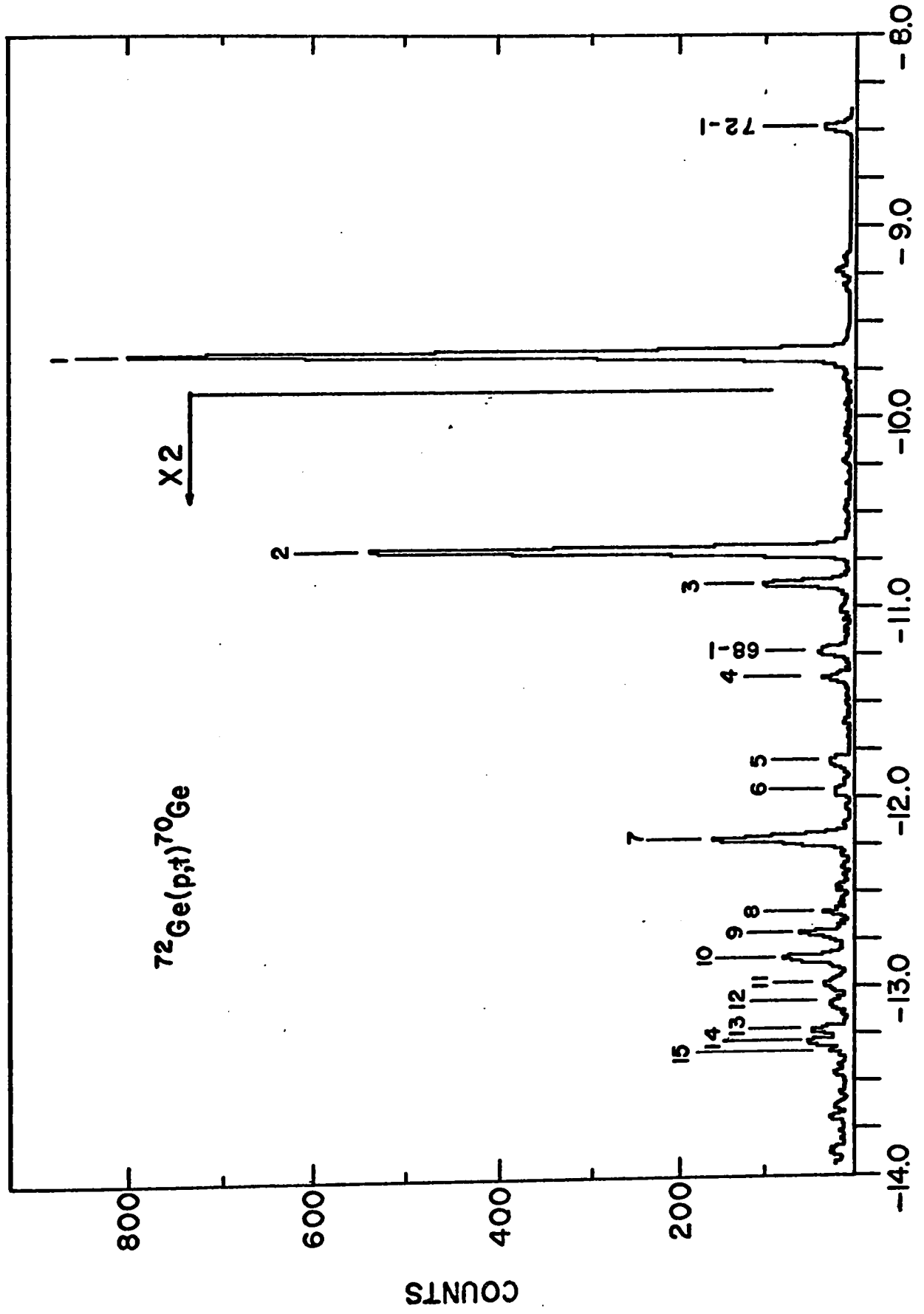


Fig. 9 Summed Q value spectrum of the $^{72}$Ge(p,t)$^{70}$Ge reaction.

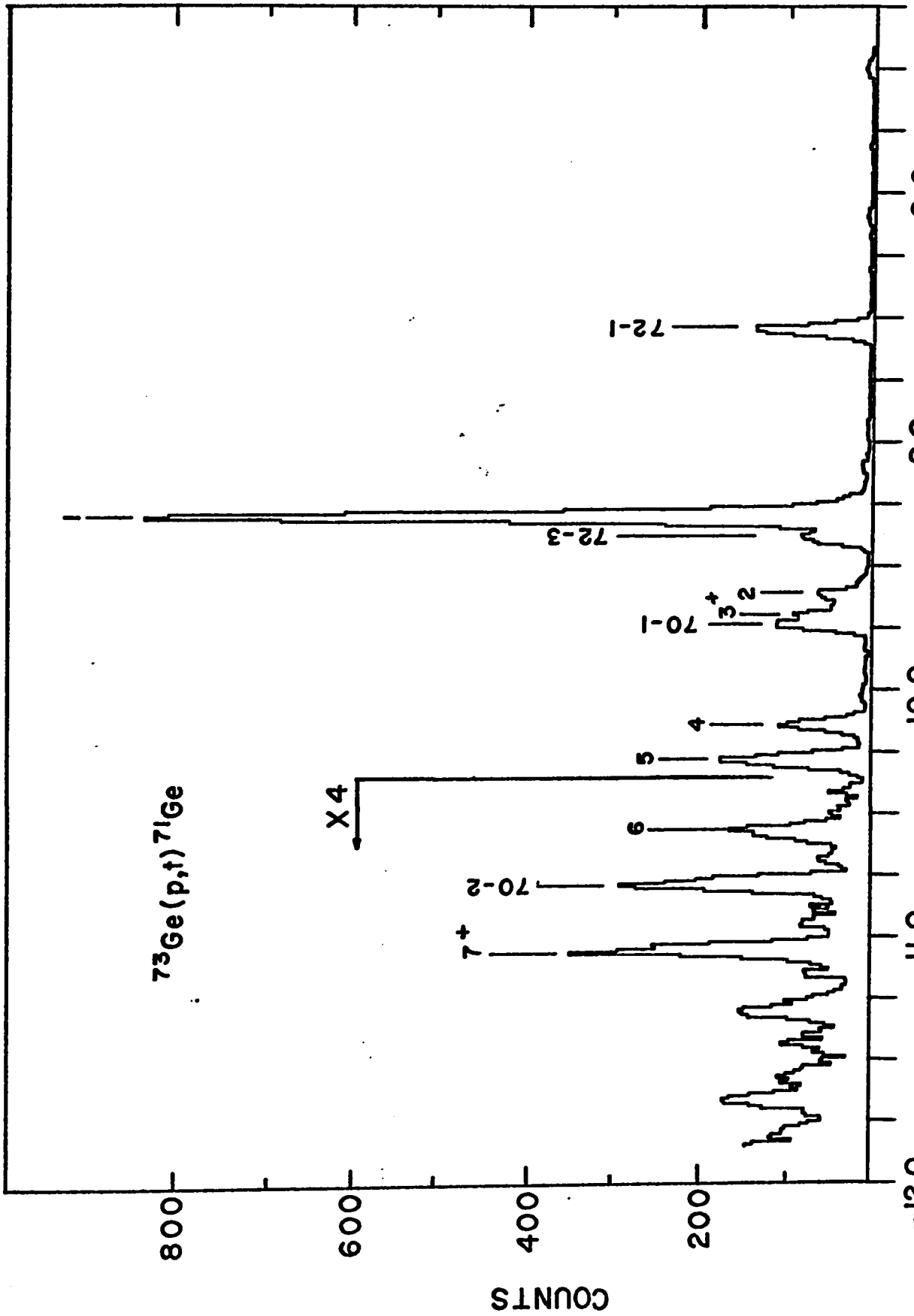


Fig. 10 Summed Q value spectrum of the $^{73}Ge(p,t)^{71}Ge$ reaction.

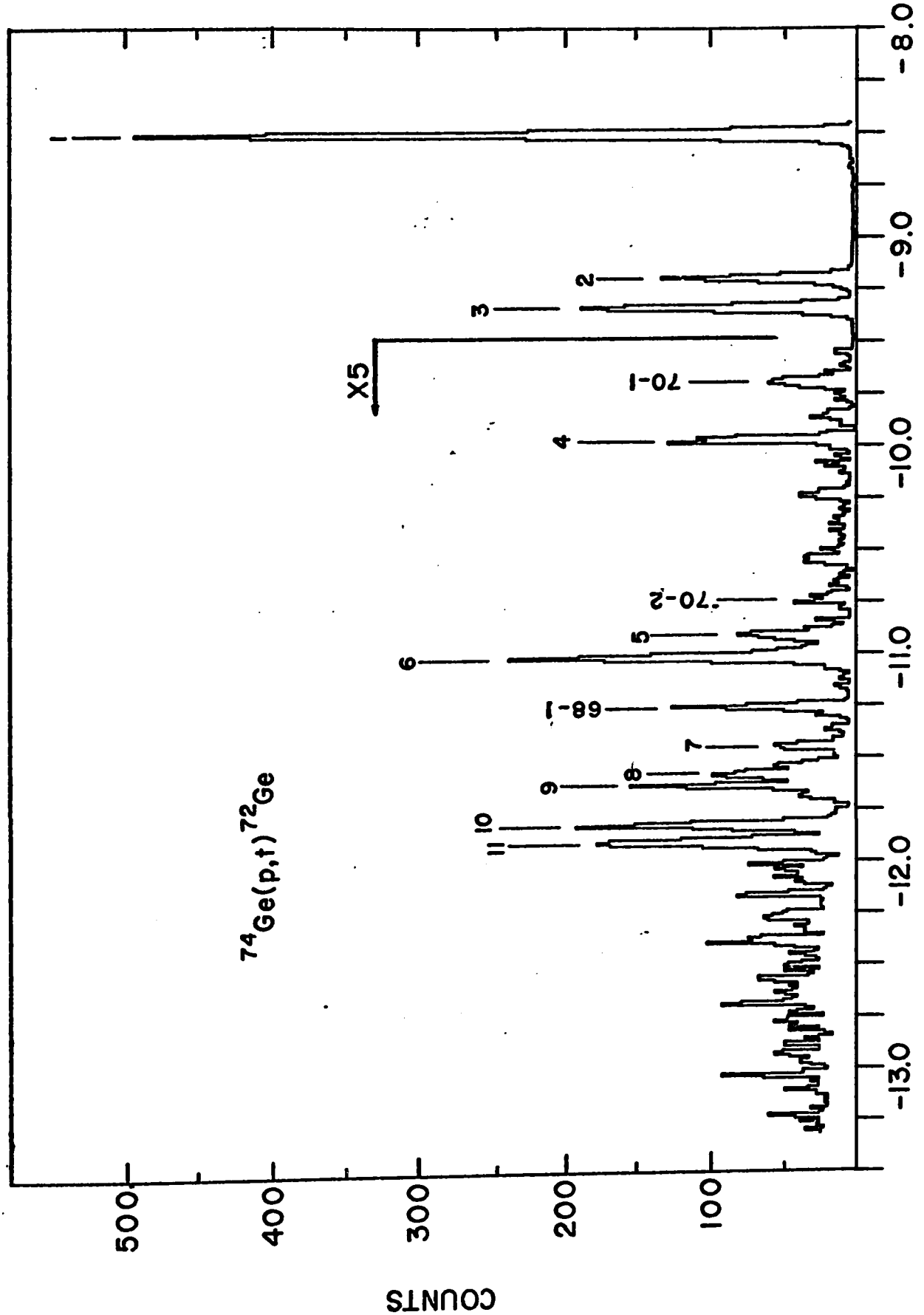


Fig. 11 Summed Q value spectrum of the $^{74}$Ge(p,t)$^{72}$Ge reaction.

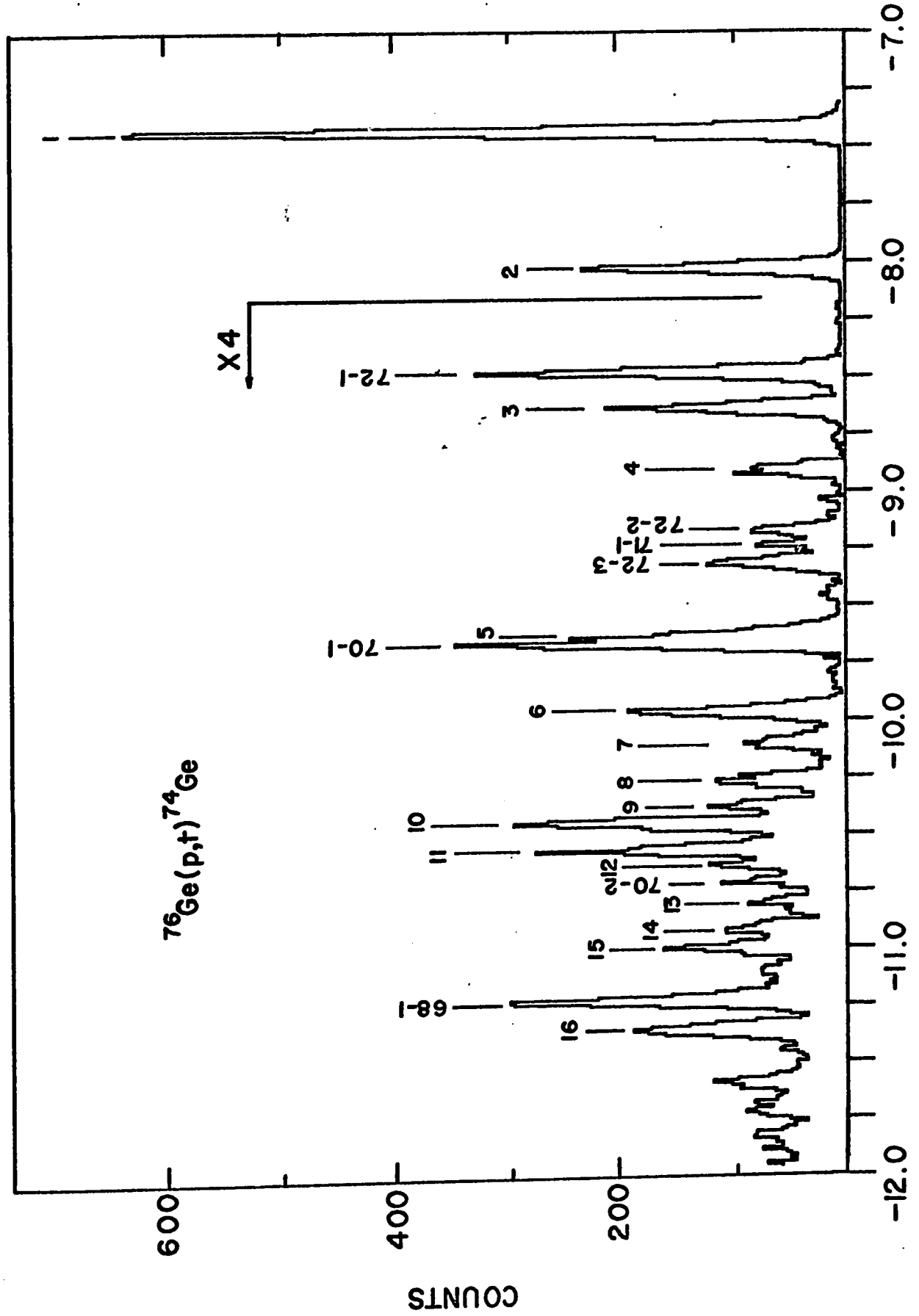


Fig. 12 Summed Q value spectrum of the $^{76}Ge(p,t)^{74}Ge$ reaction.

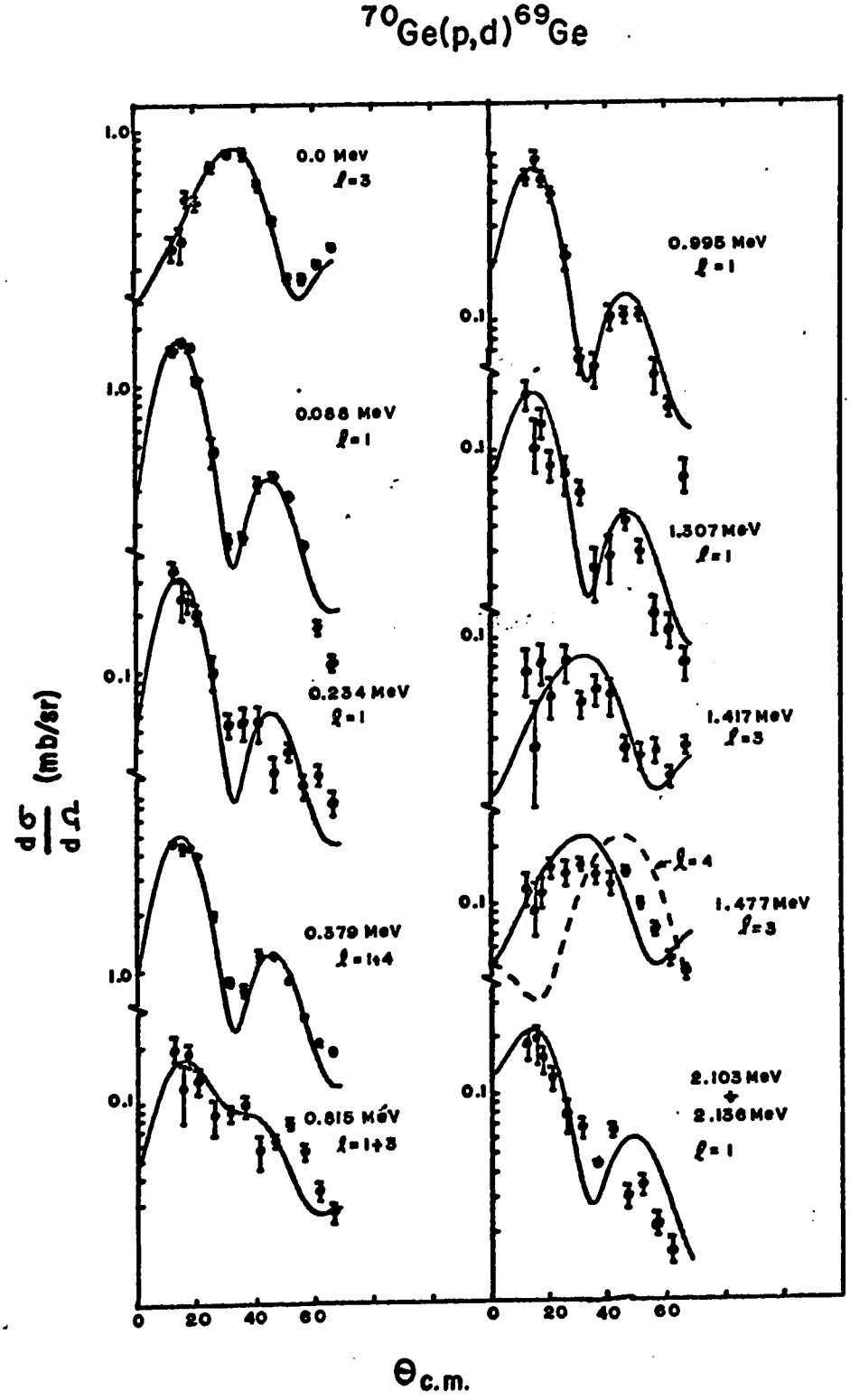


Fig. 13 Angular distributions from the $^{70}Ge(p,d)^{69}Ge$ reaction.

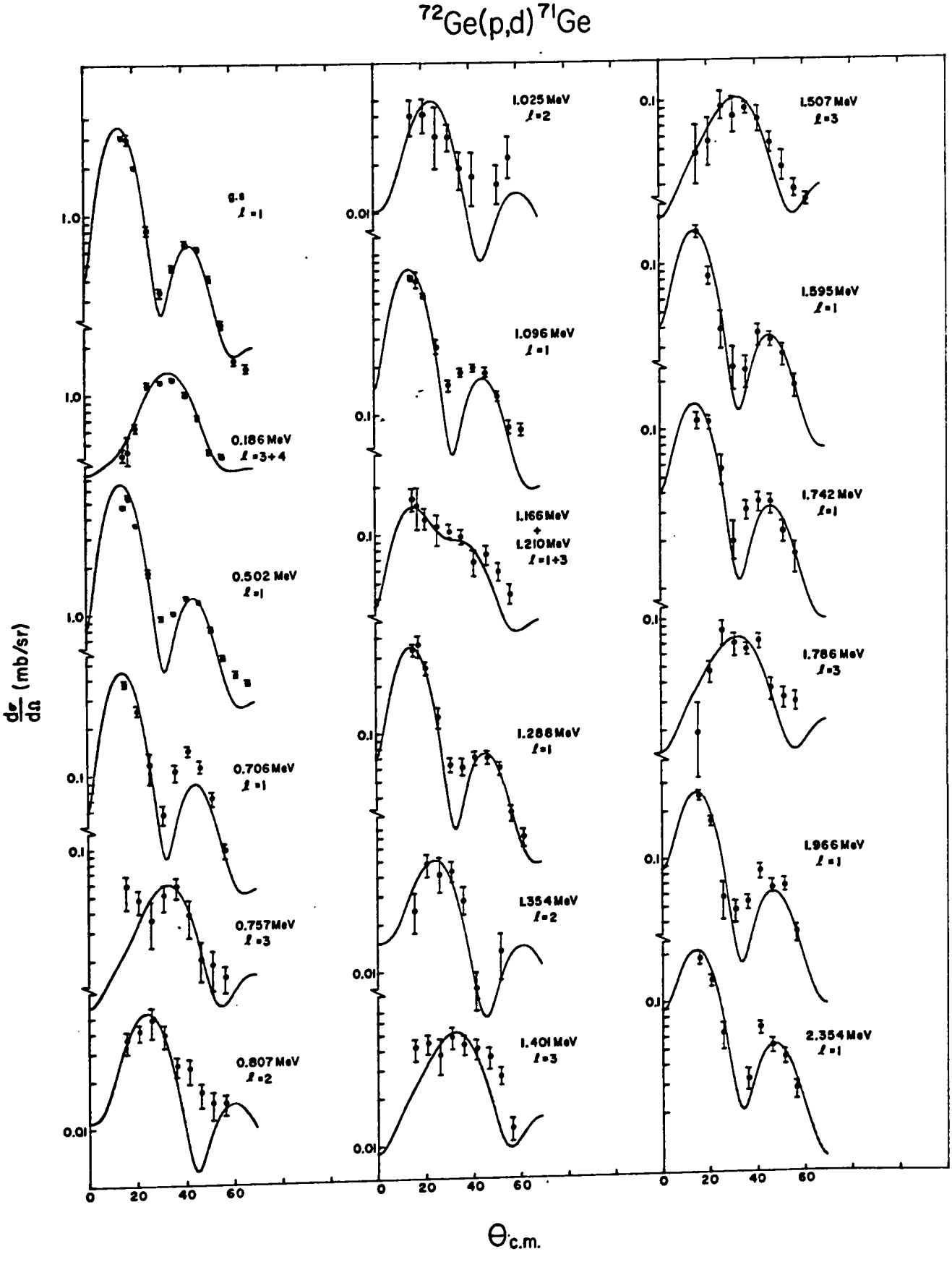


Fig. 14 Angular distributions from the $^{72}Ge(p,d)^{71}Ge$ reaction.

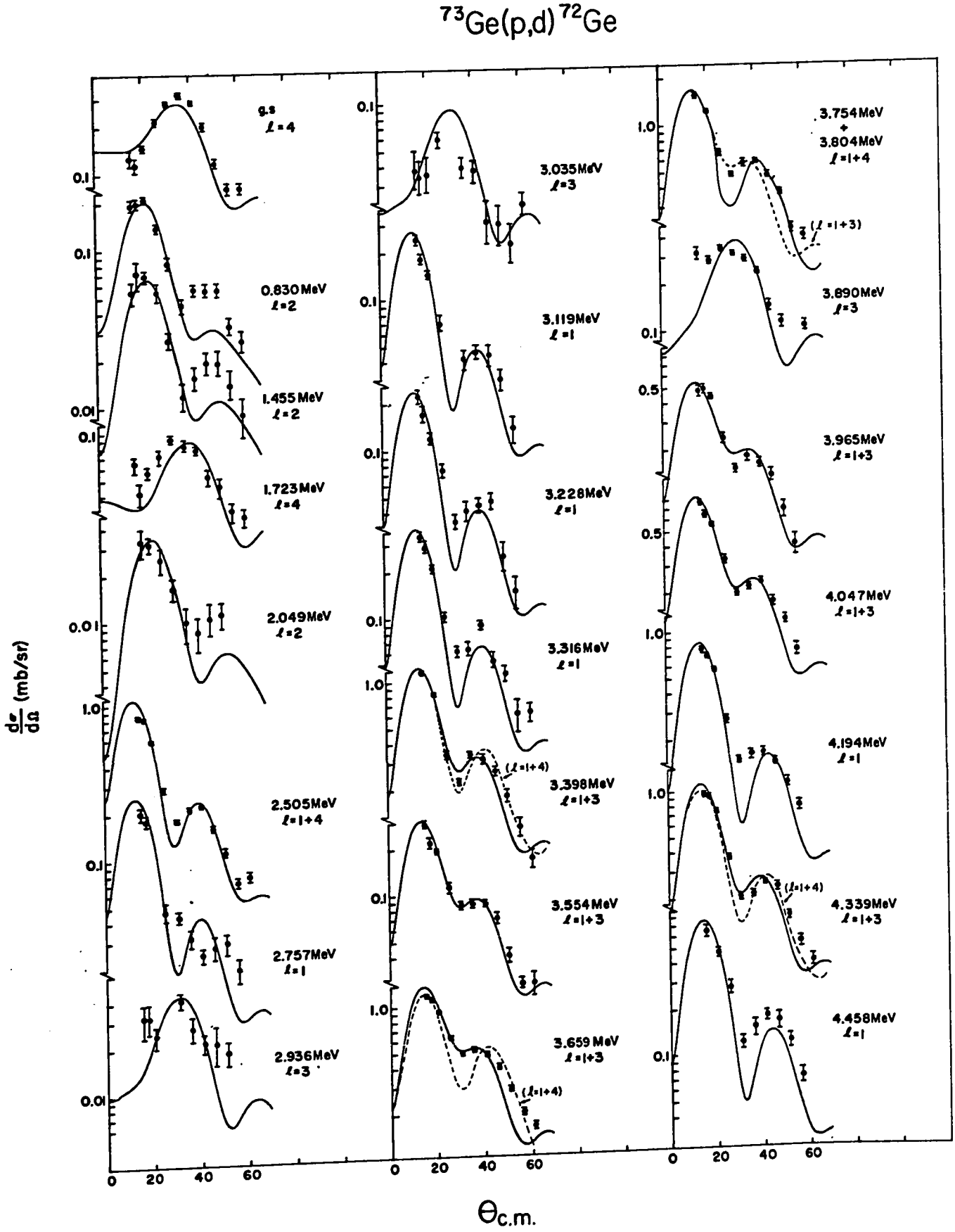


Fig. 15 Angular distributions from the $^{73}Ge(p,d)^{72}Ge$ reaction.

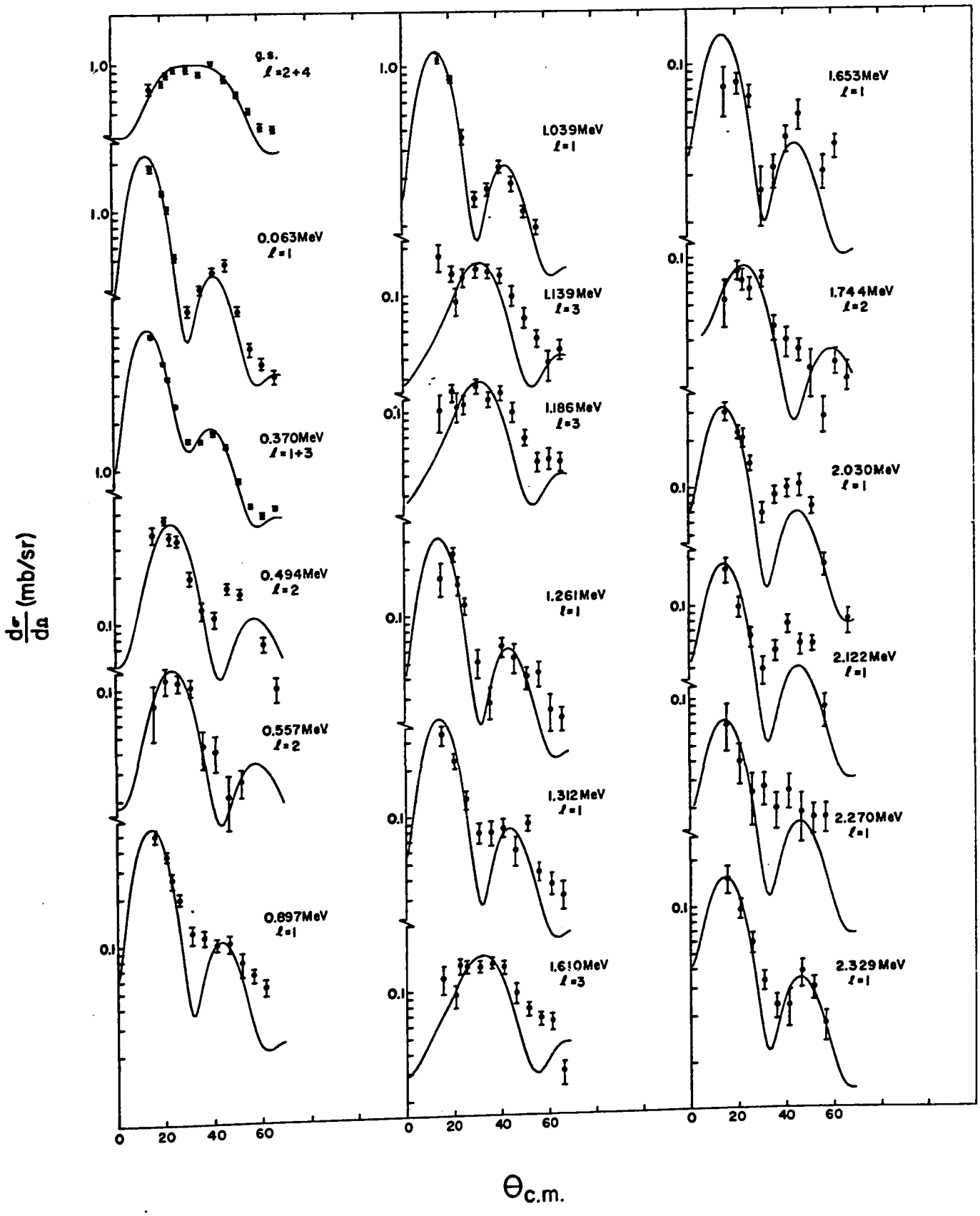


Fig. 16 Angular distributions from the $^{74}Ge(p,d)^{73}Ge$ reaction.

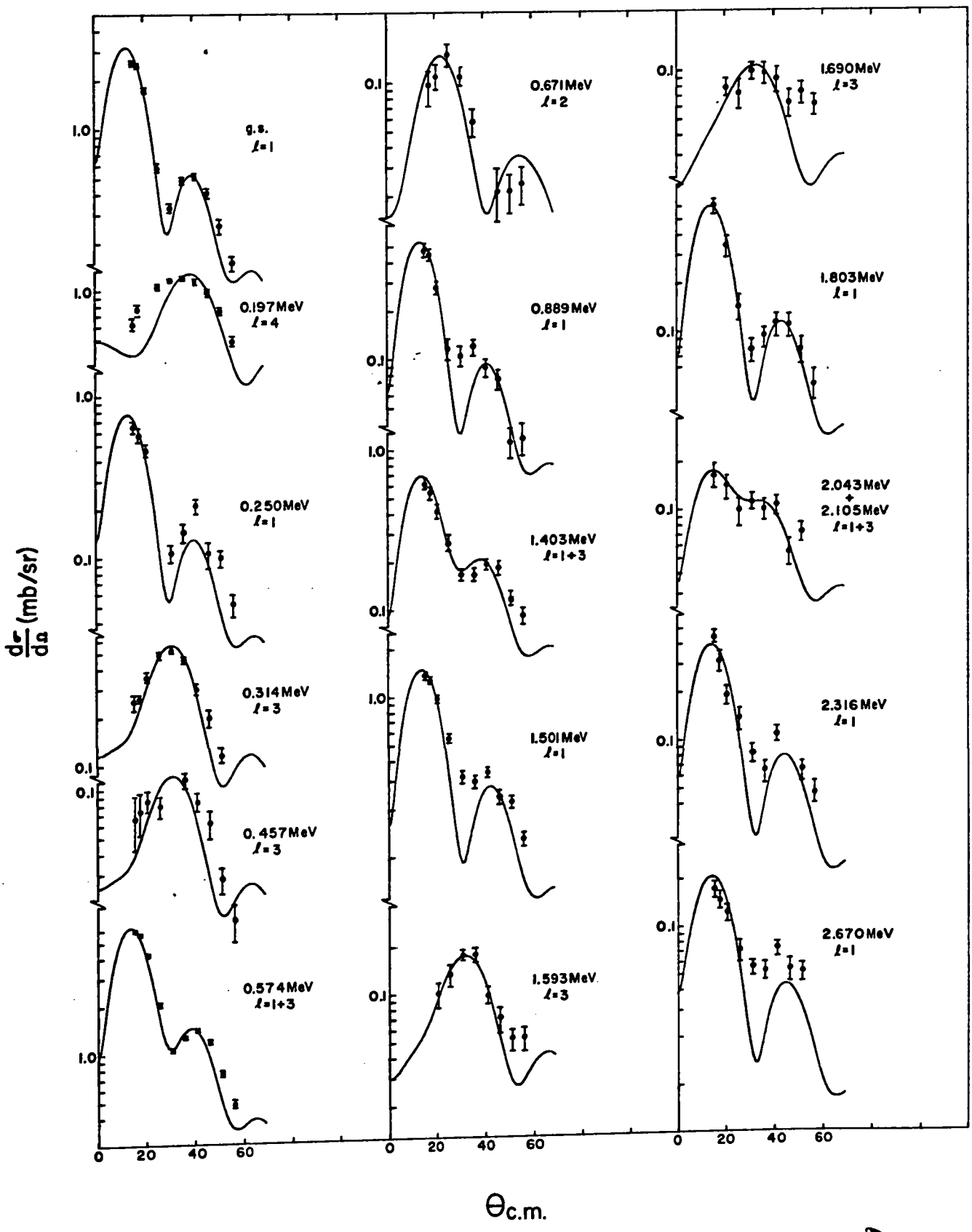


Fig. 17 Angular distributions from the $^{76}Ge(p,d)^{75}Ge$ reaction.

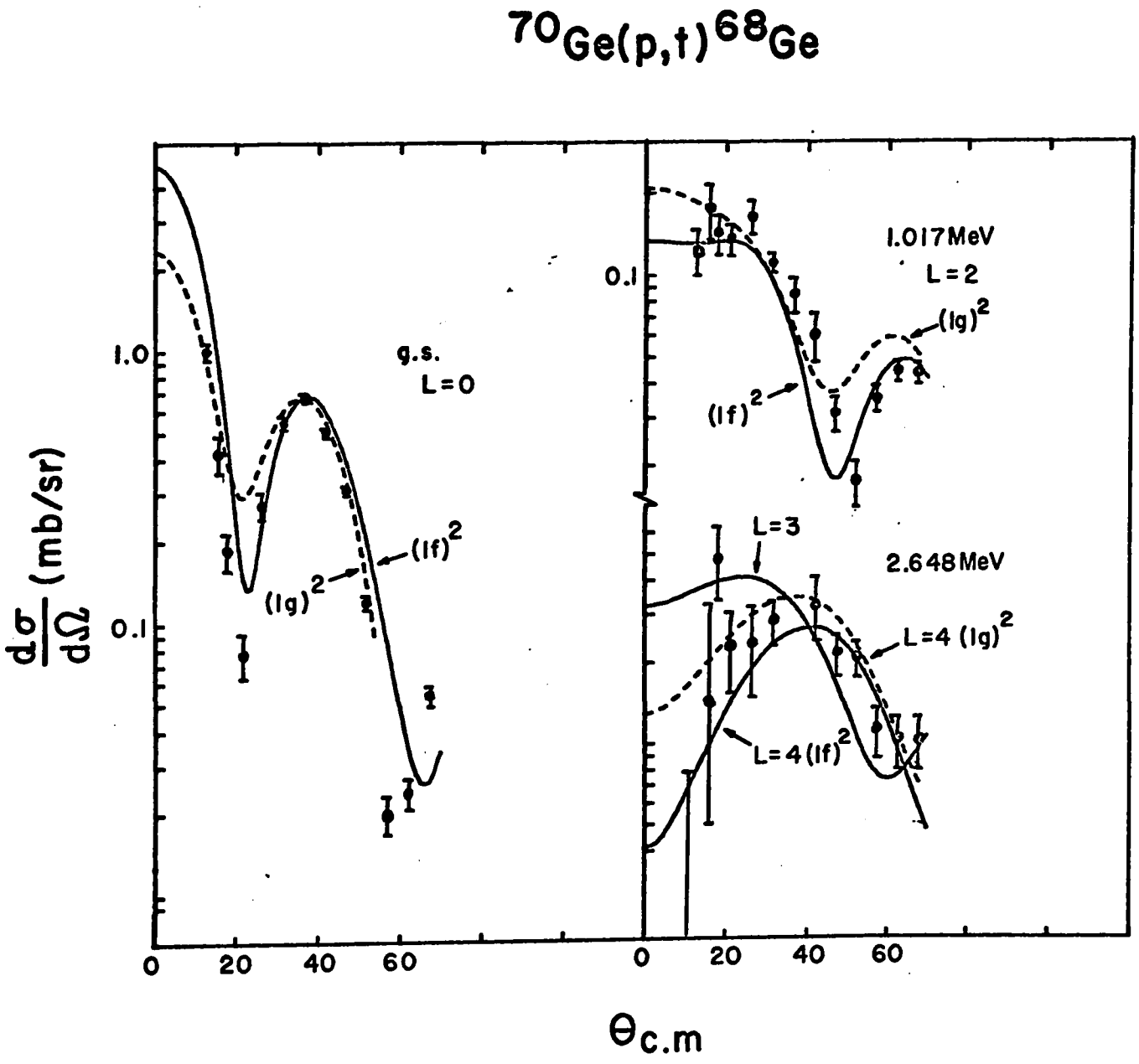


Fig. 18 Angular distributions from the $^{70}Ge(p,t)^{68}Ge$ reaction.

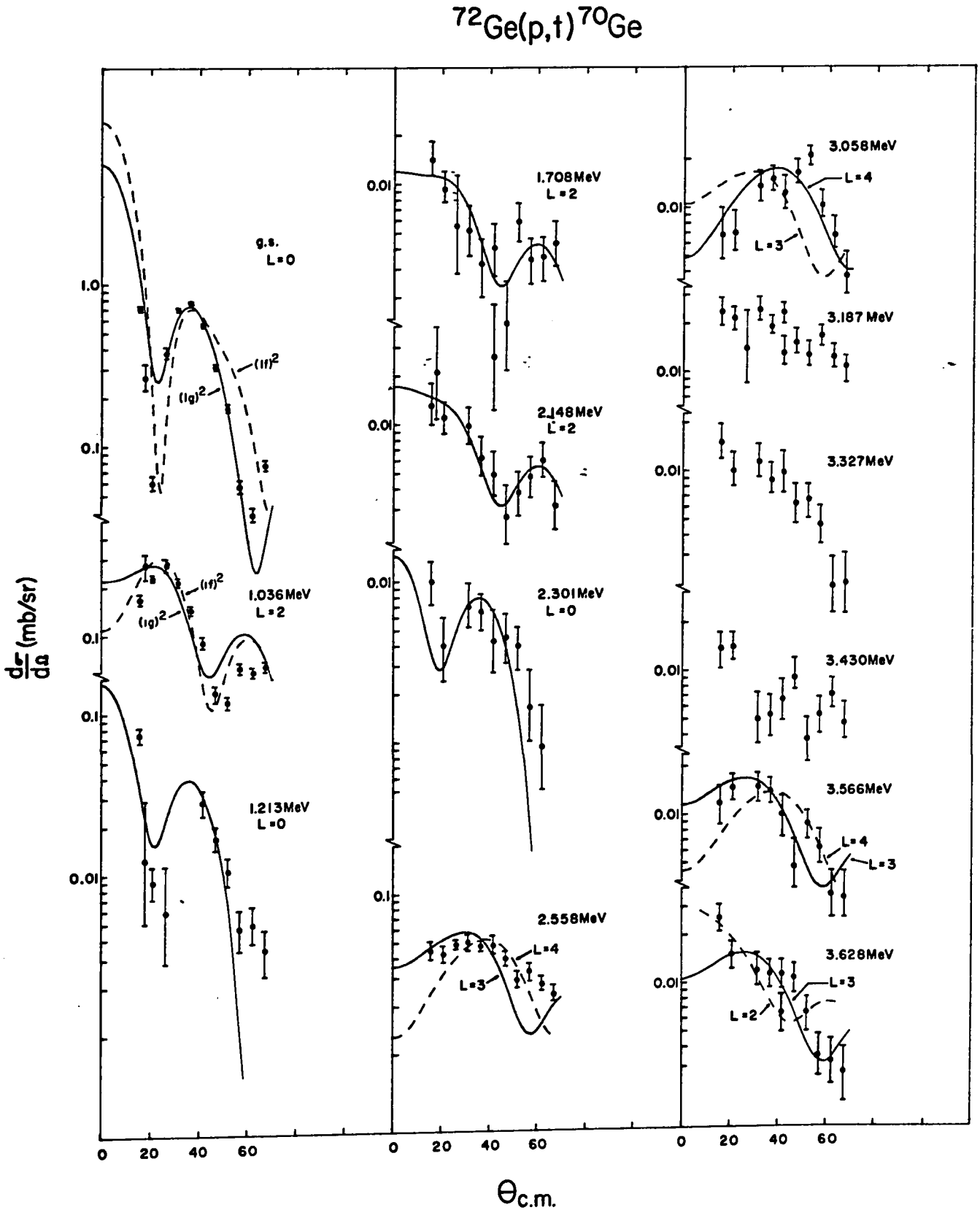


Fig. 19 Angular distributions from the $^{72}Ge(p,t)^{70}Ge$ reaction.

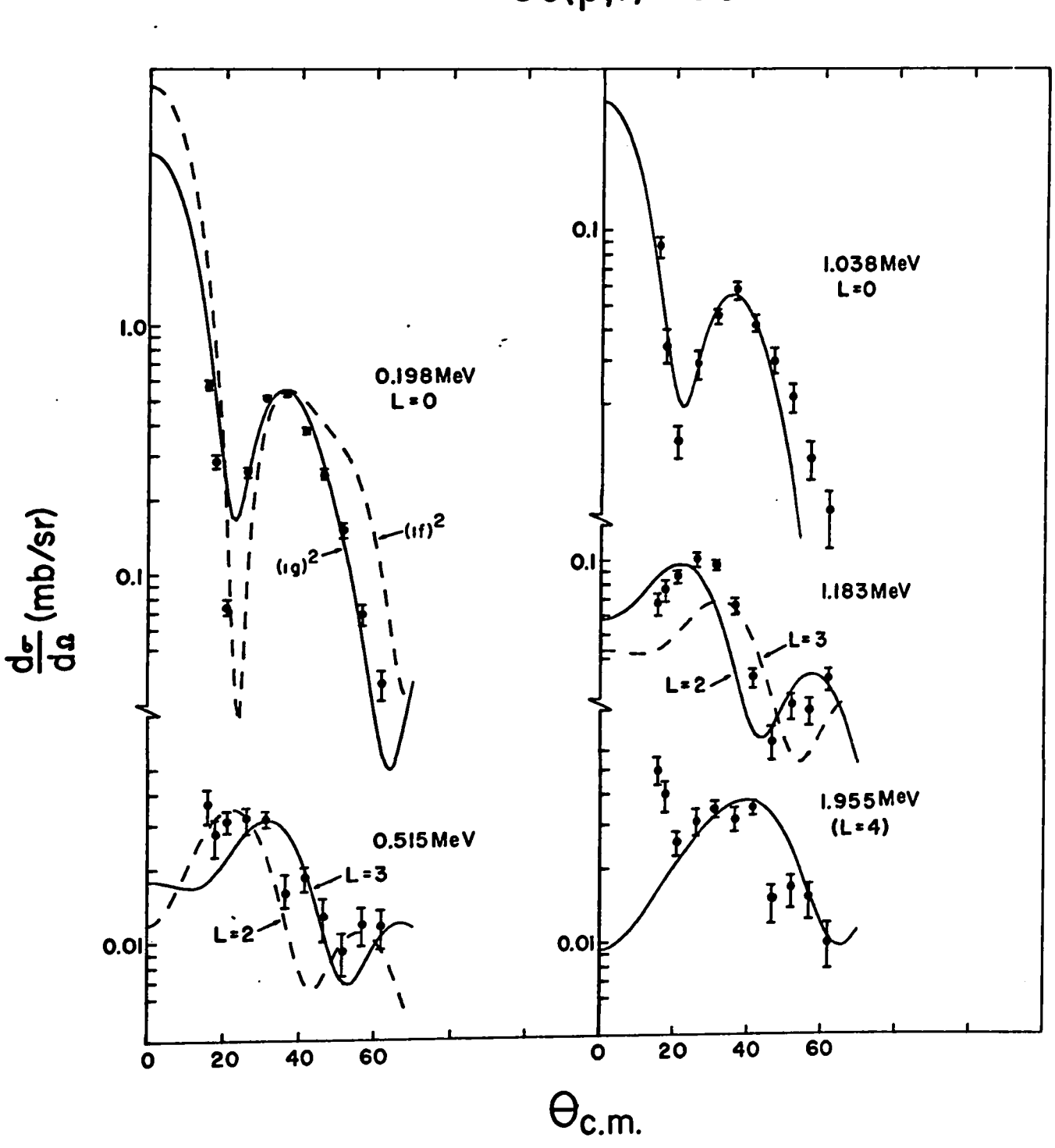


Fig. 20 Angular distributions from the $^{73}Ge(p,t)^{71}Ge$ reaction.

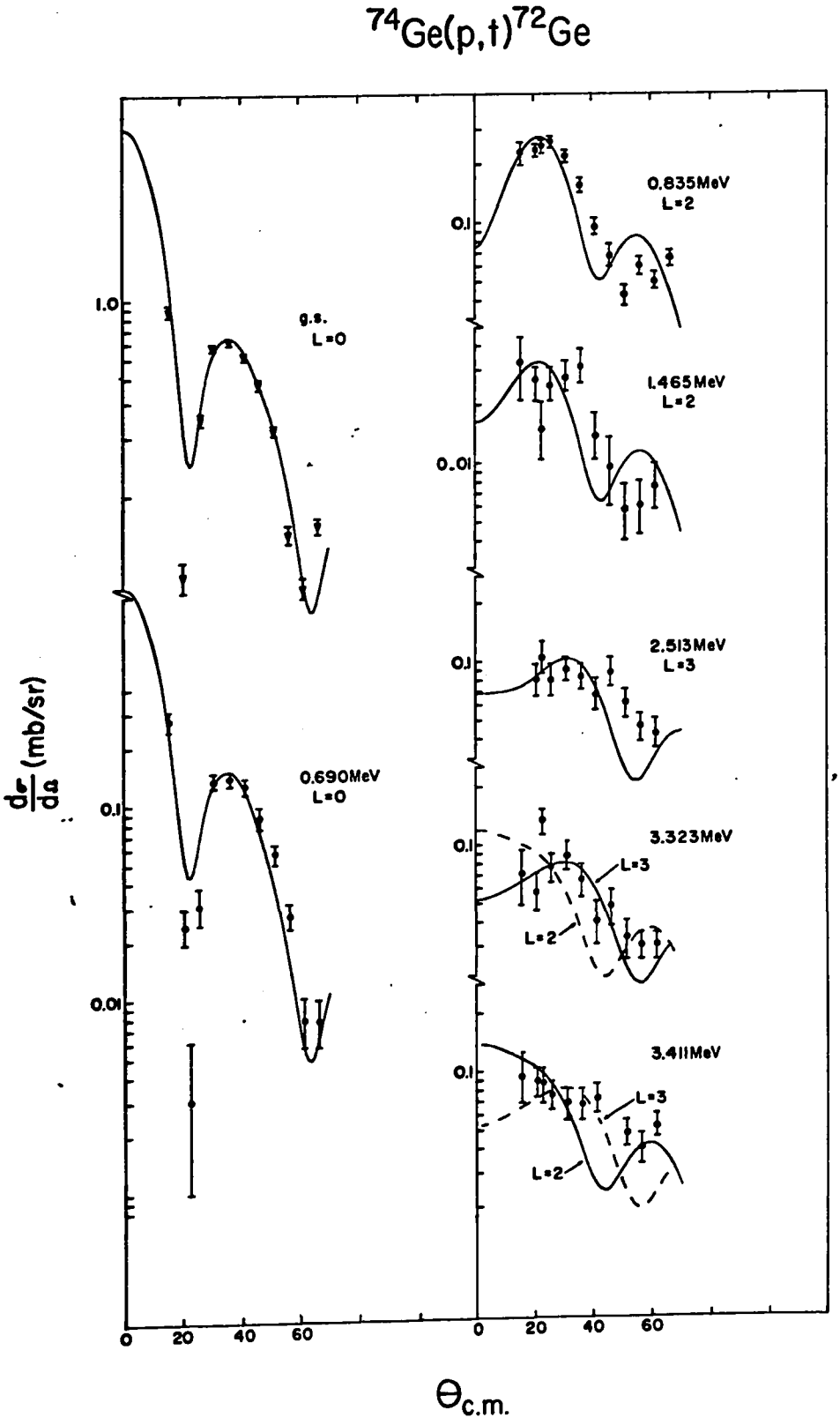


Fig. 21 Angular distributions from the $^{74}Ge(p,t)^{73}Ge$ reaction.

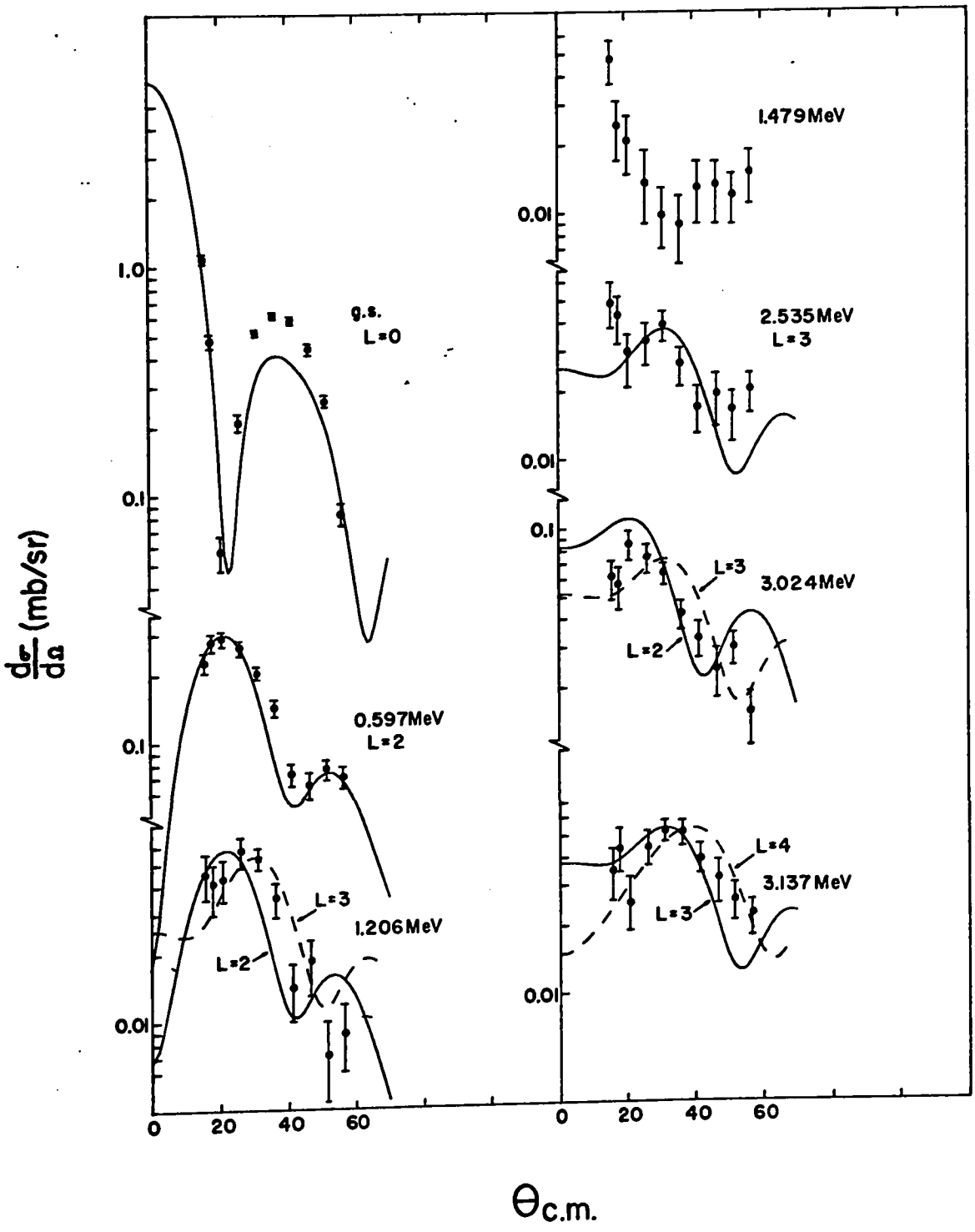


Fig. 22 Angular distributions from the $^{76}Ge(p,t)^{74}Ge$ reaction.

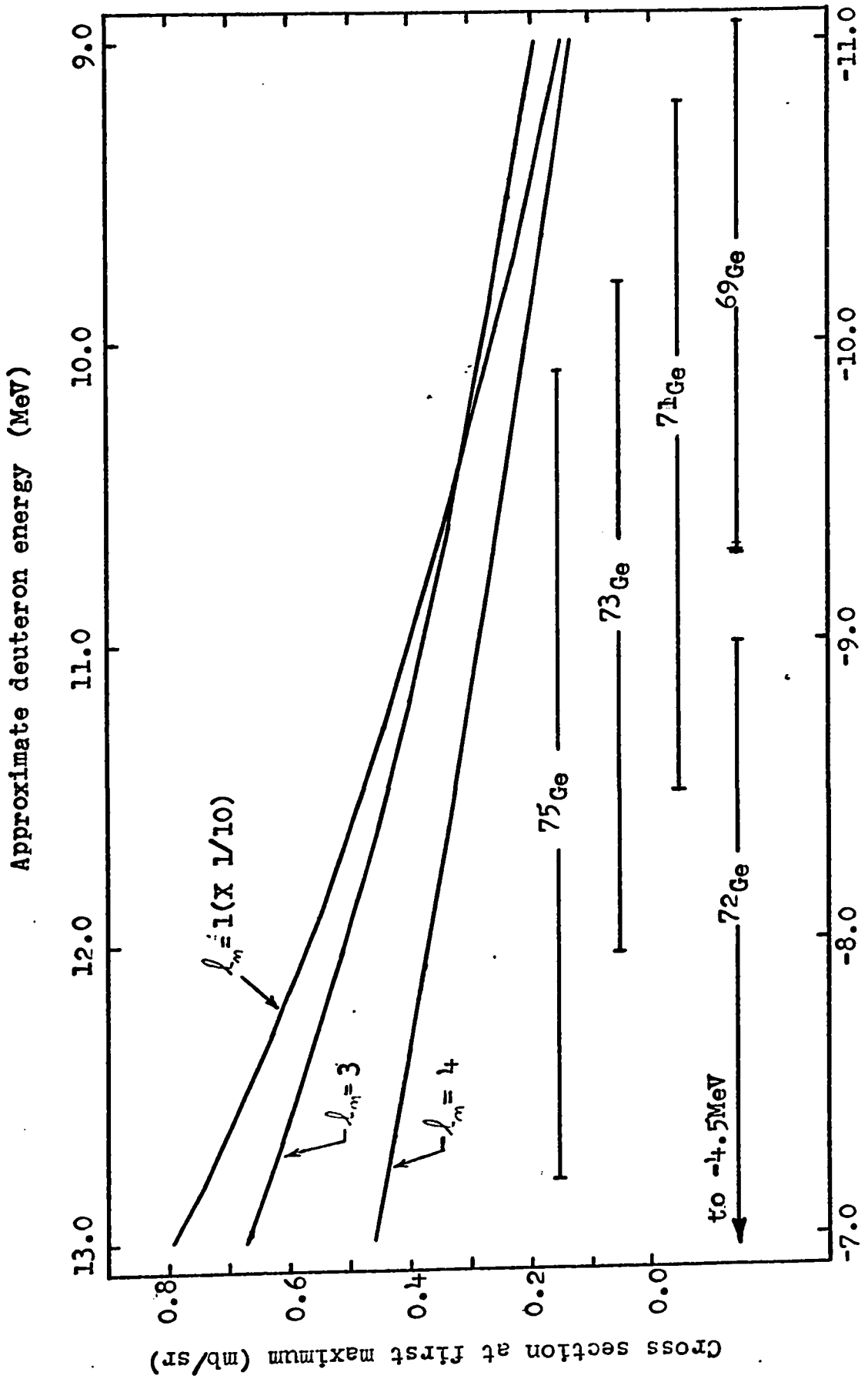


Fig. 23 Q dependence of the DWBA cross sections.

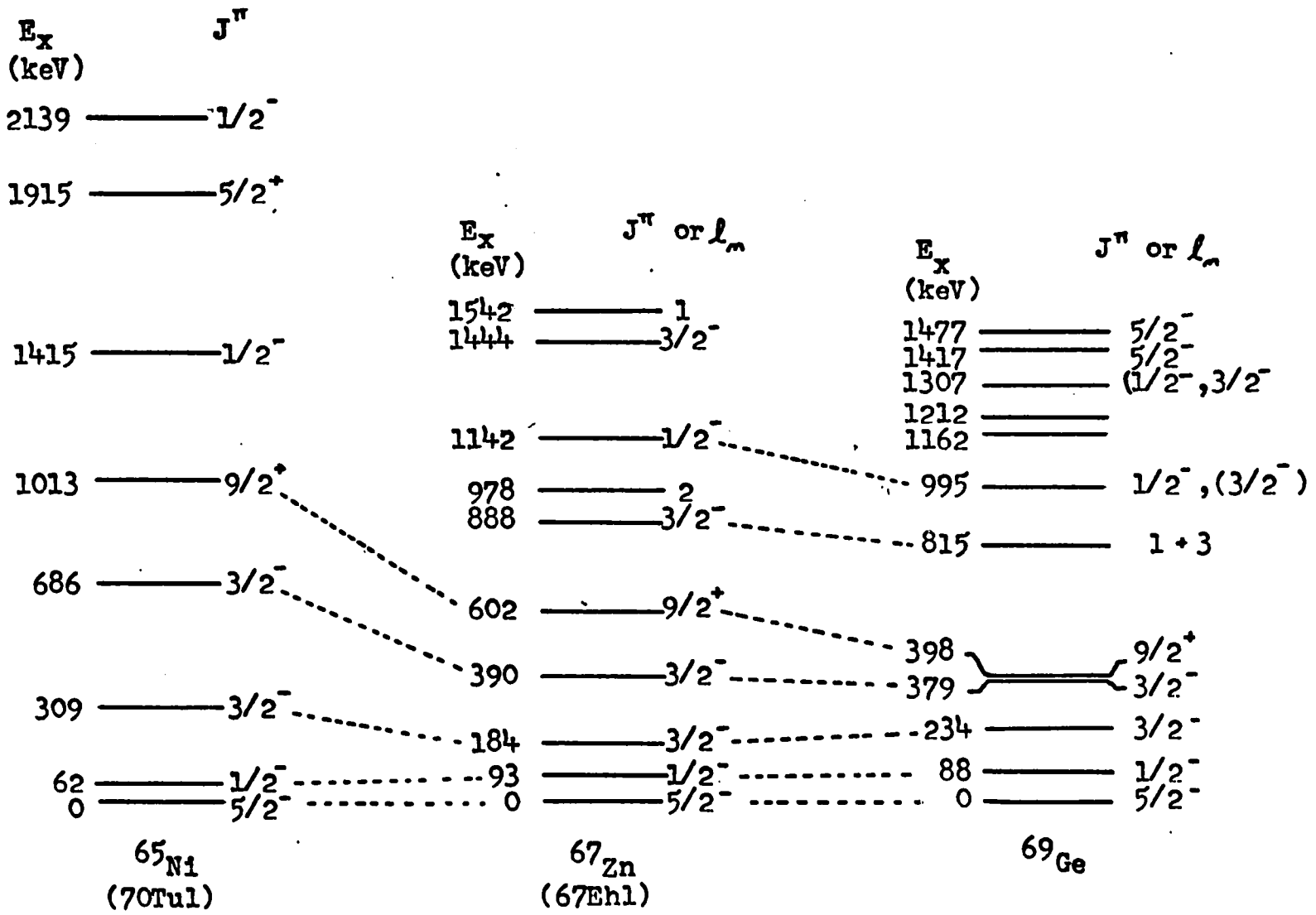


Fig. 24 Low lying levels of some N = 37 nuclei.

# $^{72}Ge$

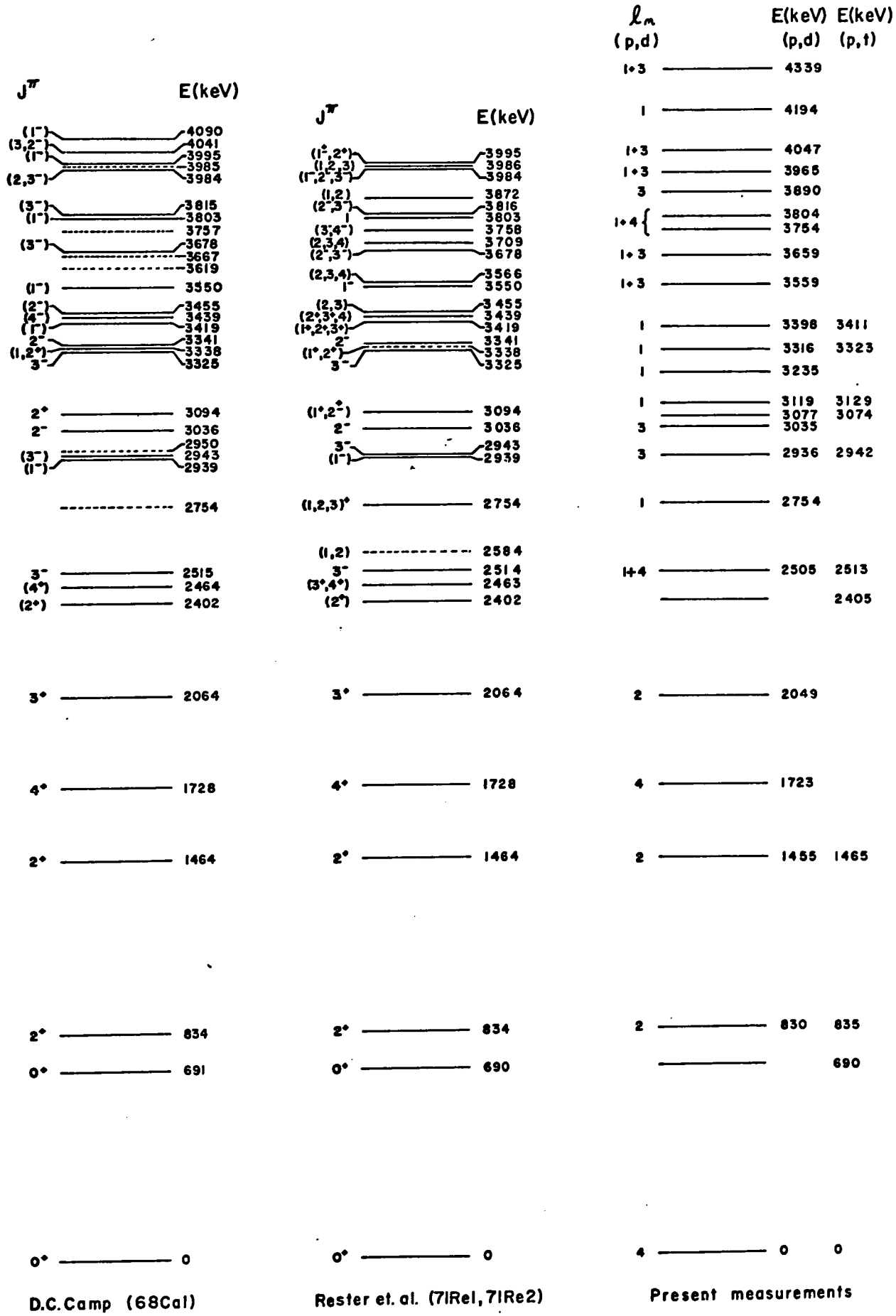


Fig. 25 Energy levels of $^{72}Ge$.

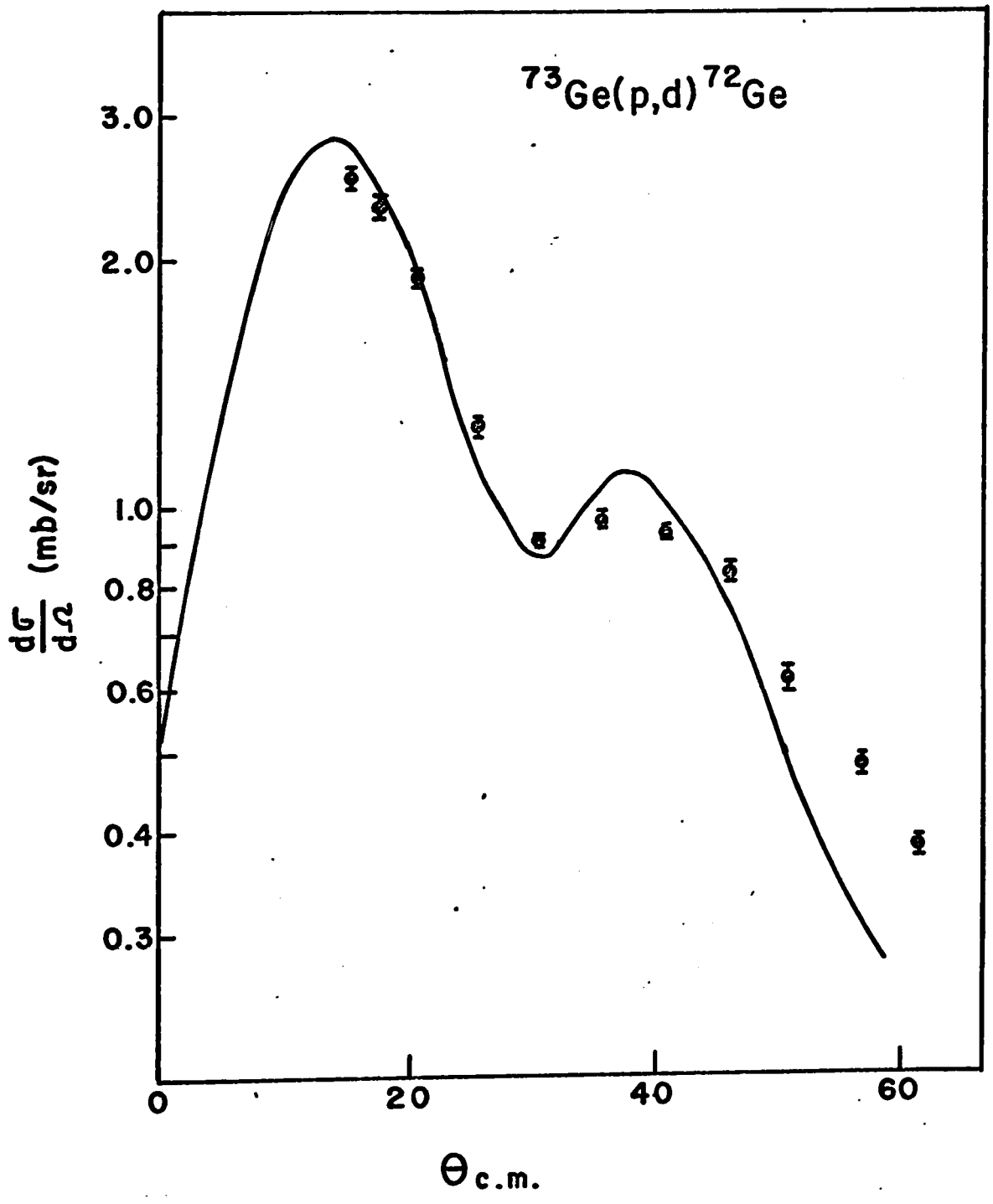


Fig. 26 Angular distribution of many unresolved peaks between 4.5 and 5.5 MeV. The solid curve is the DWBA prediction for $\ell_n$=1+3+4.

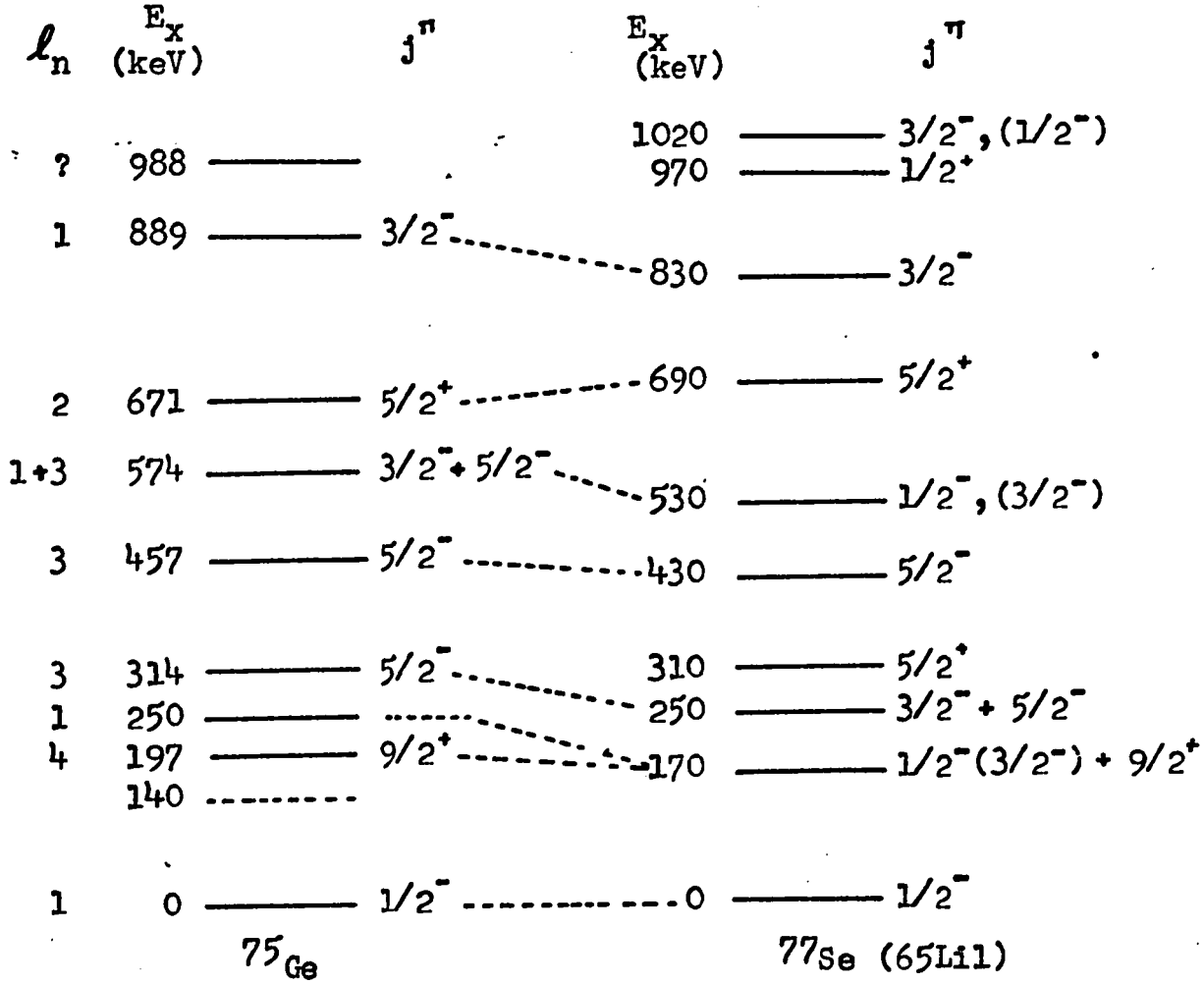


Fig. 27 Low lying levels of some N = 43 nuclei.

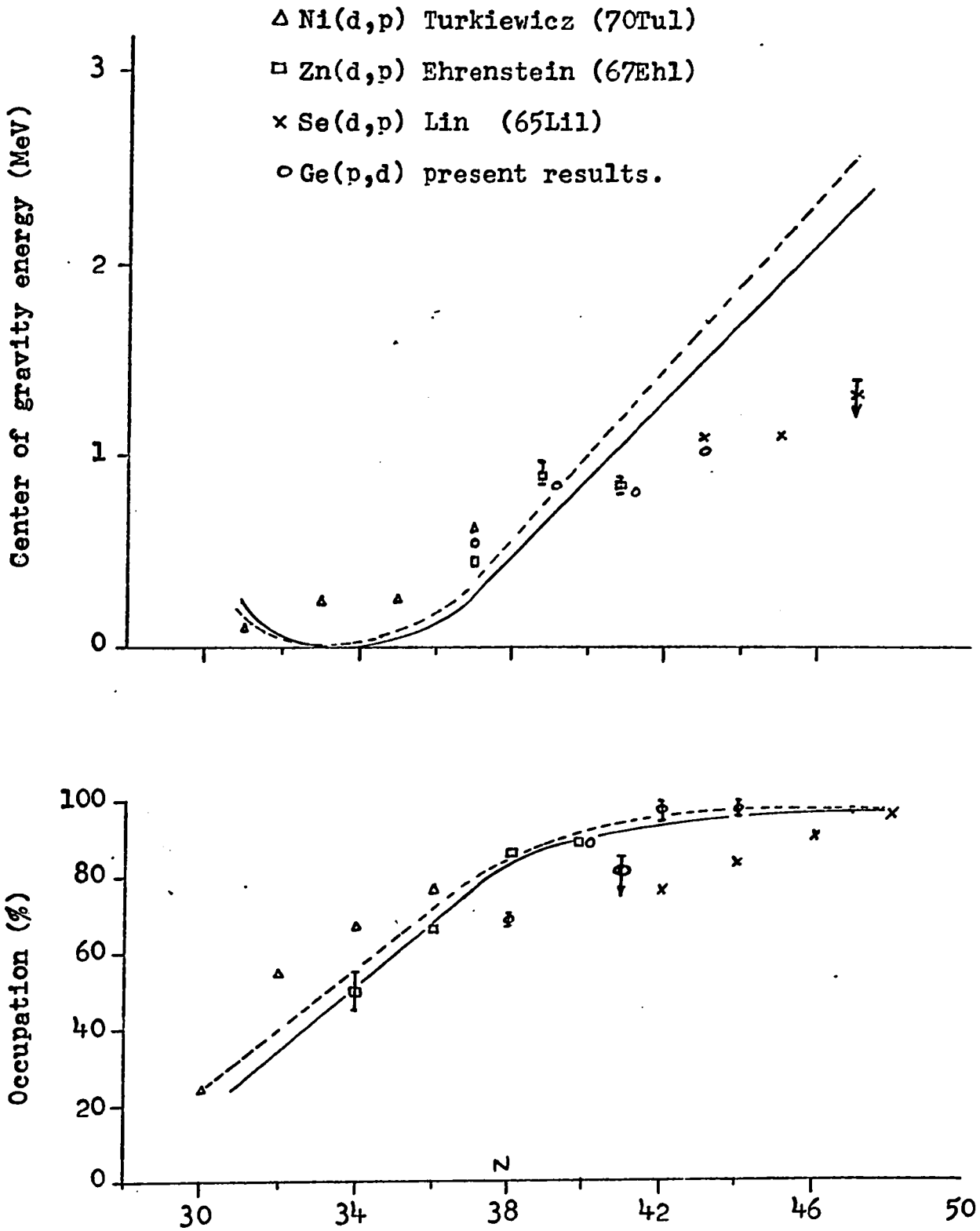


Fig. 28 Occupation number (%) and center of gravity energy of the $p_{3/2}$ shell.

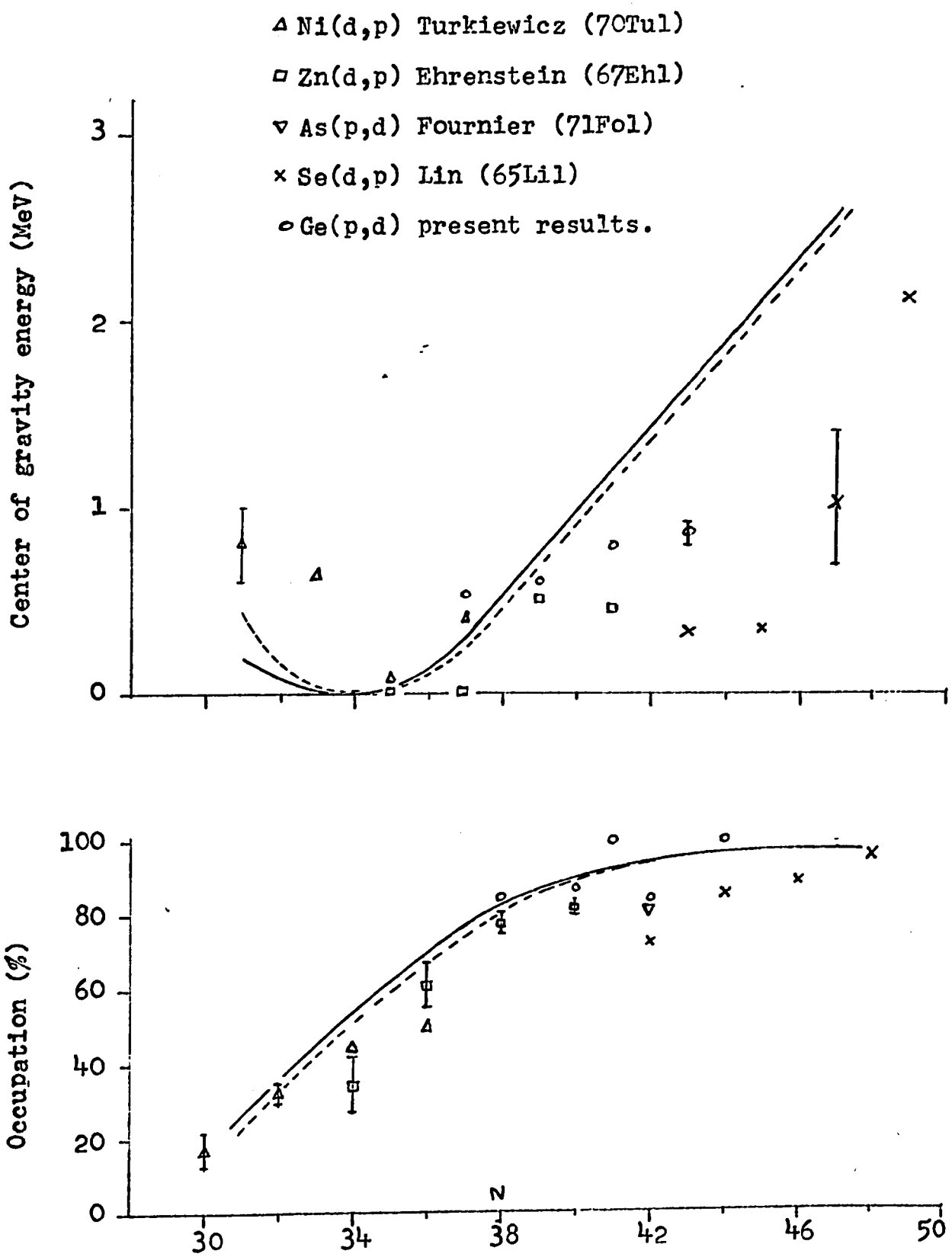


Fig. 29 Occupation number and center of gravity energy of the $1f_{5/2}$ shell.

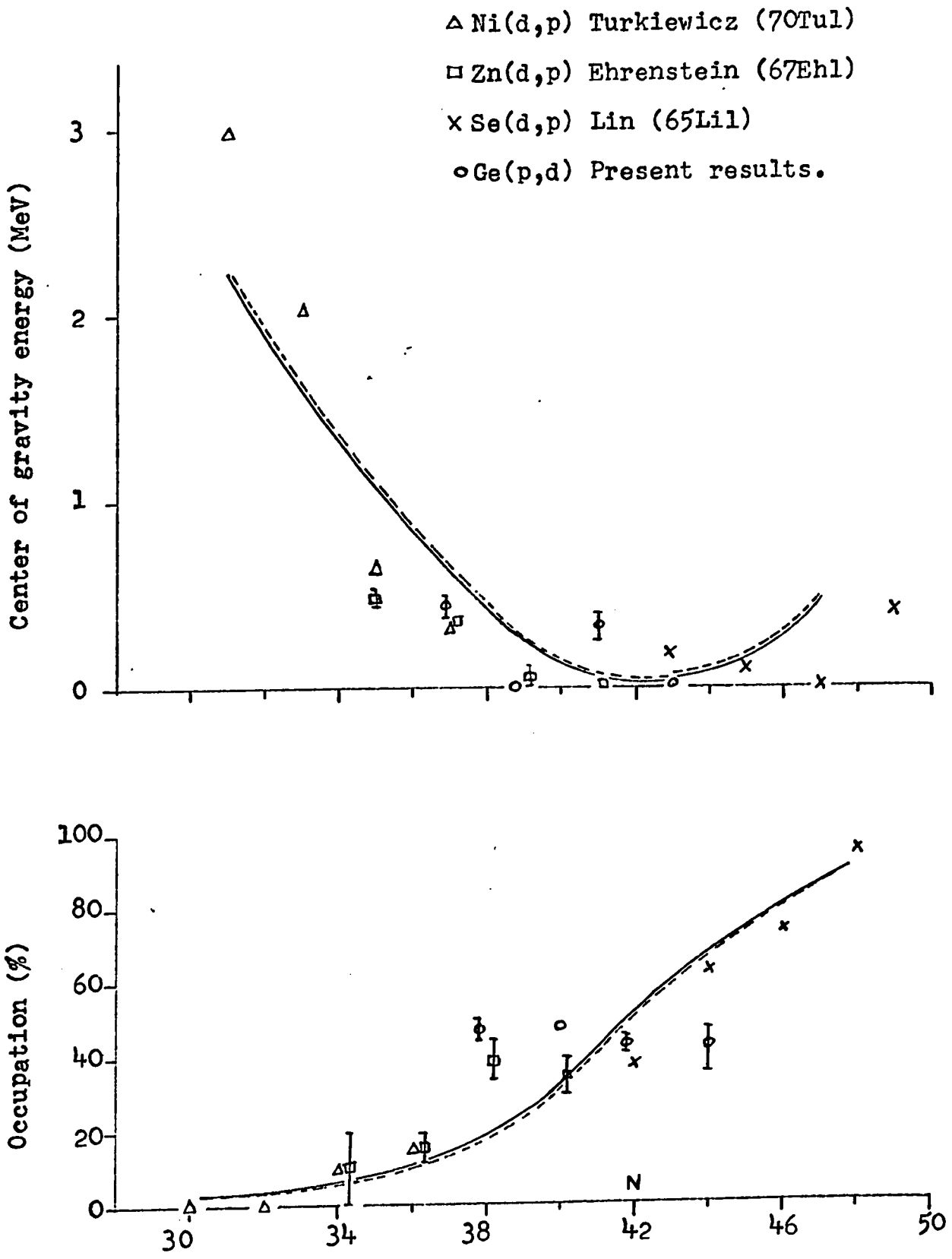


Fig. 30 Occupation number and center of gravity energy of the $2p_{1/2}$ shell.

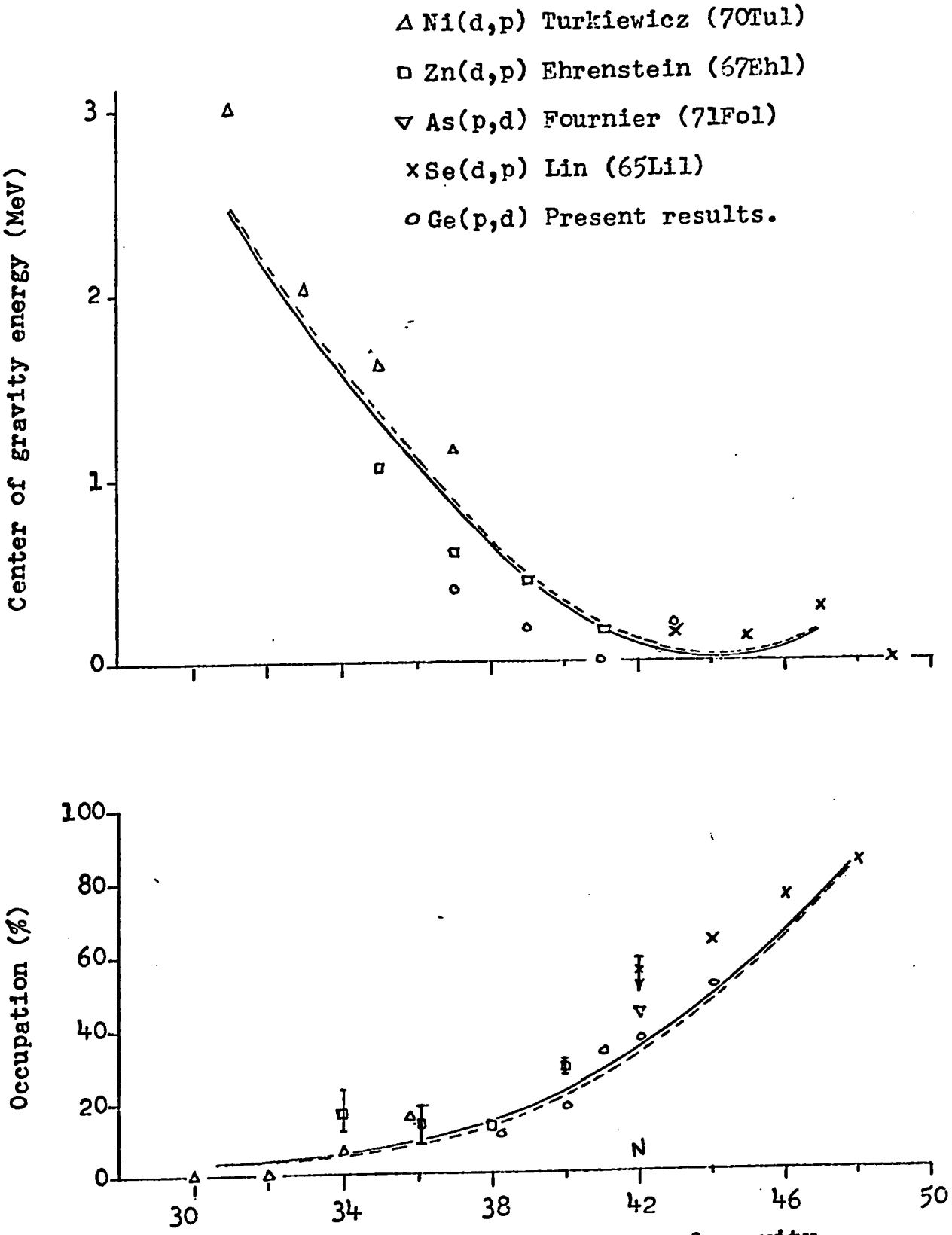


Fig. 31 Occupation number and center of gravity energy of the $1g_{9/2}$ shell.

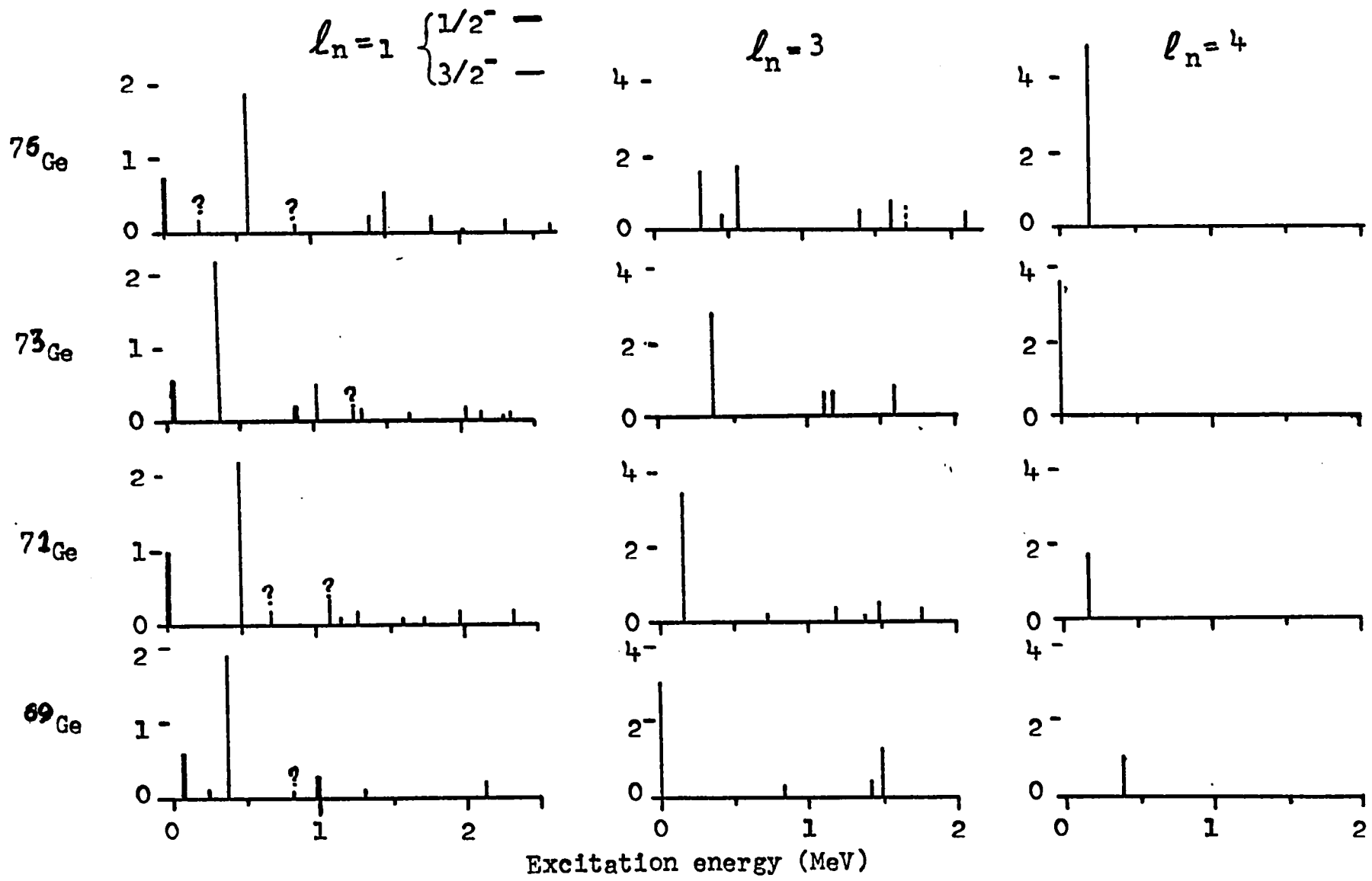


Fig. 32 Spectroscopic strength distribution.

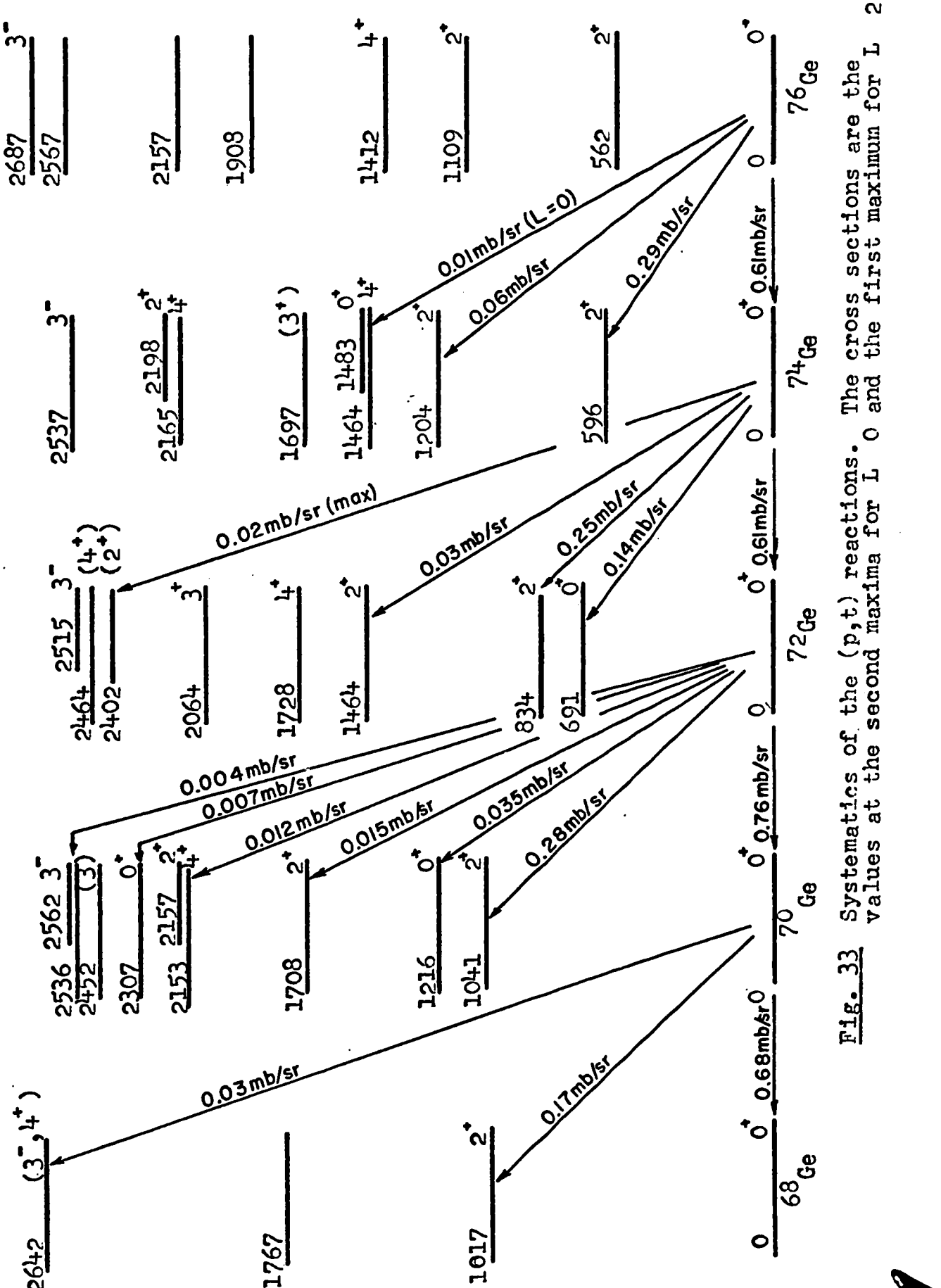


Fig. 33 Systematics of the (p,t) reactions. The cross sections are the values at the second maxima for L = 0 and the first maximum for L = 2.

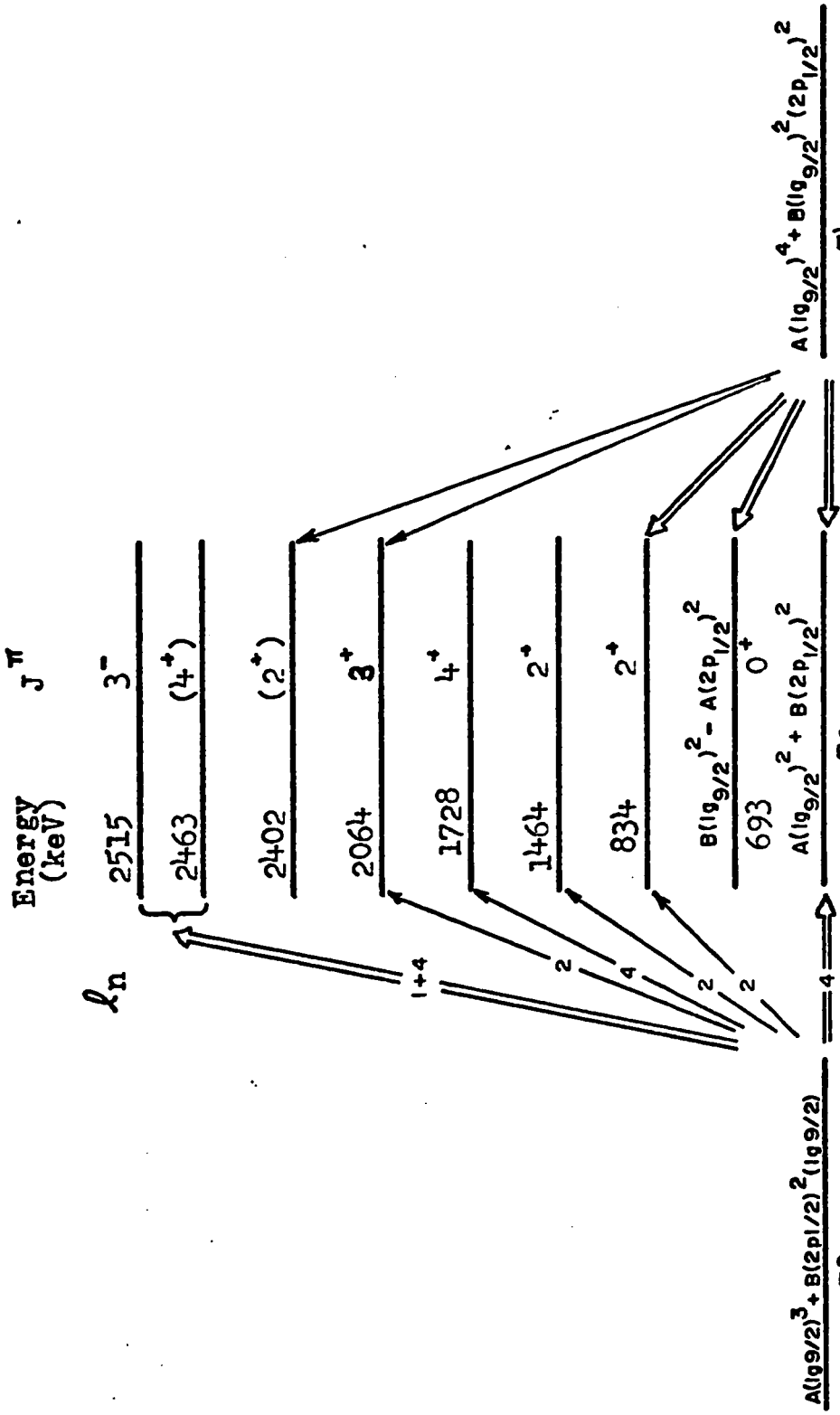


Fig. 34 Low lying levels of $^{72}$Ge populated by the $^{73}$Ge(p,d)$^{72}$Ge and $^{74}$Ge(p,t)$^{72}$Ge reactions.

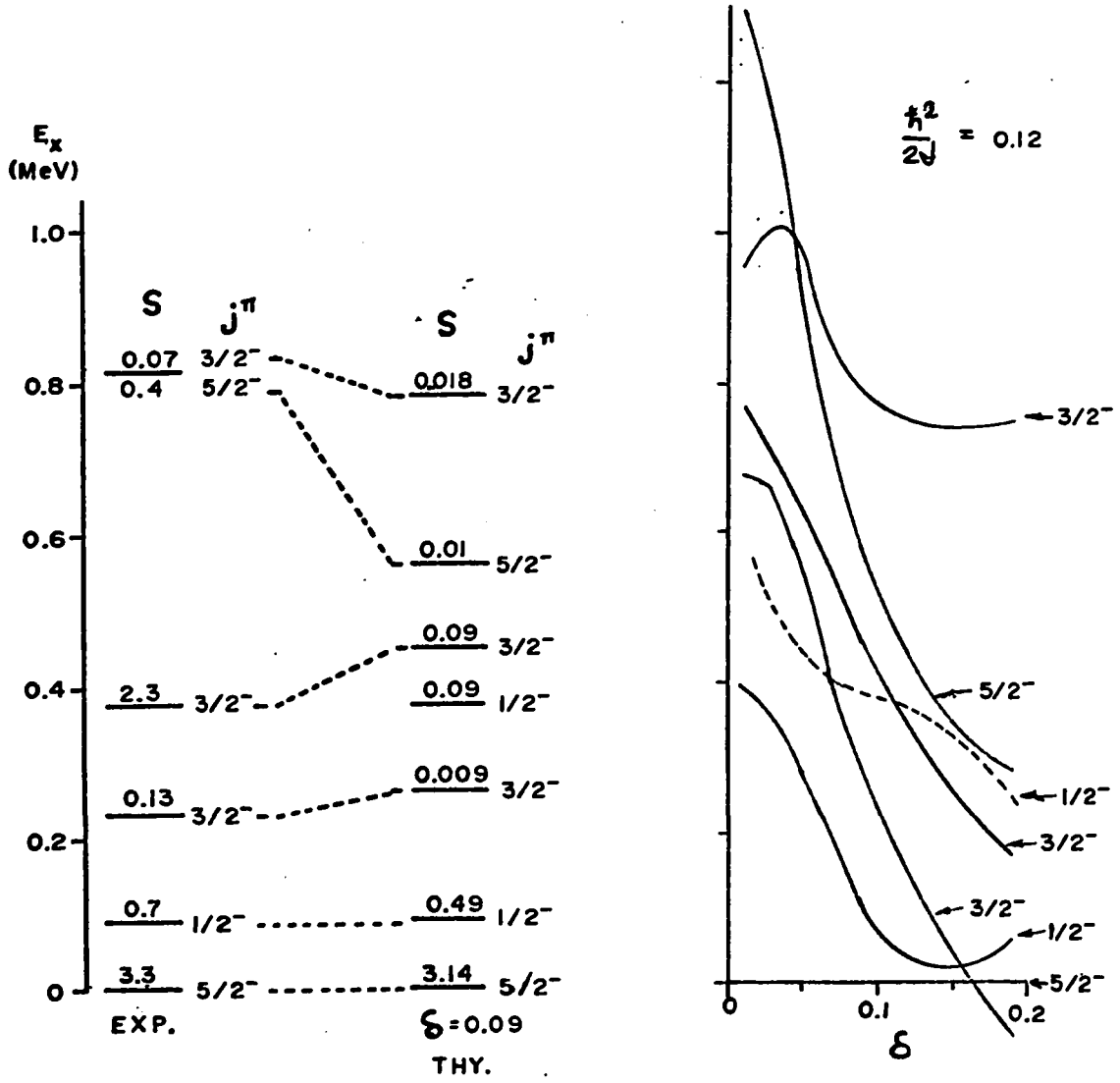


Fig. 35 Experimental and theoretical low lying levels of $^{69}Ge$.

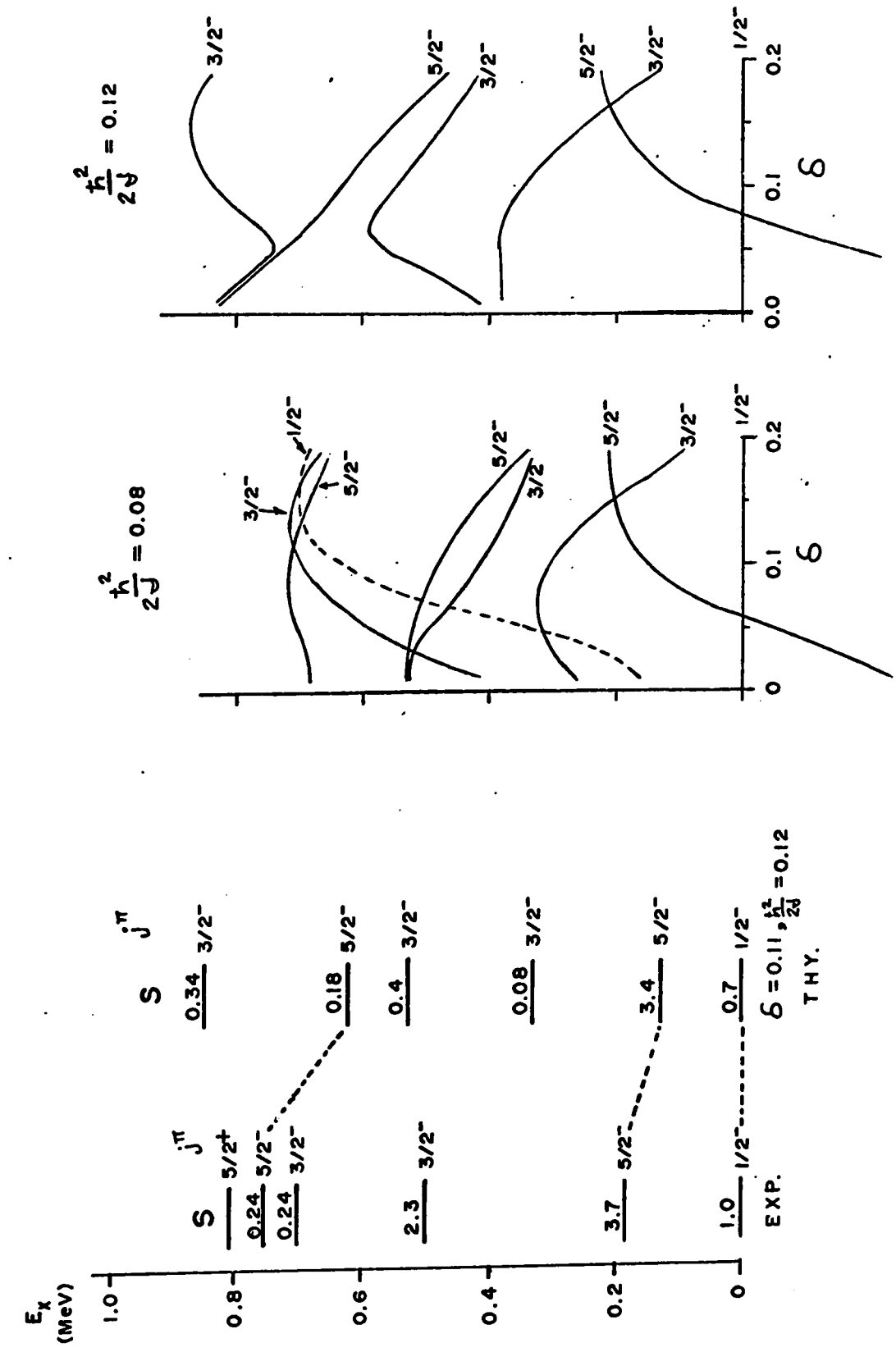


Fig. 36 Theoretical and experimental low lying levels of $^{71}$Ge.

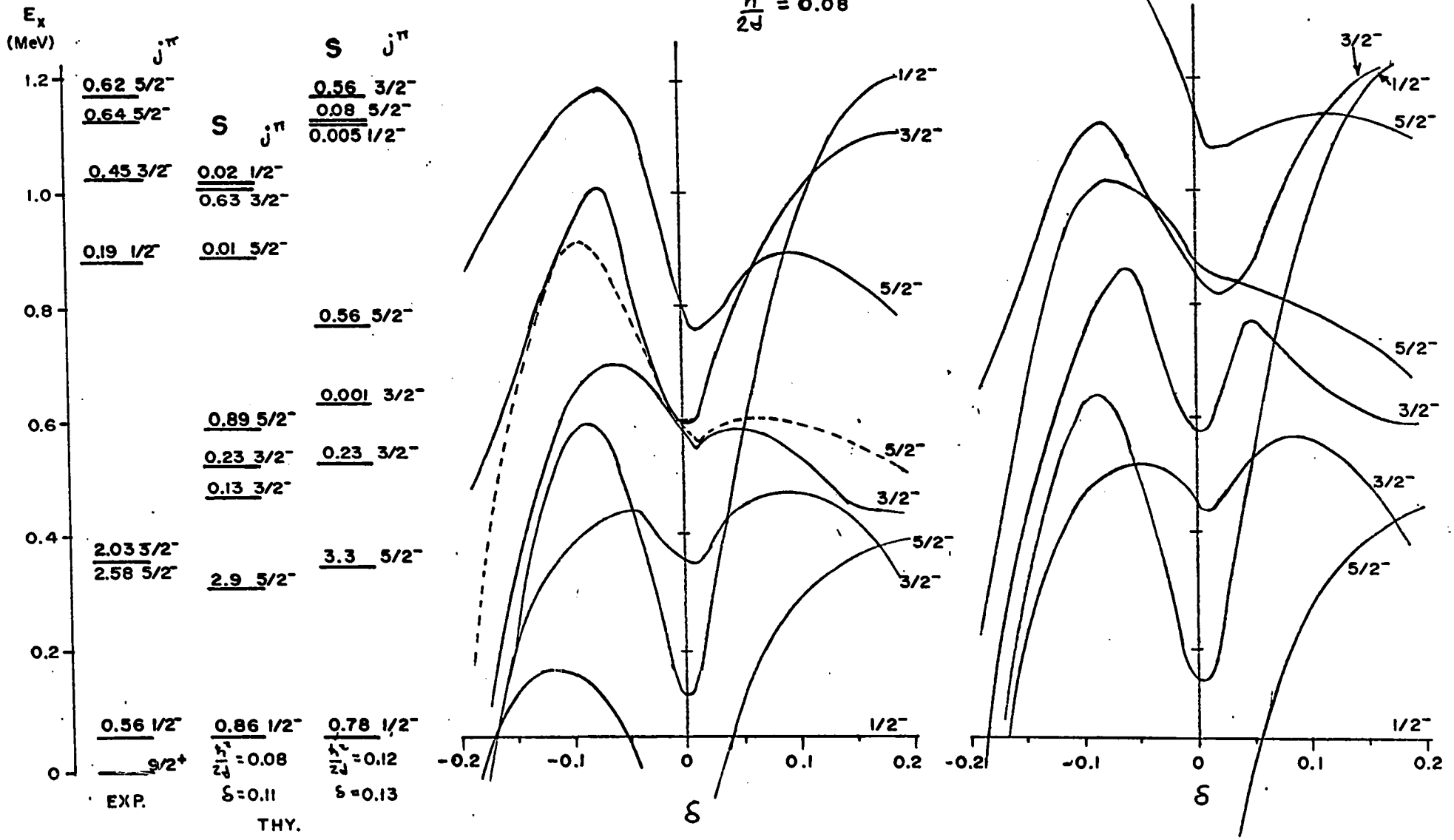


Fig. 37 Experimental and theoretical low lying levels of $^{73}$Ge.

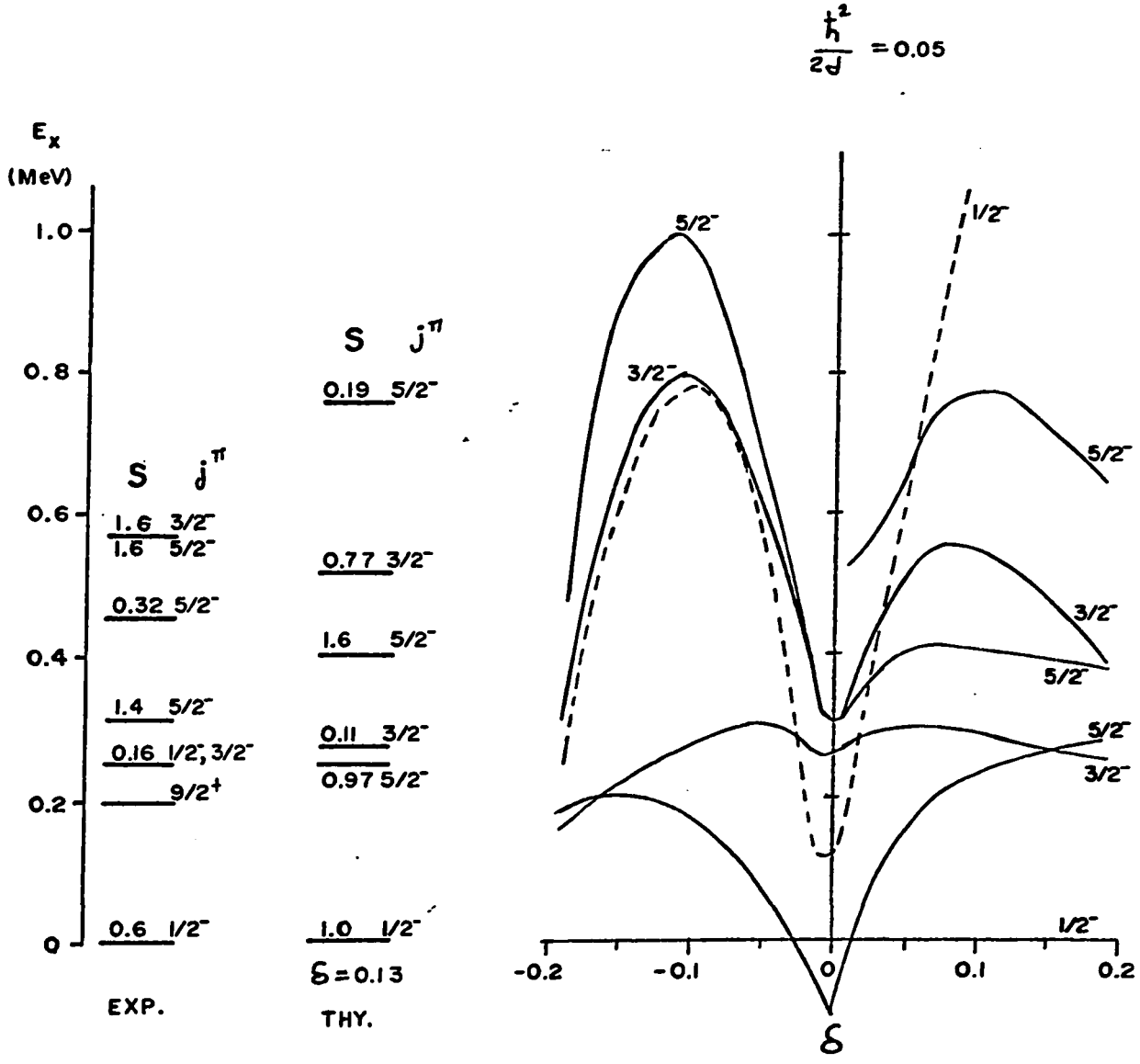


Fig. 38 Experimental and theoretical low lying levels of $^{75}$Ge.

# PART II

## 1.- INTRODUCTION.

In first order, the (p,t) reaction is usually considered as the transfer of a two neutron cluster to the proton, leaving the daughter nucleus in its final nuclear state. However, when the final nuclear state has a large parentage with an excited state in the parent nucleus or the ground state (or an excited state) of the daughter nucleus, a two step mechanism can take place in which there is pick-up of a neutron pair and inelastic scattering in the entrance or exit channel, or both. Numerical calculations by Ascuito and Glendenning (70Asl) indicate that the direct one step predicted cross sections can be enhanced by a factor of 5 when the two step process is taken into account. Furthermore, they point out that the shapes of the calculated angular distributions are not changed significantly by the two step mechanism, so that the most likely way to detect it is by the changed overall magnitude from the DWBA prediction.

$^{26}$Mg is in a mass region of permanent deformation and well developped rotational bands. In general, nuclei with permanent deformation have large inelastic cross sections to the excited states which are members of the ground state rotational band. One would therefore expect some transitions seen in the $^{26}$Mg(p,t)$^{24}$Mg reaction to be

enhanced by the two step process, especially those to the excited states of the ground state rotational band of $^{24}Mg$. Since the wave function of $^{26}Mg$ is fairly well known, the transition strength to levels in $^{24}Mg$ can be calculated and any major discrepancy between the predicted and measured transition strength could be interpreted as being due to the two step process.

The interpretation of $^{26}Mg$ in terms of a neutron pair in deformed Nilsson orbits has been made by several authors, who deduced its configuration from the low lying level structure of $^{25}Mg$ and through measurements of spectroscopic factors in single nucleon transfer reactions. From the work of Hamburger and Blair (60Hal), Cujec (64Cul), Dehnhard and Yntema (67Del), and Kroon et. al. (71Krl) has emerged a reasonably consistent description of $^{26}Mg$ in terms of neutron pairs in Nilsson orbits 5, 9 and 11.

The $^{26}Mg(p,t)^{24}Mg$ reaction has previously been investigated by Cosper et. al. (67Col). They showed that the dependence of the transition strength to the ground and first excited state on incident beam energy is consistent with direct pick-up DWBA theory. Angular distributions to several of the lower levels in $^{24}Mg$ have also been measured by Reynolds (66Rel).

## 2.- THEORY

Glendenning (65Gl1) has described a formalism for treating the direct one step two nucleon transfer reaction. For an even-even target nucleus, the differential cross section contains a coherent sum (65Gl1) of the partial amplitudes $B^M_{NLSJ}$ :

$$\sum_M \left| \sum_N G_{NLSJ} \, B^M_{NLSJ}(\vec{k}_1, \vec{k}_2) \right|^2 ,$$

where $B^M_{NLSJ}(\vec{k}_1, \vec{k}_2)$ is the partial DWBA reaction amplitude corresponding to the pick-up of a single particle (or cluster) with quantum numbers NLSJM, and $\vec{k}_1$ and $\vec{k}_2$ are the linear momentum in the entrance and exit channels, respectively. In the structure factor (65Gl1)

$$G_{NLSJ} = g \sum_r \beta_{rLSJ} \; \Lambda_n \; \langle nO, NL; L | n_1 \ell_1, n_2 \ell_2; L \rangle$$

$\beta_{rLSJ}$ involves the overlap of the (A + 2) nucleons in the target nucleus with the A nucleons in the residual nucleus coupled to a dineutron, $\Lambda_n$ (defined in Ref. 65Gl1) involves the corresponding overlap of the triton and the proton coupled to a dineutron and the Moshinsky bracket couples the two picked-up neutrons with quantum numbers $n_1 \ell_1$ and $n_2 \ell_2$ to a dineutron NL in which the neutrons have a relative motion nO. g can take two values, namely:

$$g = 1 \quad \text{if } n_1\ell_1j_1 = n_2\ell_2j_2$$
$$g = \sqrt{2} \quad \text{otherwise.}$$

The rest of this chapter will be spent on deriving an appropriate formulae to calculate the structure factor $G_{NLSJ}$ for deformed nuclei. The method used to calculate the overlap $\langle (A+2) | \; A \dot{\times} \text{dineutron} \rangle$ is to expand the Nilsson states which are assumed to describe the two valence neutrons in the deformed target into a basis of good $\ell sj$ states. These states are then coupled together and inserted into the formulae for the two nucleon pick-up amplitudes of Glendenning (65Gl1) which is given for good shell model states.

Let ${}^{T}\psi_{I_TM_TK_T}^{(A+2)}$ be the wave function of the target nucleus, ${}^{R}\psi_{I_RM_RK_R}^{(A)}$ that of the residual nucleus and ${}^{D}\Phi_{J_DM_D}^{(2)}$ that of the dineutron, where I, M and K are the spin of the particular nucleus, its projection on a space fixed axis and its projection on the body fixed axis, respectively. Then the overlap $\mathcal{J}_{TR}$ is defined as:

$$(1) \quad \mathcal{J}_{TR} = \left\langle {}^{T}\psi_{I_TM_TK_T}^{(A+2)} \;\middle|\; \left[ {}^{R}\psi_{I_RM_RK_R}^{(A)} \dot{\times} {}^{D}\Phi_{J_DM_D}^{(2)} \right]_{I_TM_TK_T} \right\rangle$$

where the sign $\dot{\times}$ means vector coupling of the angular

momentum. A Nilsson wave function is used to describe the target nucleus:

$$(2) \quad {}^{T}\psi^{(A+2)}_{I_T M_T K_T} = \sqrt{\frac{2I_T+1}{8\pi^2}} \int d^3\Omega \; D^{M_T K_T}_{I_T}(\Omega) \; \chi_{K_T}(\Omega, A+2) \; ,$$

where $\Omega$ represents the three Euler angles which relate the body fixed axis to the space fixed one, $D(\Omega)$ is the rotation matrix which transforms the wave functions from the body fixed axis to the space fixed one, and $\chi_{K_T}(\Omega, A+2)$ is the intrinsic wave function of the nucleons in the body fixed system of axis.

Two neutrons can be factored out of the intrinsic wave function:

$$(3) \quad \chi_{K_T}(\Omega, A+2) = \binom{N_n+2}{2}^{-1/2} \chi_{K_T-K}(\Omega, A) \; \chi_{K}(\Omega, 2) \; ,$$

one can further expand:

$$(4) \quad \chi_{K}(\Omega, 2) = \sqrt{1/2} \left[ \phi^{\Omega}_{k_1}(1) \, \phi^{\Omega}_{k_2}(2) - \phi^{\Omega}_{k_1}(2) \, \phi^{\Omega}_{k_2}(1) \right] ,$$

where $K = k_1 + k_2$, $\binom{N_n+2}{2}^{-1/2}$ is used to normalize equation (3) since there are $\binom{N_n+2}{2}$ ways of choosing two neutrons from a total of $N_n+2$, and equation (4) is the antisymmetric wave function of the two neutrons which were factored out. The intrinsic neutron wave functions $\phi^{\Omega}_{k}$ can be expanded in terms of good shell model states:

$$(5) \qquad \phi^{\Omega}_{k_i} = \sum_{m_i j_i m_i} \phi^{m_i}_{(i)\, n_i j_i} \; c^{n_i j_i}_{k_i} \; D^{*\, m_i k_i}_{(\Omega)\, j_i} \quad ,$$

where $c^{nj}_{k}$ is the Nilsson expansion coefficients of orbit k in terms of the harmonic oscillator basis. Using equations 3, 4 and 5, equation 2 can be rewritten:

$$(6) \qquad {}^{T}\Psi_{I_T M_T K_T (A+2)} \doteq \sqrt{\frac{2I_T+1}{8\pi^2}} \binom{N_n+2}{2}^{-1/2} \sqrt{1/2} \sum_{\gamma_1 \gamma_2} c^{n_1 j_1}_{k_1} \; c^{n_2 j_2}_{k_2} \times$$

$$\times \left[ \phi_{\gamma_1}(1)\, \phi_{\gamma_2}(2) - \phi_{\gamma_1}(2)\, \phi_{\gamma_2}(1) \right] \times$$

$$\times \int d^3\Omega \; D^{M_T K_T}_{(\Omega)\, I_T} \; D^{*\, m_1 k_1}_{(\Omega)\, j_1} \; D^{*\, m_2 k_2}_{(\Omega)\, j_2} \; \chi_{(\Omega, A)\, K_T - k_1 - k_2} \quad ,$$

where $\gamma_i = n_i j_i m_i$.

Using the symmetry properties of the Clebsh Gordan coefficients, the transformation property:

$$D^{m_1 k_1}_{(\Omega)\, j_1} \; D^{m_2 k_2}_{(\Omega)\, j_2} = \sum_{J} \langle j_1 j_2 m_1 m_2 \,|\, J m_1+m_2 \rangle \; \langle j_1 j_2 k_1 k_2 \,|\, J k_1+k_2 \rangle \; D^{m_1+m_2, k_1+k_2}_{(\Omega)\, J}$$

and the relation

$$D^{*\, MK}_{(\Omega)\, J} = (-)^{M-K} \; D^{-M\ -K}_{(\Omega)\, J} \quad ,$$

it is easy to show that:

$$D^{(\Omega)}_{I_T}{}^{M_T K_T} \; D^{*(\Omega)}_{j_1}{}^{m_1 k_1} \; D^{*(\Omega)}_{j_2}{}^{m_2 k_2} = \sum_{J'J} \left(\frac{2J'+1}{2J+1}\right) \langle j_1 j_2 m_1 m_2 | J m_1+m_2 \rangle$$

$$\langle j_1 j_2 k_1 k_2 | J k_1+k_2 \rangle \; \langle J' J, M_T - m_1 - m_2, m_1+m_2 | I_T M_T \rangle$$

$$\langle J' J, K_T - k_1 - k_2, k_1+k_2 | I_T K_T \rangle \; D^{(\Omega)}_{J'}{}^{M_T - m_1 - m_2, K_T - k_1 - k_2} \quad ,$$

so that equation 6 can be rewritten:

$$(7) \quad {}^{T}\psi^{(A+2)}_{I_T M_T K_T} = \sqrt{\frac{2I_T+1}{8\pi^2}} \binom{N_n+2}{2}^{-1/2} \sqrt{1/2} \sum_{\substack{\gamma_1 \gamma_2 \\ J'J}} c^{n_1 j_1}_{k_1} \; c^{n_2 j_2}_{k_2}$$

$$\left(\frac{2J'+1}{2J+1}\right) \langle j_1 j_2 m_1 m_2 | J m_1+m_2 \rangle \langle j_1 j_2 k_1 k_2 | J k_1+k_2 \rangle$$

$$\langle J' J K_T - k_1 - k_2, k_1+k_2 | I_T K_T \rangle \langle J' J M_T - m_1 - m_2, m_1+m_2 | I_T M_T \rangle$$

$$\left[\phi_{\gamma_1}(1)\,\phi_{\gamma_2}(2) - \phi_{\gamma_1}(2)\,\phi_{\gamma_2}(1)\right] \int d^3\Omega \; D^{(\Omega)}_{J'}{}^{M_T - m_1 - m_2, K_T - k_1 - k_2} \; \chi^{(\Omega, A)}_{K_T - k_1 - k_2}$$

Rewriting:

$$\psi^{(A)}_{J', M_T - m_1 - m_2, K_T - k_1 - k_2} = \sqrt{\frac{2J'+1}{8\pi^2}} \int d^3\Omega \; D^{(\Omega)}_{J'}{}^{M_T - m_1 - m_2, K_T - k_1 - k_2} \; \chi^{(\Omega, A)}_{K_T - k_1 - k_2}$$

which is analogous to equation 2, allows to rewrite equation 7 as:

$$(8)\quad {}^{T}\psi^{(A+2)}_{I_T M_T K_T} = \sqrt{\frac{2J'+1}{2I_T+1}} \binom{N_n+2}{2}^{-1/2} \sqrt{1/2} \sum_{\gamma_1 \gamma_2 J' j} c^{n_1 j_1}_{k_1} c^{n_2 j_2}_{k_2}$$

$$\langle j_1 j_2 m_1 m_2 | J m_1+m_2 \rangle \langle j_1 j_2 k_1 k_2 | J k_1+k_2 \rangle$$

$$\langle J' J M_T - m_1 - m_2, m_1+m_2 | I_T M_T \rangle \langle J' J K_T - k_1 - k_2, k_1+k_2 | I_T K_T \rangle$$

$$\left[\phi_{\gamma_1}(1)\,\phi_{\gamma_2}(2) - \phi_{\gamma_1}(2)\,\phi_{\gamma_2}(1)\right] \psi^{(A)}_{J', M_T - m_1 - m_2, K_T - k_1 - k_2}$$

The second term to the right of equation 1 is expanded as:

$$(9)\quad \left[{}^{R}\psi^{(A)}_{I_R M_R K_R} \times {}^{D}\Phi^{(2)}_{J_D M_D}\right]_{I_T M_T K_T} = \sum_{M_D} \langle I_R J_D M_R M_D | I_T M_T \rangle \; {}^{R}\psi^{(A)}_{I_R M_R K_R} \; {}^{D}\Phi^{(2)}_{J_D M_D} ,$$

which corresponds to the vector coupling of a nucleus of spin $I_R$ and projection $M_R$ on the space fixed axis to a dineutron which has quantum numbers $J_D$ and $M_D$.

If we assume that the reaction proceeds via the pick-up of neutrons in states $n'_1 \ell'_1 j'_1$ and $n'_2 \ell'_2 j'_2$, then it is possible to expand the dineutron wave function in terms of these single particle shell model states:

$$(10)\quad {}^{D}\Phi^{(2)}_{J_D M_D} = (1+(-)^{J_D}\delta_{n_1' n_2'}\delta_{j_1' j_2'})^{-1/2}\sqrt{1/2}$$
$$\sum_{m_1' m_2'} \langle j_1' j_2' m_1' m_2' | J_D m_1'+m_2' \rangle \left[\phi_{\gamma_1'}(1)\,\phi_{\gamma_2'}(2) - \phi_{\gamma_1'}(2)\,\phi_{\gamma_2'}(1)\right]$$

which is the properly normalized and antisymmetric wave function of two identical particles. Replacing equation 10 into equation 9 yields:

$$(11)\quad \left[{}^{R}\Psi^{(A}_{I_R M_R K_R} \times {}^{D}\Phi^{(2)}_{J_D M_D}\right]_{I_T M_T K_T} = (1+(-)^{J_D}\delta_{n_1' n_2'}\delta_{j_1' j_2'})^{-1/2}$$
$$\sqrt{1/2}\sum_{M_D m_1' m_2'} \langle I_R J_D M_R M_D | I_T M_T \rangle \langle j_1' j_2' m_1' m_2' | J_D M_D \rangle$$
$$\left[\phi_{\gamma_1'}(1)\,\phi_{\gamma_2'}(2) - \phi_{\gamma_1'}(2)\,\phi_{\gamma_2'}(1)\right] {}^{R}\Psi^{(A)}_{I_R M_R K_R}$$

Inserting equations 11 and 8 into equation 1, the overlap integral becomes:

$$\mathcal{J}^{n_1' j_1', n_2' j_2'}_{TR} = \sqrt{\frac{2J'+1}{2I_T+1}}\binom{N_n+2}{2}^{-1/2}(1/2)$$
$$(1+(-)^{J_D}\delta_{n_1' n_2', j_1' j_2'})^{-1/2}\sum_{\gamma_1\gamma_2 m_1' m_2' J J' M_D} c^{n_1 j_1}_{k_1}\, c^{n_2 j_2}_{k_2}$$
$$\langle j_1 j_2 m_1 m_2 | J m_1+m_2\rangle \langle j_1' j_2' m_1' m_2' | J_D M_D\rangle \langle I_R J_D M_R M_D | I_T M_T\rangle$$
$$\langle j_1 j_2 k_1 k_2 | J k_1+k_2\rangle \langle J' J M_T - m_1 - m_2, m_1+m_2 | I_T M_T\rangle$$
$$\langle J' J K_T - k_1 - k_2, k_1+k_2 | I_T K_T\rangle \left\langle \Psi^{(A)}_{J', M_T-m_1-m_2, K_T-k_1-k_2} \middle| {}^{R}\Psi^{(A)}_{I_R M_R K_R}\right\rangle$$
$$\left\langle \left[\phi_{\gamma_1}(1)\,\phi_{\gamma_2}(2) - \phi_{\gamma_1}(2)\,\phi_{\gamma_2}(1)\right] \middle| \left[\phi_{\gamma_1'}(1)\,\phi_{\gamma_2'}(2) - \phi_{\gamma_1'}(2)\,\phi_{\gamma_2'}(1)\right]\right\rangle$$

The two integrations yield $J' = I_R$, $M_R = M_T - m_1 - m_2$, $K_R = K_T - k_1 - k_2$ and a factor 2 $\delta_{\gamma_1 \gamma_1'} \delta_{\gamma_2 \gamma_2'}$, so that:

$$\mathcal{J}^{n_1 j_1, n_2 j_2}_{TR} = \sqrt{\frac{2I_R+1}{2I_T+1}} \binom{N_n+2}{2}^{-1/2} \left[1 + (-)^{J_D} \delta_{n_1 n_2} \delta_{j_1 j_2}\right]^{-1/2}$$

$$\sum_{m_1 m_2 J M_D} c^{n_1 j_1}_{k_1} \; c^{n_2 j_2}_{k_2}$$

$$\langle j_1 j_2 m_1 m_2 | J m_1 + m_2 \rangle \; \langle j_1 j_2 m_1 m_2 | J_D M_D \rangle$$

$$\langle I_R J_D M_T - M_D, M_D | I_T M_T \rangle \langle I_R J M_T - M_D, M_D | I_T M_T \rangle$$

$$\langle j_1 j_2 k_1 k_2 | J k_1 + k_2 \rangle \; \langle I_R J K_T - k_1 - k_2, k_1 + k_2 | I_T K_T \rangle$$

Summing first over $m_1$ and $m_2$ yields $\delta_{JJ_D}$ for the first two Clebsh Gordan coefficients; Summing afterwards over $M_D$ yields 1 for the third and fourth Clebsh Gordan coefficients, so that the overlap integral reduces to:

$$\mathcal{J}^{n_1 j_1, n_2 j_2}_{TR} = \sqrt{\frac{2I_R+1}{2I_T+1}} \binom{N_n+2}{2}^{-1/2} \left[1 + (-)^{J_D} \delta_{n_1 n_2} \delta_{j_1 j_2}\right]^{-1/2}$$

$$c^{n_1 j_1}_{k_1} \; c^{n_2 j_2}_{k_2} \langle j_1 j_2 k_1 k_2 | J k_1 + k_2 \rangle \langle I_R J K_R K_T - K_R | I_T K_T \rangle$$

In the notation of Glendenning (65G11):

$$\beta^{n_1 j_1, n_2 j_2}_{LSJ} = \binom{N_n+2}{2}^{1/2} \begin{bmatrix} \ell_1 & s_1 & j_1 \\ \ell_2 & s_2 & j_2 \\ L & S & J \end{bmatrix} \mathcal{J}^{n_1 j_1, n_2 j_2}_{TR} \; ,$$

and the complete structure factor for pick-up of a neutron from orbit $k_1$ and another neutron from orbit $k_2$ becomes:

$$G^{k_1k_2}_{NLSJ} = \sum_{n_1j_1n_2j_2} g \left[1+(-)^{J_D}\delta_{n_1n_2}\delta_{j_1j_2}\right]^{-1/2} \sqrt{\frac{2I_R+1}{2I_T+1}}\; c^{n_1j_1}_{k_1}\, c^{n_2j_2}_{k_2}$$
$$\langle j_1j_2k_1k_2|Jk_1+k_2\rangle \langle I_RJK_T-k_1-k_2,k_1+k_2|I_TK_T\rangle$$
$$\begin{bmatrix}\ell_1 & s_1 & j_1\\ \ell_2 & s_2 & j_2\\ L & S & J\end{bmatrix} \bigcap_n \langle nO,NL;L|n_1\ell_1,n_2\ell_2;L\rangle \quad .$$

If the target wave function is expressed as:

$$\sum_{k_1k_2} V_{k_1k_2}|k_1\rangle|k_2\rangle \quad ,$$

where $V_{k_1k_2}$ is the probability amplitude that one of the picked-up neutrons will be in orbit $|k_1\rangle$ and the other in orbit $|k_2\rangle$, then the complete structure factor will be given by:

$$G_{NLSJ} = \sum_{k_1k_2} G^{k_1k_2}_{NLSJ}\; V_{k_1k_2} \quad .$$

In the case of $^{26}$Mg where the picked-up neutrons are assumed to be paired off in a same Nilsson orbit, one has the simplification $k_1 = -k_2 = k$; it is also usual to assume that the two neutrons in the dineutron are paired to a zero spin so that $S = 0$ and $J = L$. With these assumptions the structure factor simplifies to:

$$G^{k}_{NLSJ} = \sum_{\substack{n_1 j_1 \\ n_2 j_2}} g \left[1 + (-)^{L} \delta_{n_1 n_2} \delta_{j_1 j_2}\right]^{-1/2} \sqrt{\frac{2I_R+1}{2I_T+1}} \; c^{n_1 j_1}_{k} \, \underline{c}^{n_2 j_2}_{-k}$$
$$\langle j_1 j_2 k, -k | L0 \rangle \; \langle I_R L K_T 0 | I_T K_T \rangle$$
$$\begin{bmatrix} \ell_1 & s_1 & j_1 \\ \ell_2 & s_2 & j_2 \\ L & 0 & L \end{bmatrix} \Lambda_n \; \langle n0, NL; L | n_1 \ell_1, n_2 \ell_2; L \rangle$$

## 3.- EXPERIMENTAL.

The reaction was performed with a 20 MeV proton beam, and the experimental set-up was the same as that previously described in the first part of this work. The target was a 99% enriched self supporting $^{26}Mg$ foil. The Rutherford scattering of 5 MeV $\alpha$ particles yielded a thickness of 27 $\mu g/cm^2$. Fig. 1 shows a typical triton spectrum, while Figs. 2 and 3 show the angular distributions to the $0^+$, $2^+$ and $4^+$ members of the ground state rotational band with a fitted DWBA curve. Fig. 4 shows the angular distributions to levels which are not members of the ground state rotational band.

## 4.- ANALYSIS.

Fits to the $0^+$, $2^+$ and $4^+$ members of the ground state rotational band were attempted with a zero-range, spin independent DWBA theory, using the code DWUCK (67Kul) which was modified by J. C. Hardy (70Hal) so that the bound state wave function was a product of two harmonic oscillator single particle wave functions, each of which was matched to a Hankel tail at the nuclear surface. The programme calculates the partial scattering amplitudes $B^M_{NLSJ}$ for each value of NLSJ, these are then each multiplied by the structure factor $G^k_{NLSJ}$ and summed to obtain the complete reaction amplitude for pick-up of two neutrons from Nilsson orbit k.

The optical parameters for the distorted waves are listed in Table 1 and were determined as follows. The proton optical potential parameters are fairly well known, and small changes in the values of the parameters were found to have little effect on the calculated angular distributions. The proton parameters were therefore taken to be the same as those used by Kroon et. al. (71Kr1) in their analysis of the $^{26}Mg(p,d)^{25}Mg$ at 20 MeV incident energy. The initial values of the triton optical parameters were taken from the analysis of triton elastic scattering data by Glover and Jones (66Gl1). Their parameters were

varied slightly so as to obtain an acceptable simultaneous fit to the first L= 0, 2 and 4 transitions, assuming only one value of $G_{NLSJ}$, namely $G_{3000} = G_{2202} = G_{1404} = 1$, which are normally the leading values for L= 0, 2 and 4, respectively.

The structure amplitudes $G^k_{NLSJ}$, which corresponds to pure Nilsson states, were calculated for a deformation of $\eta = 4.3$. The length parameter $\nu$ for the bound state wave function, which also enters in the structure amplitudes through the factor $\Omega_n$, was taken to be $\nu = 0.333$ fm$^{-2}$, the value which corresponds to the conventional harmonic oscillator level spacing of $41A^{-1/3}$ MeV. The corresponding length parameter for the triton wave function was taken to be $\eta = 0.242$ fm$^{-1}$ (65Gl1). Calculation of the structure amplitudes $G^k_{NLSJ}$ was made with and without major shell mixing in the wave function of the target, and the resultant values are listed in Tables 2 and 3, respectively. It is seen that the addition of major shell mixing greatly affects the calculated structure factor for pick-up of a neutron pair from orbits 9 and 11, while that of orbit 5 is not affected very much. This is understandable since orbit 5 mixes very little with the N ± 2 shells while orbits 9 and 11 mix strongly with the other N ± 2 shells (67Del).

The wave functions of $^{26}$Mg which have been deduced

by several authors from the analysis of single nucleon transfer reactions are listed in Table 4, along with the normalizations obtained by chi-square fitting the DWBA predictions to the experimental data for each case. Since the structure factor is sensitive to the phases of the wave functions, which are not determined from single nucleon transfer reactions, all relative signs are listed for each set of parameters.

If the direct one step DWBA theory was adequate in describing the (p,t) reaction on $^{26}$Mg, one would expect to find at least one line in Table 4 which would have a similar normalization for L = 0, 2 and 4. Inspection of that table shows, on the contrary, that in all the cases, the normalization varies by large factors for L = 0, 2 and 4. It also shows that the inclusion of major shell mixing has considerably improved the results by lowering considerably the normalization to the L = 4 transition which is unacceptable in the unmixed calculation.

The best relative agreement between the experimental and calculated cross sections is obtained with the set of Kroon et. al. (71Kr1) for the values of $V_5 = 0.78$, $V_9 = 0.57$ and $V_{11} = -0.30$, for which the cross sections to the $2^+$ and $4^+$ would have to be enhanced by factor of 3.5 to 5, respectively; this would be consistent with a two step process. However, the normalization constant of 266 for the ground

state transition is inconsistent with the work of Bruge and Leonard (70Br1) on the $^{58}Ni(p,^{3}He)^{56}Co$ and a recent calculation of Ball et. al. (71Ba1) on the $^{37}Cl(p,t)^{35}Cl$ reaction who find a normalization of approximately 40 for the DWBA code DWUCK in the modified form which was used in this analysis. On that ground, the wave function of Kroon et. al. (71Kr1) with all positive $V_k$ would be the best solution.

## 5.- CONCLUSIONS.

It seems that the wave function of $^{26}Mg$ with positive $V_k$ provides the best fit to the absolute cross section of the ground state transition, and that with this sign choice the DWBA theory is unable to account for the strength of the transitions to the other members of the ground state rotational band. The nearly correct ratio of cross sections which is obtained with some choice of the signs of the $V_k$ is meaningless because all the cross sections are too small by a large factor due to strong cancellation when summing the partial structure amplitudes $\sum_{l_2} V_k \, G_N^k$ .

If one assumes that the two nucleon transfer DWBA theory is correct, at least to first order, then the only explanation for the strength of the cross sections to the excited states of the ground state rotational band is that they are strongly enhanced by another reaction mechanism. The two step process is a good candidate for this reaction mechanism since the shapes of the experimental angular distributions are not too different from the calculated ones. The excitation of two members of the $K=2$ band in $^{24}Mg$, which is not allowed in this model, also indicates the presence of another reaction mechanism.

Table 1. Optical model parameters used in the analysis of the $^{26}Mg(p,t)^{24}Mg$ reaction.

| | $V_s$ (MeV) | $r_{os}$ (fm) | $a_s$ (fm) | $W_s$ (MeV) | $r_{oI}$ (fm) | $a_I$ (fm) |
|---|---|---|---|---|---|---|
| protons | 51.8 | 1.30 | 0.48 | 8.6 | 1.30 | 0.48 |
| tritons | 141.3 | 1.27 | 0.52 | 55.0 | 1.28 | 0.65 |

Table 2. Values of the structure amplitudes $G^k_{NLSJ}$ for pure Nilsson orbits calculated with major shell mixing.

| $J^\pi$ | $E_x$ (MeV) | Nilsson orbit number | $G^k_{NLSJ}$ | | | | |
|---|---|---|---|---|---|---|---|
| | | | N = 1 | N = 2 | N = 3 | N = 4 | N = 5 |
| $0^+$ | 0 | 5 | 0.0002 | -0.0.09 | 0.1802 | 0.0096 | 0.0006 |
| | | 9 | 0.0003 | -0.0055 | 0.2415 | -0.0122 | 0.0013 |
| | | 11 | 0.0007 | -0.0264 | 0.3205 | 0.0159 | 0.0009 |
| $2^+$ | 1368 | 5 | 0.0077 | -0.1515 | -0.0177 | -0.0004 | |
| | | 9 | -0.0029 | 0.0777 | -0.0350 | 0.0016 | |
| | | 11 | 0.0188 | -0.2574 | -0.0300 | -0.0005 | |
| $4^+$ | 4123 | 5 | 0.0711 | 0.0233 | 0.0004 | | |
| | | 9 | -0.2185 | 0.0028 | 0.0010 | | |
| | | 11 | 0.1129 | 0.0369 | 0.0008 | | |

Table 3. Values of the structure amplitudes $G^k_{NLSJ}$ for pure Nilsson orbits calculated without major shell mixing.

| $J^\pi$ | $E_x$ (keV) | Nilsson orbit number | $G^k_{NLSJ}$ | | |
|---|---|---|---|---|---|
| | | | N = 1 | N = 2 | N = 3 |
| $0^+$ | 0 | 5 | 0.0002 | -0.0110 | 0.1825 |
| | | 9 | 0.0005 | 0.0054 | 0.4544 |
| | | 11 | 0.0002 | -0.0109 | 0.1829 |
| $2^+$ | 1368 | 5 | 0.0078 | -0.1542 | |
| | | 9 | -0.0002 | 0.0222 | |
| | | 11 | -0.0055 | 0.1269 | |
| $4^+$ | 4123 | 5 | 0.0732 | | |
| | | 9 | 0.0013 | | |
| | | 11 | -0.0038 | | |

Table 4. DWBA normalization required to reproduce the observed angular distributions using $V_k$ values which have been deduced from single nucleon transfer reactions.

| Author | $V_5$ | $V_9$ | $V_{11}$ | DWBA normalization | | | | | |
|---|---|---|---|---|---|---|---|---|---|
| | | | | With major shell mixing. | | | Without major shell mixing. | | |
| | | | | L = 0 | L = 2 | L = 4 | L = 0 | L = 2 | L = 4 |
| Dehnhard Yntema (67Del) | 0.837 | 0.447 | 0.283 | 79 | 605 | 1040 | 55 | 1030 | 7230 |
| | 0.837 | 0.447 | -0.283 | 319 | NA | 1990 | 95 | 290 | 6580 |
| | 0.837 | -0.447 | 0.283 | 671 | 150 | NA | NA | 676 | 6950 |
| | 0.837 | -0.447 | -0.283 | NA | 576 | NA | 929 | 236 | 6340 |
| Cujec (64Cul) | 0.925 | 0.381 | | 142 | 1410 | 1670 | 78 | 399 | 5670 |
| | 0.925 | -0.381 | | 2300 | 265 | NA | NA | 316 | 5670 |
| Hamburger Blair (60Hal) | 0.911 | 0.570 | 0.2 | 97 | 590 | 1350 | 69 | 626 | 5990 |
| | 0.911 | 0.57 | -0.2 | 267 | 5784 | 2410 | 106 | 289 | 5590 |
| | 0.911 | -0.57 | 0.2 | 594 | 185 | NA | 5140 | 475 | 5820 |
| | 0.911 | -0.57 | -0.2 | NA | 497 | NA | 9370 | 238 | 5430 |
| Kroon et. al. (71Krl) | 0.78 | 0.57 | 0.3 | 68 | 761 | 805 | 44 | 148 | 8420 |
| | 0.78 | 0.57 | -0.3 | 266 | 954 | 1350 | 77 | 339 | 7760 |
| | 0.78 | -0.57 | 0.3 | 1350 | 131 | NA | 2750 | 800 | 7980 |
| | 0.78 | -0.57 | -0.3 | 793 | 462 | NA | 324 | 246 | 2720 |

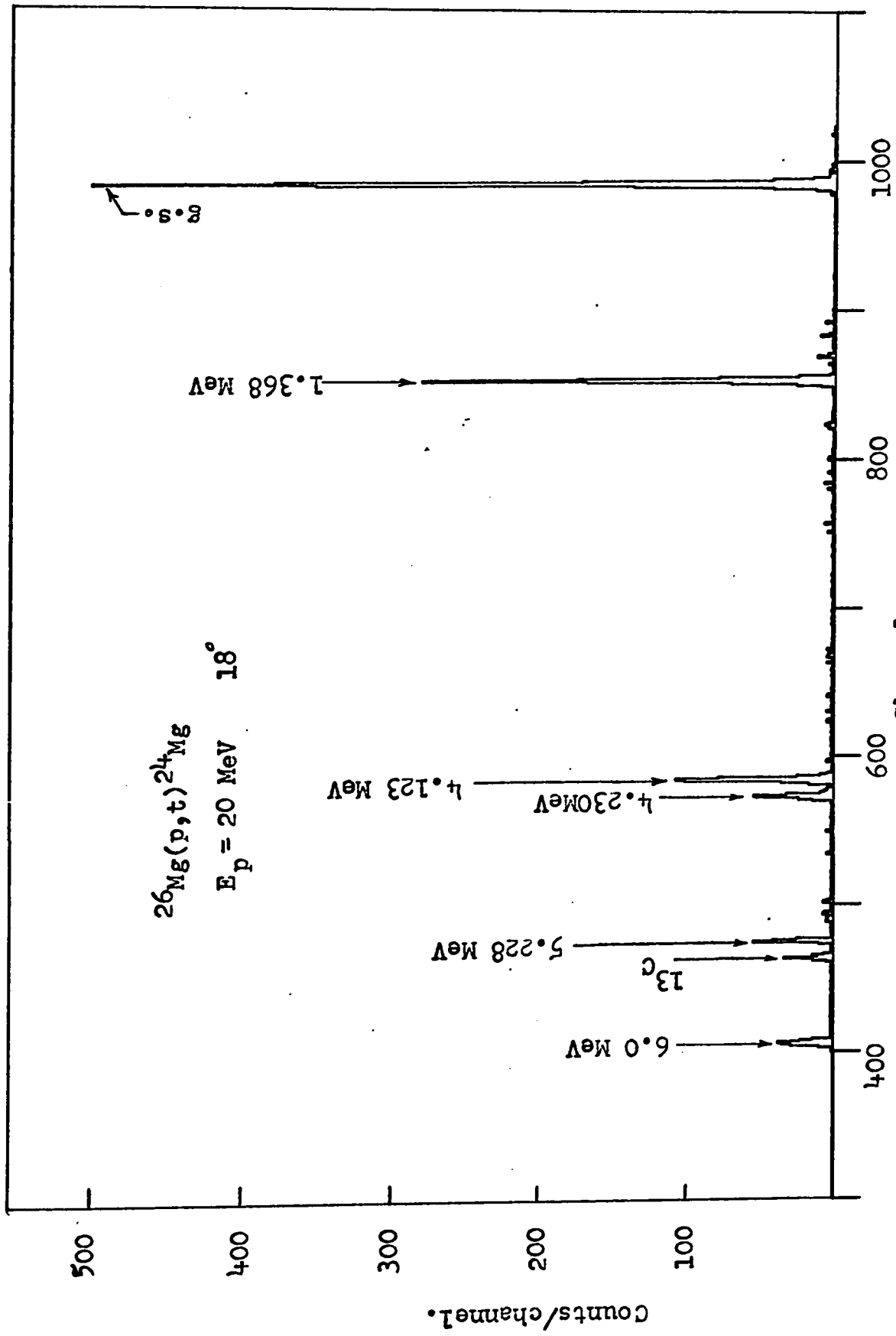


Fig. 1 Spectrum from the $^{26}Mg(p,t)^{24}Mg$ reaction.

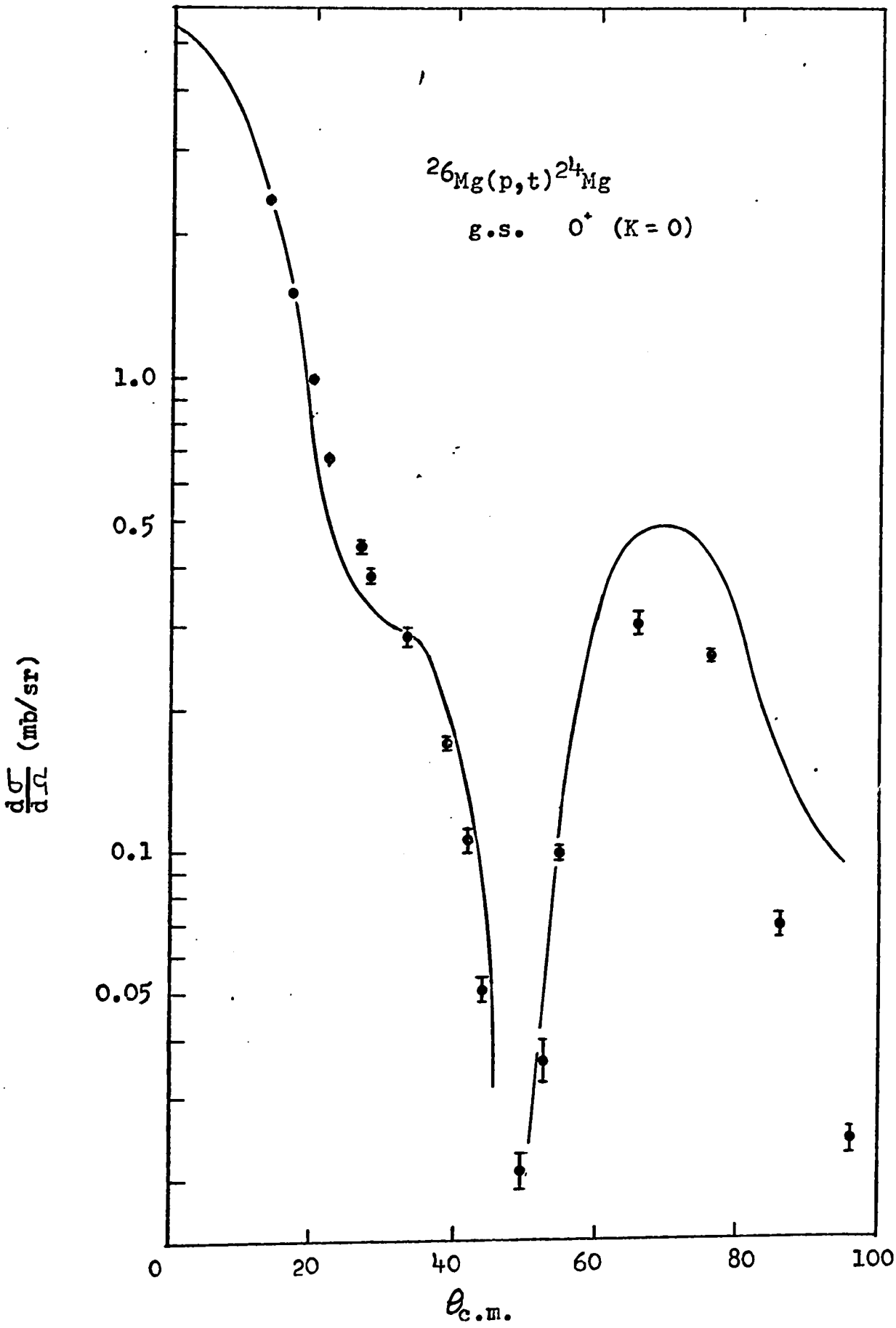


Fig. 2 Angular distribution to the ground state of $^{24}Mg$.

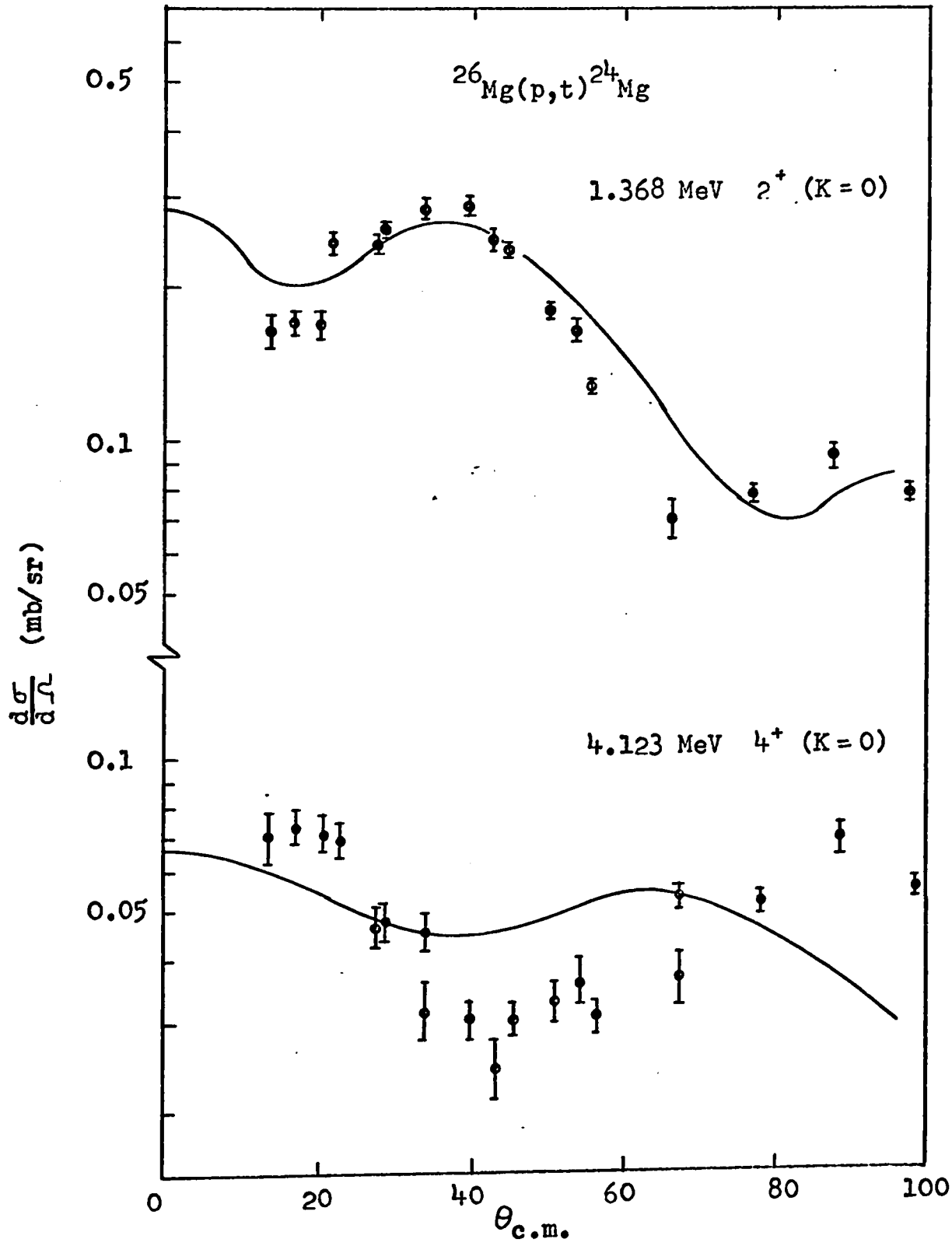


Fig. 3 Angular distribution to the $2^+$ and $4^+$ members of the ground state rotational band.

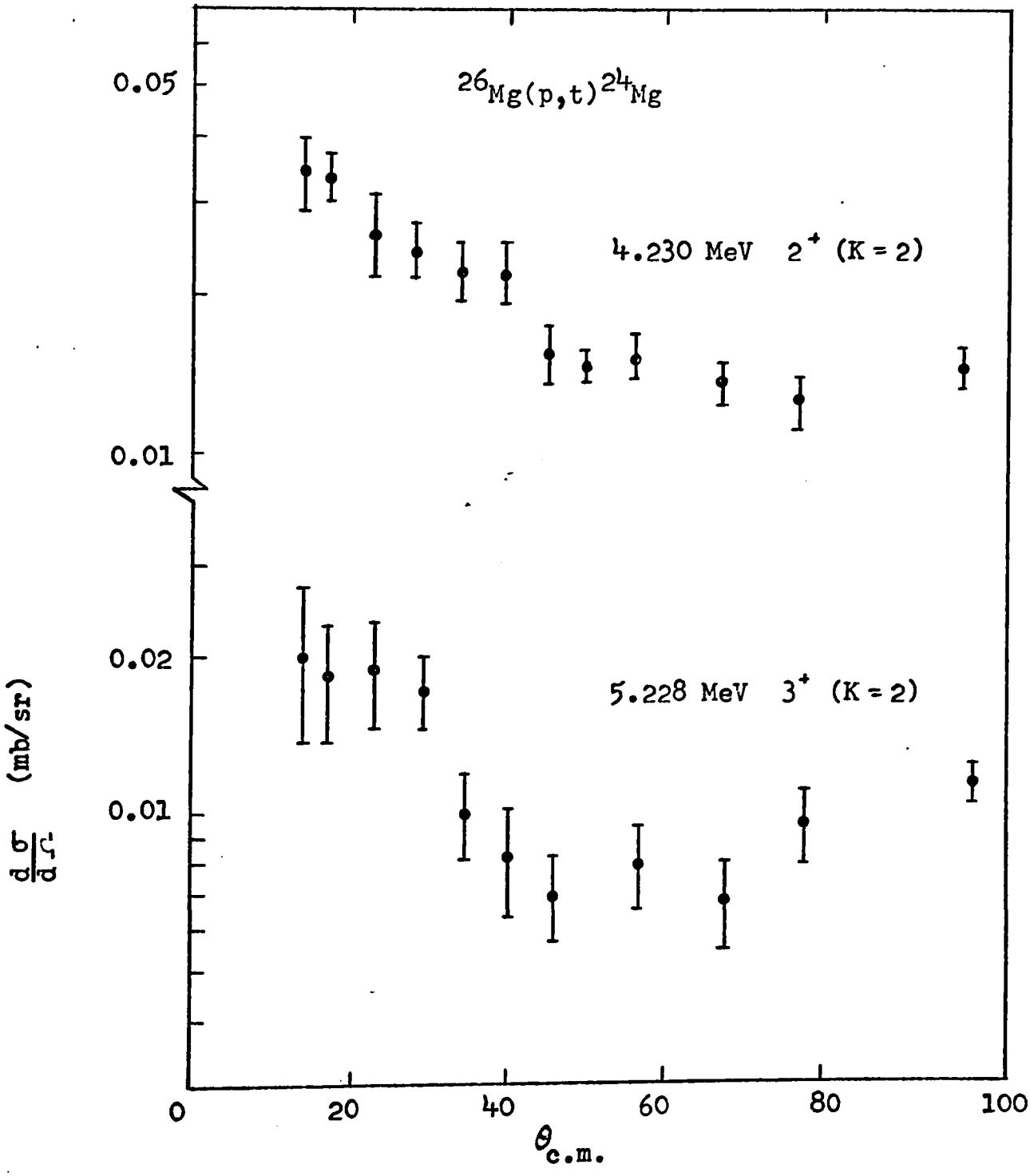


Fig. 4 Angular distribution to two members of the K = 2 band.

## APPENDIX 1.

### Cross section correction for overlapping levels.

Let target 1 consist mainly of nucleus 1 of thickness $d_1^1$ and of an impurity 2 of thickness $d_1^2$ in which $d_1^1 \gg d_1^2$. If nucleus 1 and 2 have a level which overlaps, then the area seen under the peak in the energy spectra will be:

$$A_1 = \omega N_1 ( \sigma^1 d_1^1 + \sigma^2 d_1^2 ), \qquad (1)$$

where: $\omega$ = solid angle of the detector,

$N_i$ = number of particles incident on target i ,

$\sigma^j$ = cross section of nucleus j,

$d_i^j$ = thickness of nucleus j in target i.

If target 2 has the same two nuclei with this time $d_2^1 \ll d_2^2$ , then the area seen under the peak in the energy spectrum when target 2 is bombarded will be:

$$A_2 = \omega N_2 ( \sigma^1 d_2^1 + \sigma^2 d_2^2 ). \qquad (2)$$

Equations 1 and 2 can be solved for $\sigma^1$, yielding:

$$\sigma' = \frac{\dfrac{A_1}{\omega d_1^1 N_1}}{1 - \dfrac{d_2^1 d_1^2}{d_1^1 d_2^1}} - \frac{\dfrac{A_2}{\omega d_2^2 N_2}}{\dfrac{d_1^1}{d_1^2} - \dfrac{d_2^1}{d_2^2}}$$

Using the two relations $d_1^1 \gg d_1^2$ and $d_2^2 \gg d_2^1$ the preceeding expression can be simplified to:

$$\sigma^1 \simeq \frac{A_1}{\omega d_1^1 N_1} - \frac{d_1^2}{d_1^1} \times \frac{A_2}{\omega d_2^2 N_2}$$

$$= \sigma_T^1 - \frac{d_1^2}{d_1^1} \sigma_T^2 \quad ,$$

where $\sigma_T^i$ is the cross section obtained from target i assuming it contains only nucleus i of thickness $d_i^i$.

If there are more than two overlaping levels, the formulae can be extended to:

$$\sigma^1 = \sigma_T^1 - \sum_i \frac{d_1^i}{d_1^1} \sigma_T^i$$

Since the thickness of the impurities is proportional to their % content in the target, one has:

$$\sigma^1 = \sigma_T^1 - \sum_i \frac{c_1^i}{c_1^1} \sigma_T^i \quad ,$$

where $c_j^i$ is the % content of impurity i in target j.

## REFERENCES


55Nil S.G. Nilsson, Mat. Fys. Medd. Dan. Vid. Selsk. 29, no. 16 (1955)

56Brl E. Brun, J.J. Kraushaar and W.E. Meyerhoff, Phys. Rev. 102(1956)808

59Bal B.F. Bayman, A.S. Reiner and R.K. Sheline, Phys. Rev. 115(1959)1627

60Hal E.W. Hamburger and A.G. Blair, Phys. Rev. 119(1960)777

60Kil L.S. Kisslinger and R.A. Sorensen, Mat. Fys. Dan. Vid. Selsk. 32, No. 9 (1960)

60Mal M.H. Macfarlane and J.B. French, Rev. Mod. Phys. 32(1960)567

61Dal A.S. Davydov, Nucl. Phys. 24(1961)682

61Nil S.G. Nilsson and O. Prior, Mat. Fys. Medd. Dan. Vid. Selsk. 32, No. 16 (1961)

61Yol S. Yoshida, Phys. Rev. 123(1961)2122

63Kil L.S. Kisslinger and R.A. Sorensen, Rev. Mod. Phys. 35(1963)853

63Pel F.G. Perey, Phys. Rev. 131(1963)745

63Pe2 C.M. Perey and F.G. Perey, Phys. Rev. 132(1963)755

64Cul B. Čujec, Phys. Rev. 136(1964)B1305

64Dal W. Darcey, Compt. Rend. Congr. Int. de Physique Nucléaire, Paris II (1964) p. 456

64Lel L.L. Lee Jr. and J.P. Schiffer, Phys. Rev. 136(1964)B405

64Rol J.R. Rook and D. Mitra, Nucl. Phys. 51(1964)96

64Sh1 R. Sherr, E. Rost and M.E. Rickey,
Phys. Rev. Lett. 12(1964)420

65Gl1 N.K. Glendenning, Phys. Rev. 137(1965)B102

65Li1 E.K. Lin, Phys. Rev. 139(1965)B340

66Gl1 R.N. Glover and A.D.W. Jones, Nucl. Phys. 81(1966)277

66Nd1 Nuclear Data Sheets, Nuclear Data B1-6(1966)

66Re1 G.M. Reynolds. Ph.D. Thesis, University of Minnesota (1966)

67Br1 G. Brown, J.G. Haigh, F.R. Hudson and A.E. Macgregor,
Nucl. Phys. A101(1967)163

67Co1 S.W. Cosper, H. Brunnader, J. Cerny and R.L. McGrath,
Phys. Lett. 25B(1967)324

67De1 D. Dehnhard and J.L. Yntema, Phys. Rev. 160(1967)964

67Eh1 D. von Ehrenstein and J.P. Schiffer,
Phys. Rev. 164(1967)1374

67Fo1 C.M. Fou, R.W. Zurmühle and J.M. Joyce,
Nucl. Phys. A97(1967)458

67Ha1 J.C. Hafele, E.R. Flynn and A.G. Blair,
Phys. Rev. 155(1967)1238

67Ja1 A.A. Jaffee, Conference on Atomic Masses, 1967, p.615

67Kr1 M. Kregar and B. Elbek, Nucl. Phys. A93(1967)49

67Kr2 M. Kregar and M.V. Mihailović, Nucl. Phys. A93(1967)402

67Ku1 P.D. Kuntz, University of Colorado 1967 (unpublished)

68Ba1 J.B. Ball and C.B. Fulmer, Phys. Rev. 172(1968)1199

68Ca1 D.C. Camp, Nucl. Phys. A121(1968)561

68Go1 L.H. Goldman, Phys. Rev. 165(1968)1203

68Ot1 H. Ottmar, Z. Phys. 209(1968)44

68Pal D.M. Van Patter, P.F. Hinrichsen and M.H. Shapiro, Bull. Am. Phys. Soc. 13(1968)1427

68Ral M.N. Rao, J. Rapaport, A. Sperduto and D.L. Smith, Nucl. Phys. A121(1968)1

68Rul A.P. de Ruiter, H. Verheul and J. Kinijn, Nucl. Phys. A116(1968)473

68Scl W. Scholz and F.B. Malik, Phys. Rev. 176(1968)1355

69Gll N.K. Glendenning, Proceedings of the International Conference on Nuclear States, Montreal 1969, p.245

69Hel G. Heymann, P. van der Merwe, I.J. van Heerden and I.C. Dormehl, Z. Phys. 218(1969)137

69Hil B. Hird and R.W. Ollerhead, Nucl. Inst. and Methods 71(1969)231

69Hi2 P.F. Hinrichsen, D.M. Van Patter and M.H. Shapiro, Nucl. Phys. A123(1969)250

69Iml N. Imanishi, M. Sakisaka and F. Fukuzawa, Nucl. Phys. A125(1969)626

69Mol W.G. Monahan and R.G. Arns, Phys. Rev. 184(1969)1135

70Asl R.J. Ascuito and N.K. Glendenning, Phys. Rev. C2(1970)415 and Phys. Rev. C2(1970)1260

70Brl G. Bruge and R.F. Leonard, Phys. Rev. C2(1970)2200

70Chl Christiansen et. al. Phys. Rev. Lett. 21(1968)554 and Phys. Rev. C1(1970)613

70Cul T.H. Curtis, H.F. Lutz and W. Bartolini, Phys. Rev. C1(1970)1418

70Ehl D. von Ehrenstein, G.C. Morrison, J.A. Nolen Jr. and N. Williams, Phys. Rev. C1(1970)2066

70Grl J.A.R. Griffith, M. Irshad, O.Karban and S. Roman, Nucl. Phys. A146(1970)193

70Hal J.C. Hardy, Private Communication

70Kyl J. Kyles, J.C. McGeorge, F. Shaikh and J. Byrne, Nucl. Phys. A150(1970)143

70Mal J.G. Malan, J.W. Tepel and J.A.M. de Villiers, Nucl. Phys. A143(1970)53

70Mol R. Moreh and O. Shahal, Phys. Rev. C2(1970)2217

70Mul S. Muszynski and S.K. Mark, Nucl. Phys. A142(1970)459

70Nol E. Nolte, W. Kutschera, Y. Shida and H. Morinaga, Phys. Lett. 33B(1970)294

70Oll A.F. Oluwole, G. Schmelling and A. Shugart, Phys. Rev. C2(1970)228

70Tul I.M. Turkiewicz, P. Beuzit, J. Delauany and J.P. Fouan, Nucl. Phys. A143(1970)641

71Bal G. Ball et. al. To be published

71Cal D.C. Camp, D.R. Fielder and B.P. Foster, Nucl. Phys. A163(1971)145

71Fol R. Fournier, B. Hird, L. Hsu, J. Kroon and G. Ball, to be published

71Krl J. Kroon, R. Fournier, R.J.W. Hodgson, B. Hird, R.W. Ollerhead and F. Ingebretsen, Nucl. Phys. to be published.

71Mul G. Murray, N.E. Sanderson and J.C. Willmott, Nucl. Phys. A171(1971)435

71Pal T. Paradellis, A. Houdayer and S.K. Mark, Nucl. Phys. to be published

71 Rel A.C. Rester, A.V. Ramayya, J.H. Hamilton, D. Krmpotic and P. Venugopala Rao, Nucl. Phys. A162(1971)461

71Re2 A.C. Rester, J.H. Hamilton, A.V. Ramayya and Noar R. Johnson, Nucl. Phys. A162(1971)481

## CURRICULUM VITAE

NAME: Rodolphe Fournier

BORN: Quebec, Canada 1942.

EDUCATED:

SECONDARY: Ecole Secondaire St. Michel,
Sillery, Québec

UNIVERSITY: Université Laval, Québec
B.Sc. Génie Physique 1960-1965
M.Sc. Physique Nucléaire 1966-1968
University of Ottawa 1968-1971

ERRATA

After completion of the thesis, a phase error was found in the calculation of the unmixed $c_k^{nj}$ coefficients which were used in the calculation of the structure factors for the $^{26}Mg(p,t)^{24}Mg$ reaction. Tables 3 and 4 of the second part should read as in the following pages.

There is now agreement on the relative cross sections for the set $V_5$ 0.78, $V_9$ -0.57 and $V_{11}$ -0.3. This solution is again unacceptable due to the high normalization of 1000, so that the final conclusions remain unchanged.

Table 3. Values of the structure amplitudes $G^k_{NLSJ}$ for pure Nilsson orbits calculated without major shell mixing.

(CORRECTION TO PAGE 157)

| $J^\pi$ | $E_x$ (keV) | Nilsson orbit number | $G^k_{NLSJ}$ N = 1 | N = 2 | N = 3 |
|---|---|---|---|---|---|
| $0^+$ | 0 | 5 | 0.0002 | -0.0110 | 0.1825 |
| | | 9 | 0.0003 | -0.0069 | 0.2505 |
| | | 11 | 0.0003 | -0.0028 | 0.3190 |
| $2^+$ | 1368 | 5 | 0.0078 | -0.1542 | |
| | | 9 | -0.0030 | 0.0731 | |
| | | 11 | -0.0010 | -0.0577 | |
| $4^+$ | 4123 | 5 | 0.0732 | | |
| | | 9 | -0.2188 | | |
| | | 11 | 0.1184 | | |

Table 4. DWBA normalization required to reproduce the observed angular distributions using $V_K$ values which have been deduced from single nucleon transfer reactions.

(CORRECTION TO PAGE 158)

| Author | $V_5$ | $V_9$ | $V_{11}$ | DWBA normalization | | | | | |
|---|---|---|---|---|---|---|---|---|---|
| | | | | With major shell mixing. | | | Without major shell mixing. | | |
| | | | | L = 0 | L = 2 | L = 4 | L = 0 | L = 2 | L = 4 |
| Dehnhard Yntema (67Del) | 0.837 | 0.447 | 0.283 | 79 | 605 | 1040 | 72 | 246 | $10^6$ |
| | 0.837 | 0.447 | -0.283 | 319 | NA | 1990 | 293 | 12875 | 5177 |
| | 0.837 | -0.447 | 0.283 | 671 | 150 | NA | 526 | 130 | 686 |
| | 0.837 | -0.447 | -0.283 | NA | 576 | NA | 4023 | 903 | 1612 |
| Cujec (64Cul) | 0.925 | 0.381 | | 142 | 1410 | 1670 | 129 | 541 | $10^5$ |
| | 0.925 | -0.381 | | 2300 | 265 | NA | 1624 | 246 | 1115 |
| Hamburger Blair (60Hal) | 0.911 | 0.570 | 0.2 | 97 | 590 | 1350 | 88 | 260 | $10^5$ |
| | 0.911 | 0.57 | -0.2 | 267 | 5784 | 2410 | 241 | 1820 | 19833 |
| | 0.911 | -0.57 | 0.2 | 594 | 185 | NA | 458 | 150 | 889 |
| | 0.911 | -0.57 | -0.2 | NA | 497 | NA | 51820 | 537 | 1716 |
| Kroon et. al. (71Krl) | 0.78 | 0.57 | 0.3 | 68 | 761 | 805 | 63 | 294 | 24647 |
| | 0.78 | 0.57 | -0.3 | 266 | 954 | 1350 | 249 | $10^6$ | 2388 |
| | 0.78 | -0.57 | 0.3 | 1350 | 131 | NA | 989 | 125 | 538 |
| | 0.78 | -0.57 | -0.3 | 793 | 462 | NA | 1025 | 996 | 1189 |